

# Light Scattering in Water

Mike Twardowski

*Harbor Branch Oceanographic Institute  
Ft. Pierce, FL*

[mtwardowski@fau.edu](mailto:mtwardowski@fau.edu)

[http://www.fau.edu/hboi/ocean\\_optics](http://www.fau.edu/hboi/ocean_optics)



# Brief Background...

PhD	Oceanography, Biophysics – University of Rhode Island (Percy Donaghay)	1998
Postdoc	Environmental Optics Fellowship – Oregon State University (Ron Zaneveld)	1998-2000

## CURRENT POSITIONS

Director, Center for Marine Applied Technology and Engineering (C-MATE)	2021-present
Professor, <i>Harbor Branch Oceanographic Institute, FAU</i>	2015-present
Affiliate Professor, <i>Ocean Engineering, FAU</i>	2017-present
President, <i>Sunstone Scientific LLC</i>	2017-present
Senior Engineer, <i>SEACORP Inc.</i>	2015-present

## FORMER POSITION

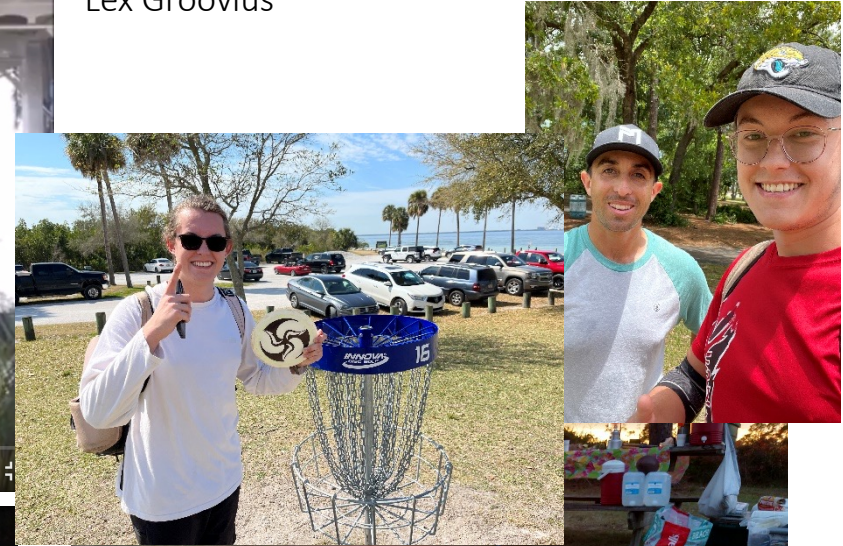
Director of Research and Vice President, <i>WET Labs, Inc.</i>	2000-2015
--	-----------

- Ocean optics research: basic and applied
- Sensor development: fundamental optics, imaging systems
- Modeling: radiative transfer theory, imaging and visibility
- NASA PACE Science Team





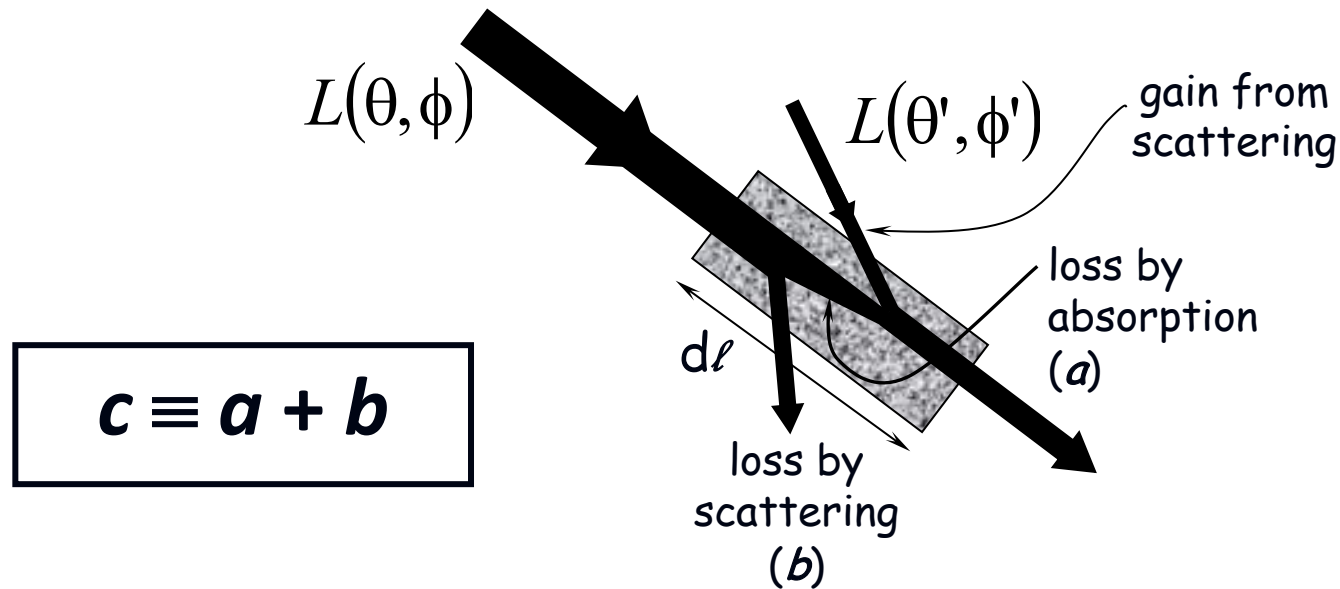
“Lex Groovius”



BIOSOPE, led by Villefranche (2004)



# Radiative Transfer in the Ocean



## Inherent Optical Properties (IOPs)

*Depend only on substances in water*

[Attenuation (c), Absorption (a), Scattering (b), and related subfractions]

## Apparent Optical Properties (AOPs)

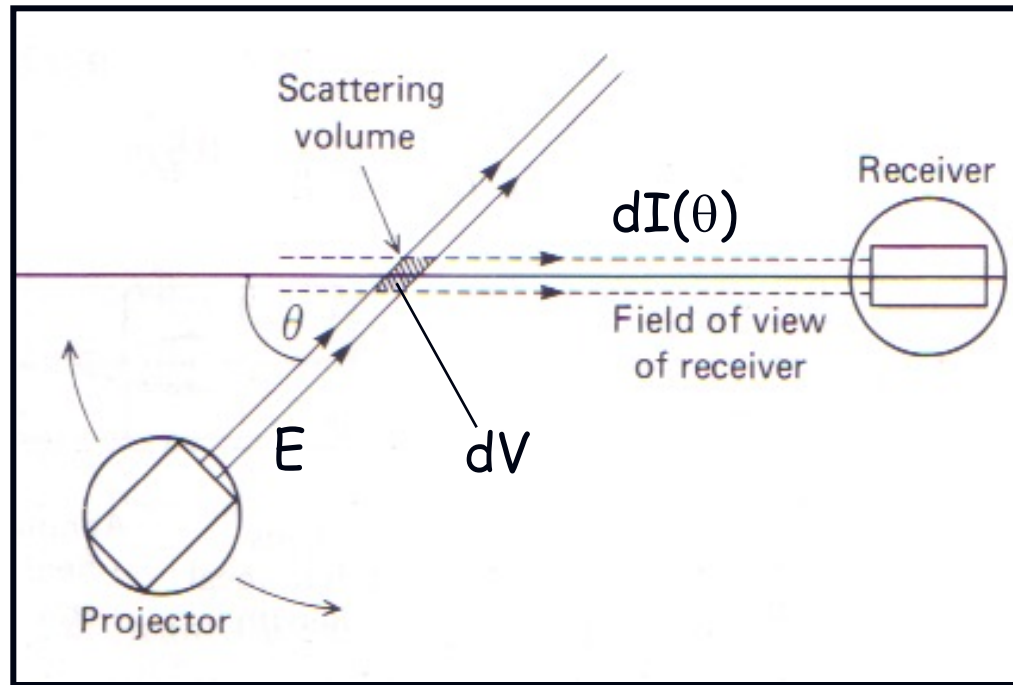
*Depend on substances in water AND ambient light field*

[Reflectance (R), Diffuse attenuation (K), and related parameters]



# Volume Scattering Function (VSF) defined

$$\beta(\theta) = \frac{dI(\theta)}{EdV} = \frac{W \cdot sr^{-1}}{W \cdot m^{-2} \cdot m^3} = m^{-1} \cdot sr^{-1}$$



$dI(\theta)$  radiant flux  
in direction  
 $d\theta$  ( $W \text{ sr}^{-1}$ )

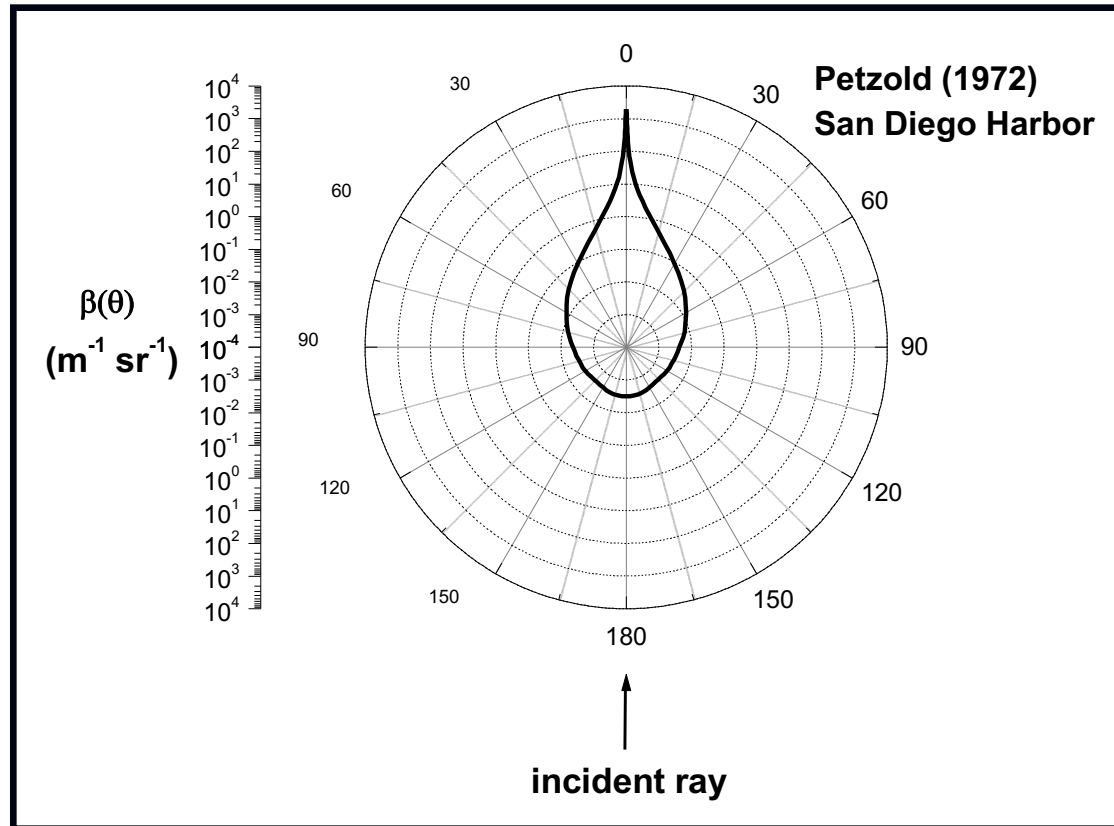
$dV$  elemental  
volume ( $m^3$ )

$E$  incident  
irradiance  
( $W \text{ m}^{-2}$ )

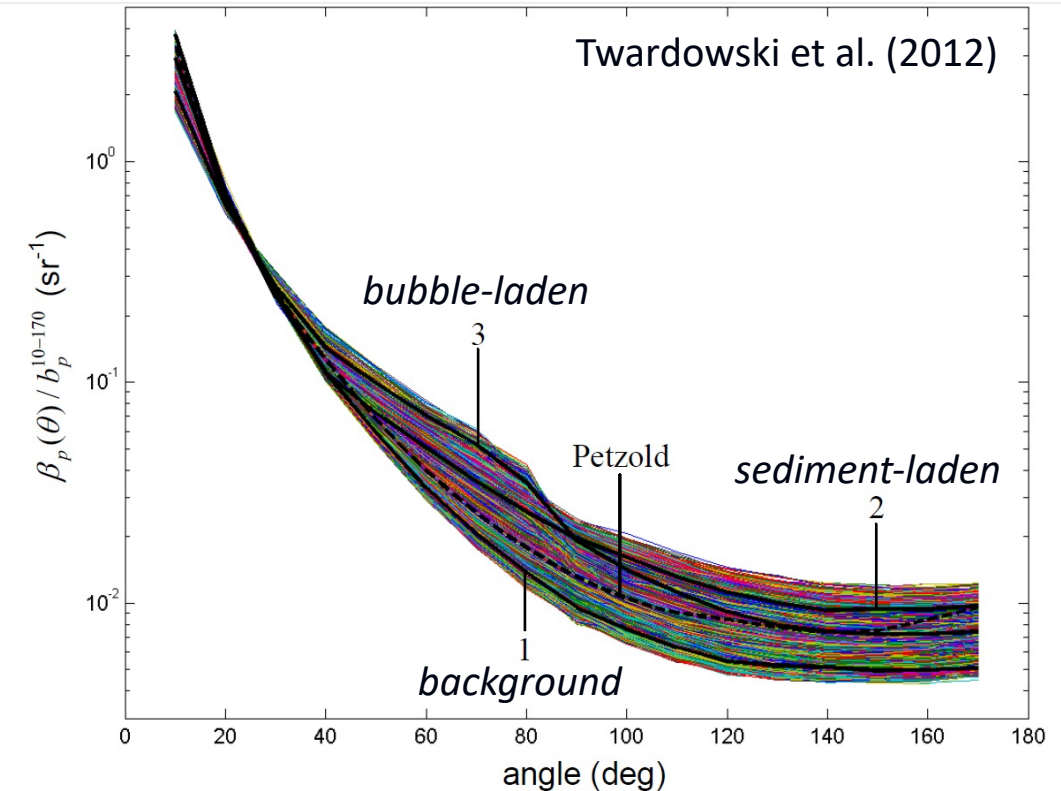
# Typical VSF

\*Log  
Scale  
~10<sup>7</sup>  
Dynamic  
range

\*Very  
steeply  
forward  
peaked



Scripps Pier, 2008



Typically, only ~0.3-3% of scattering ( $b$ ) is backscattering ( $b_b$ )  
(however, in clear waters,  $b_w$  can increase this %)

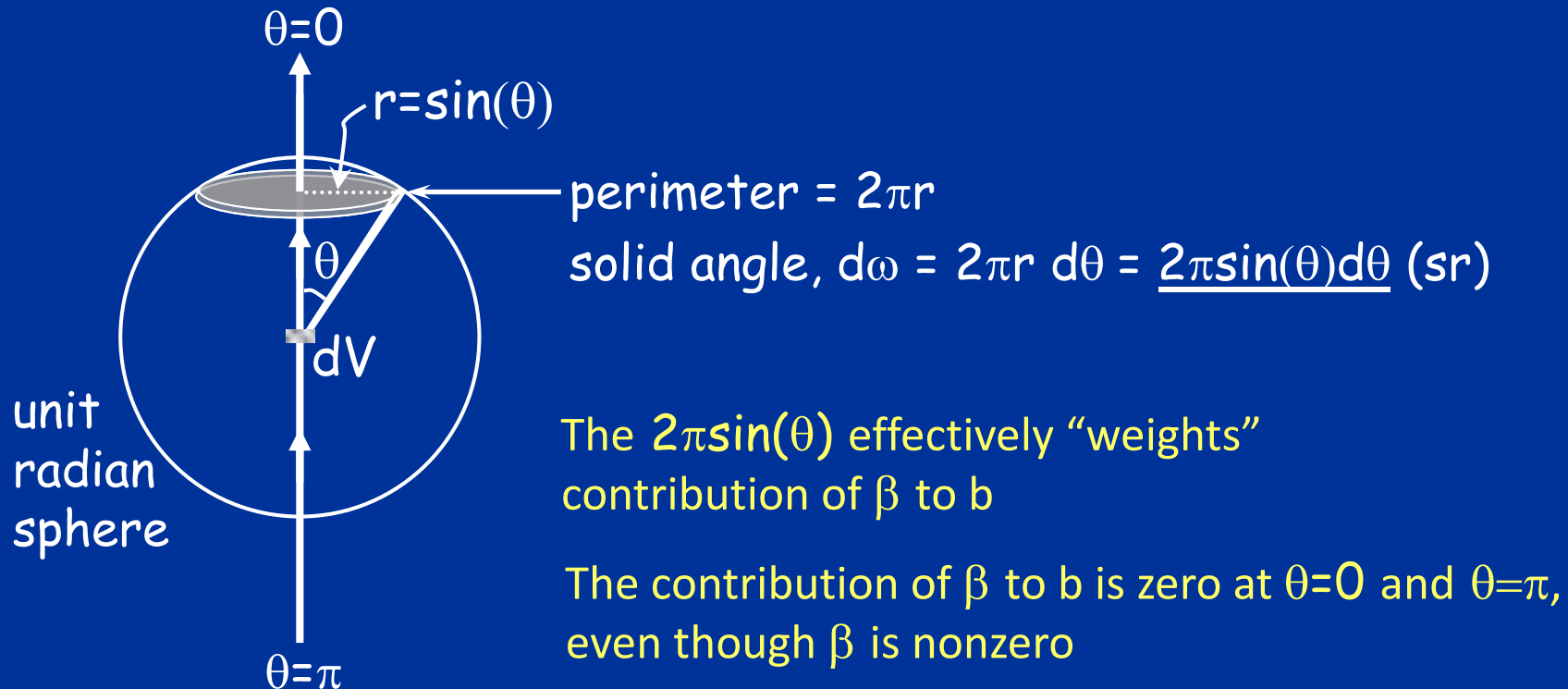


# VSF integration to obtain $b$

Remember...

$$b = 2\pi \int_0^{\pi} \sin(\theta) \beta(\theta) d\theta$$

Assuming  
azimuthal  
symmetry



# Scattering components

Can partition with respect to constituent components..., e.g.:

$$b_t(\lambda) = b_w(\lambda) + b_p(\lambda) \quad \text{units m}^{-1}, \text{ can further partition } b_p$$

Also with respect to angular distribution:

$$b_x = 2\pi \int_i^j \sin(\theta) \beta(\theta) d\theta$$

Total scattering

set  $x = t$

$[i, j] = [0, \pi]$

Forward scattering

set  $x = f$

$[i, j] = [0, \pi/2]$

Backscattering

set  $x = b$

$[i, j] = [\pi/2, \pi]$



# Primary scattering components in water

- Pure seawater (molecular)
- Turbulence (i.e., refractive index discontinuities)
- Particles
- Bubbles

# Other scattering properties from VSF

Phase function:

$$\tilde{\beta}(\theta) = \frac{\beta(\theta)}{b} \quad \text{units (sr}^{-1}\text{)}$$

Backscattering ratio:

$$\widetilde{b_b} = \frac{b_b}{b}$$

Asymmetry parameter (mean cosine):

$$g = \langle \cos(\theta) \rangle = 2\pi \int_0^\pi \tilde{\beta}(\theta) \cos(\theta) \sin(\theta) d\theta$$

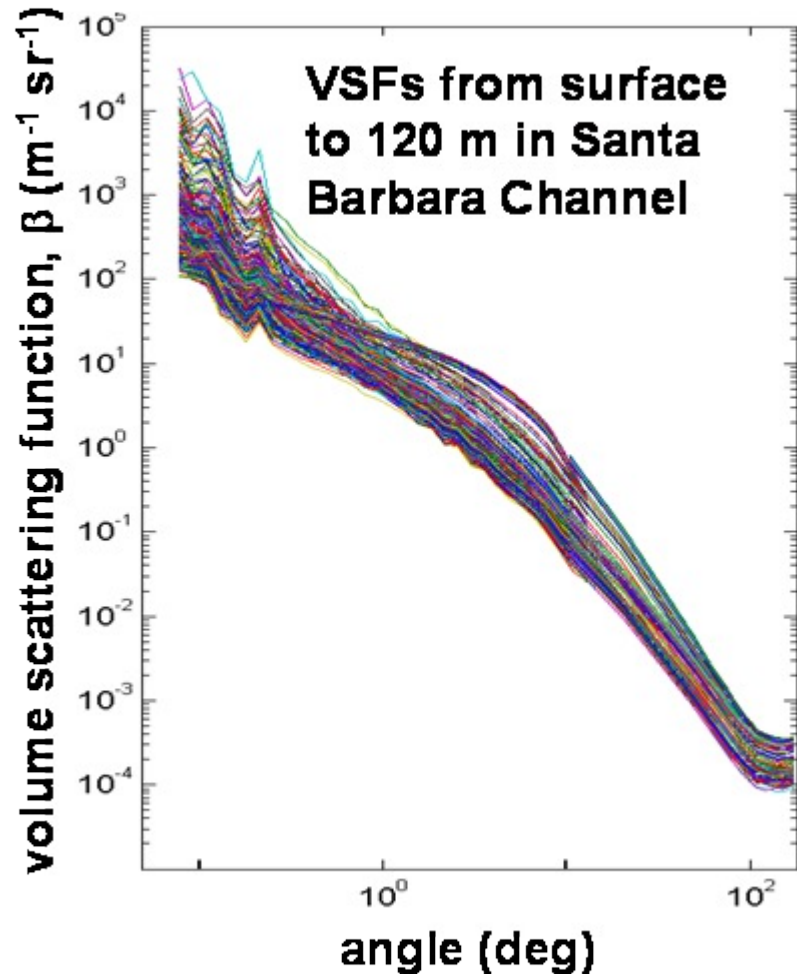
If symmetric around  $90^\circ$ ,  $g = 0$

If highly skewed  $g \rightarrow 1$

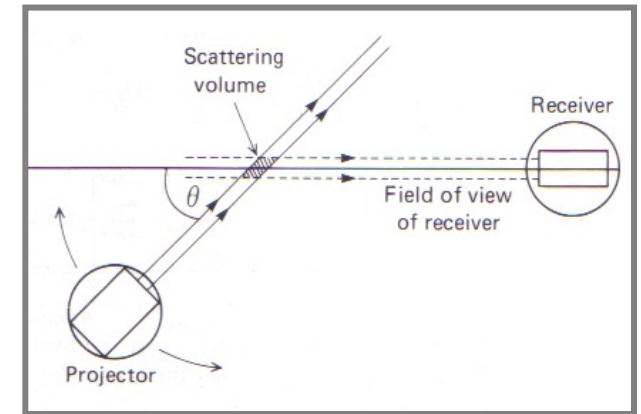
unitless



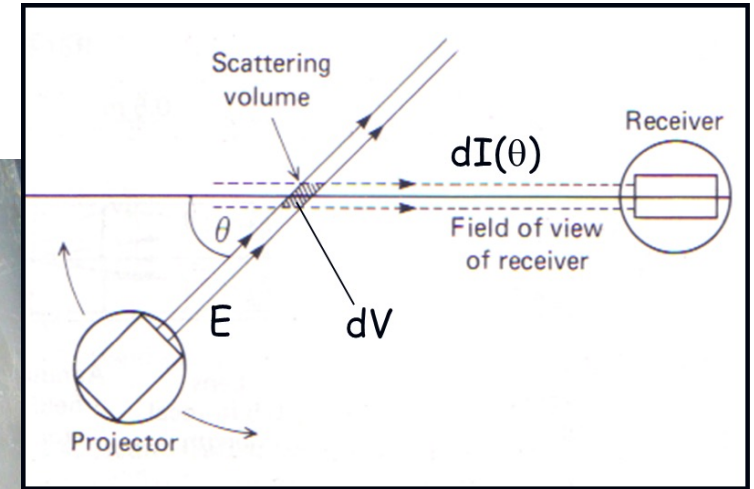
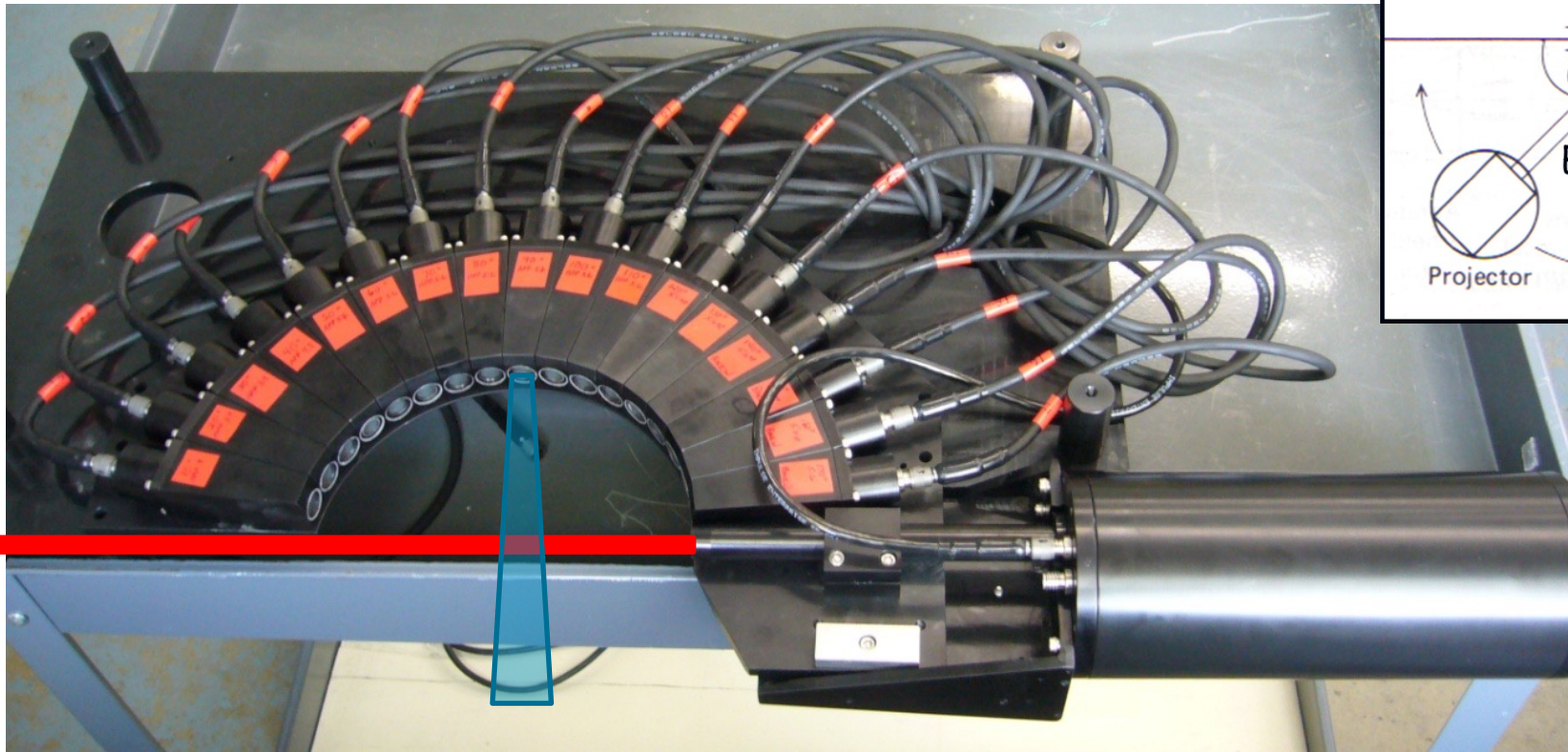
# VSF Measurement Considerations



- 6+ orders of magnitude variation in intensity from the near-forward to backward in single VSF
- several orders of magnitude natural dynamic range in intensity at any single angle
- rapid temporal variability in particle fields in surface waters
- rejecting ambient light is challenging at surface, particularly for low scattering signals in the backward
- calibration without absolute “standard”
- Errors can grow at higher turbidities and pathlengths



# Measuring the VSF: MASCOT (HBOI-FAU)

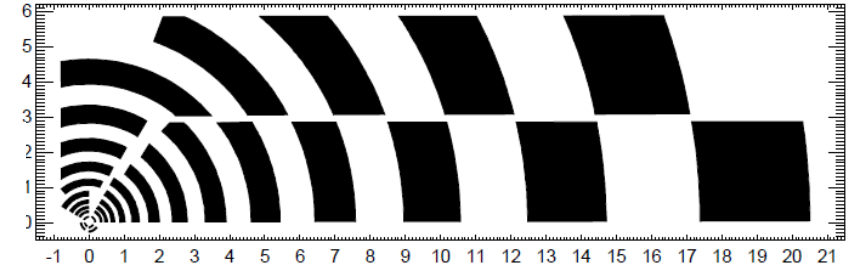
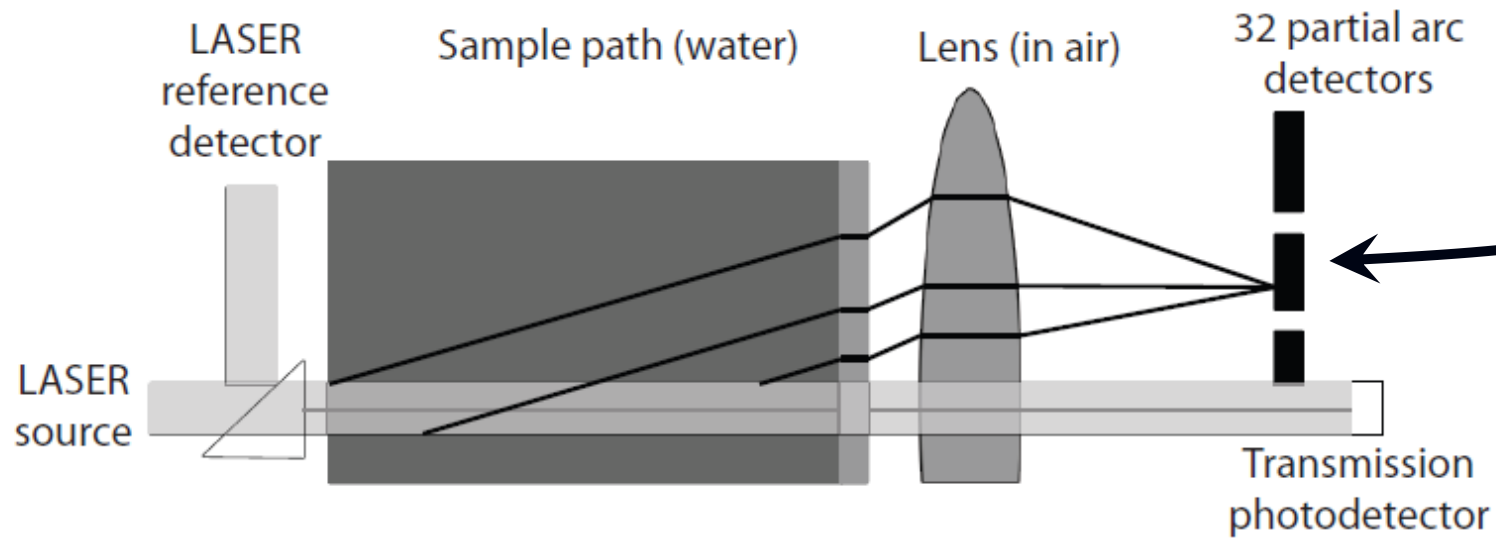


- Measures VSF from  $10^\circ$  to  $170^\circ$
- $0.8$ - $5^\circ$  detector FOVs
- 20 Hz sampling rate
- Wedge depolarizer on source



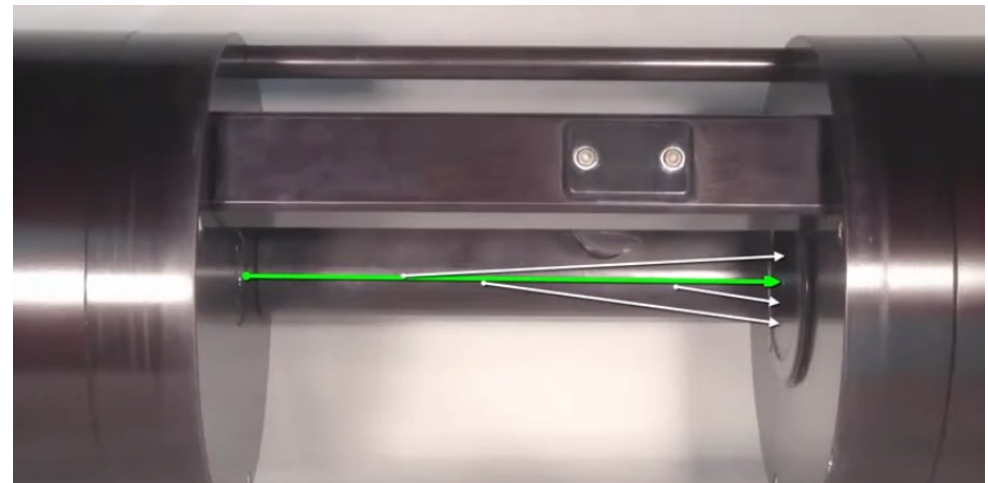
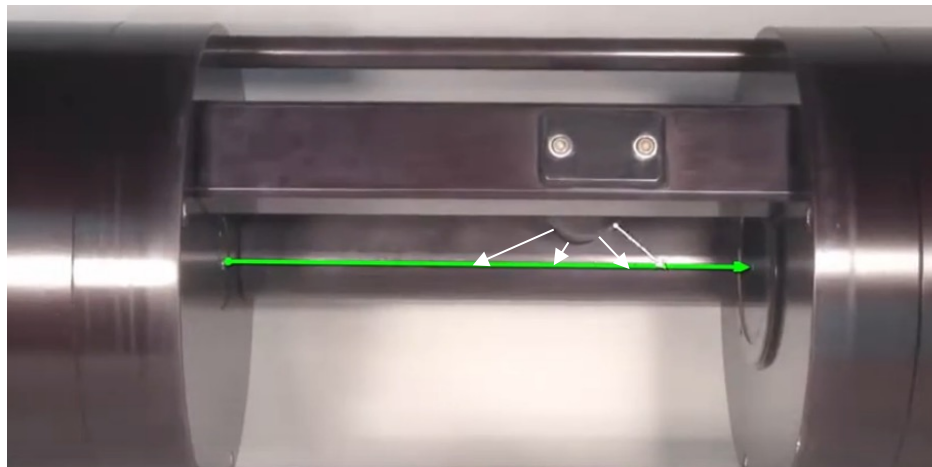
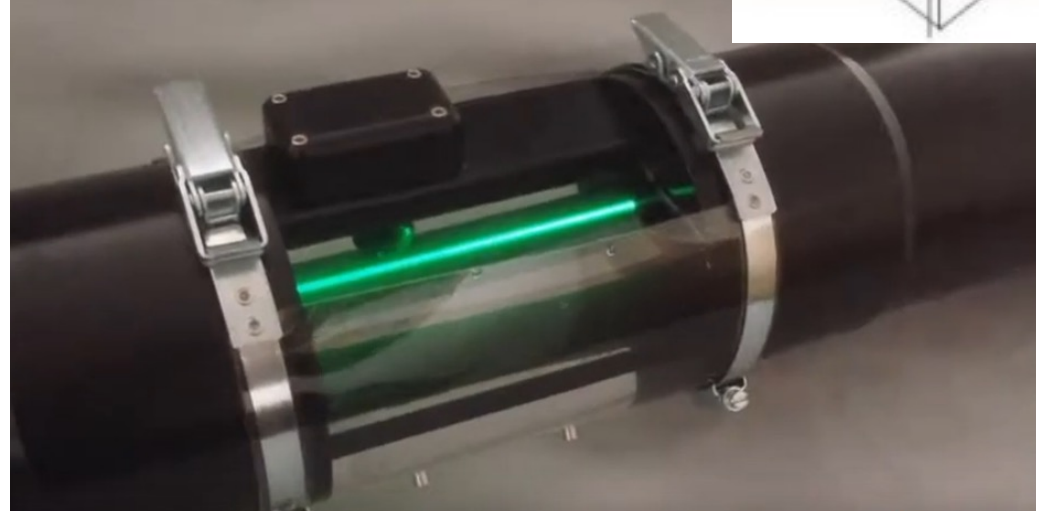
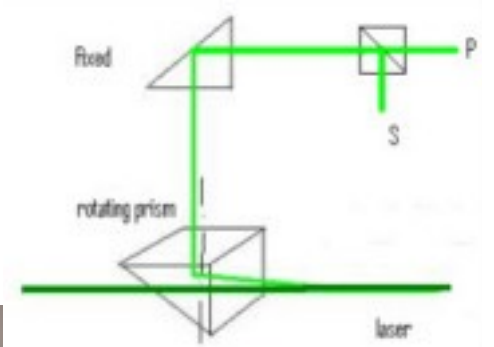
# LISST-100X (Sequoia Scientific)

near-forward scattering (diffractometry)



# LISST-VSF (Sequoia Scientific)

Full volume scattering function (and linear pol)



<https://www.youtube.com/watch?v=E4wt5LLhUK8>

# Hyper-bb (Sequoia Scientific)

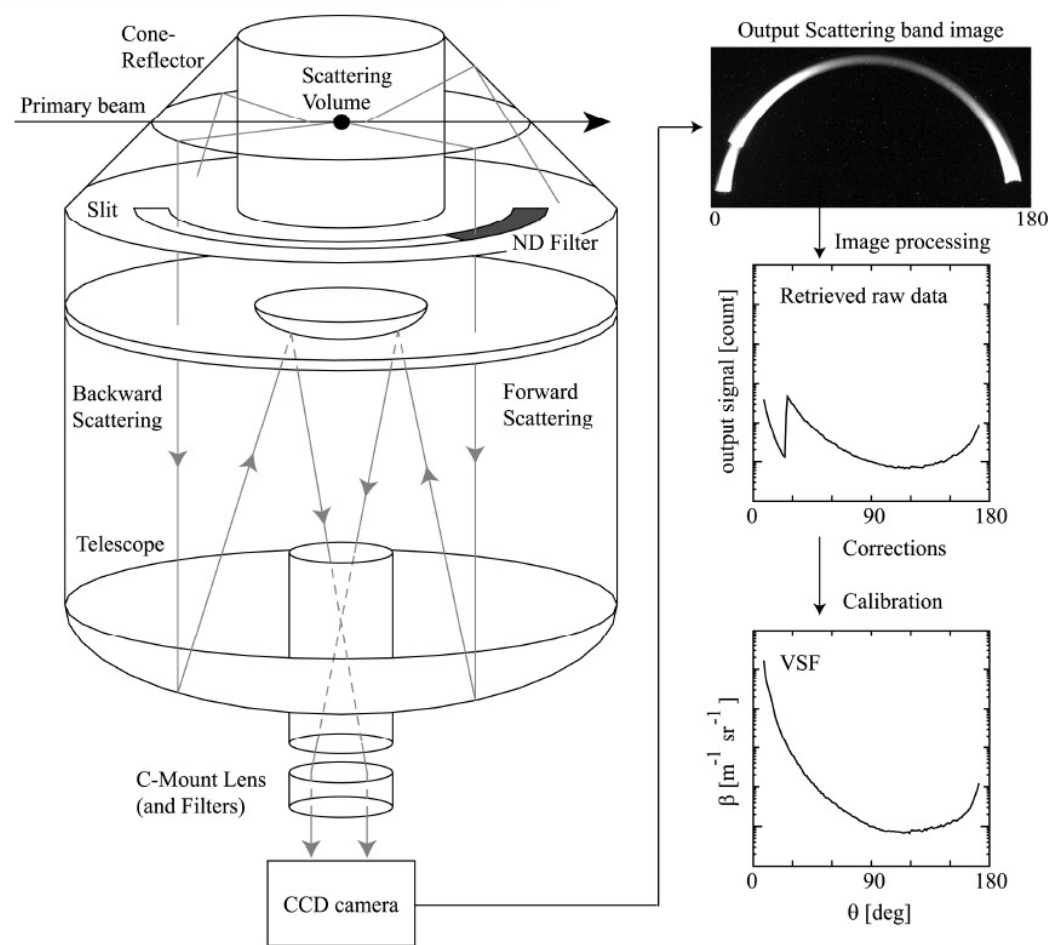
Hyperspectral  $\beta(135^\circ)$  from 430 to 700 nm





# I-VSF

## Helmholtz-Zentrum Geesthacht (HZG)

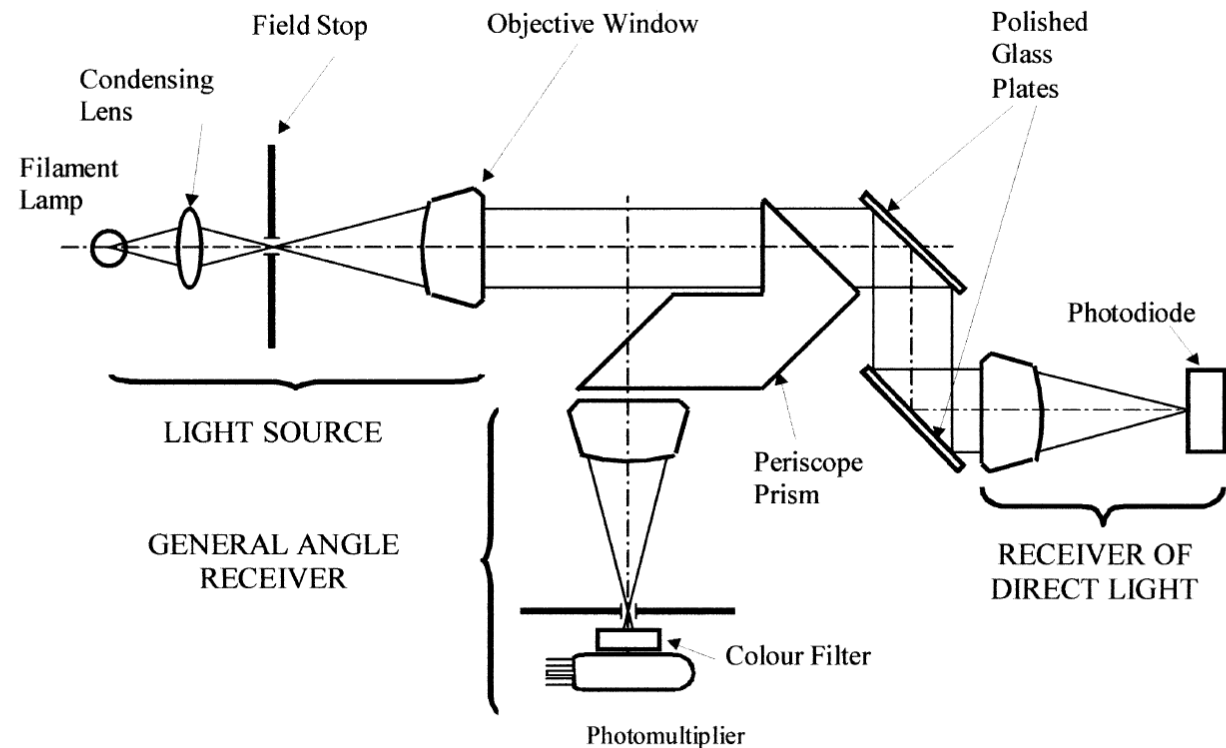


Tan et al. (2013)

# Measuring the VSF: MVSM

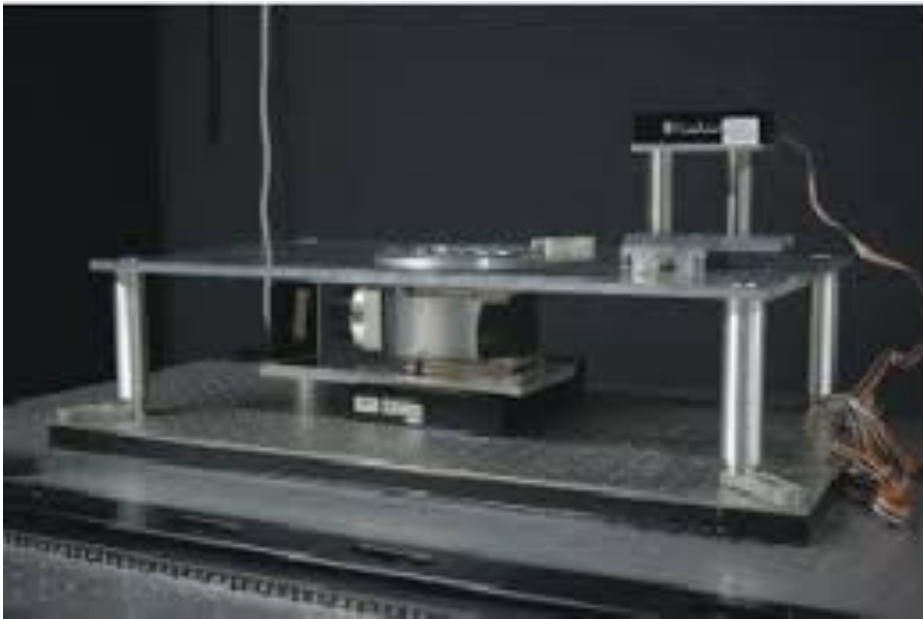
(Marine Hydrophysical Institute, Academy of Sciences of the Ukraine)

See Zhang and Gray et al. pubs

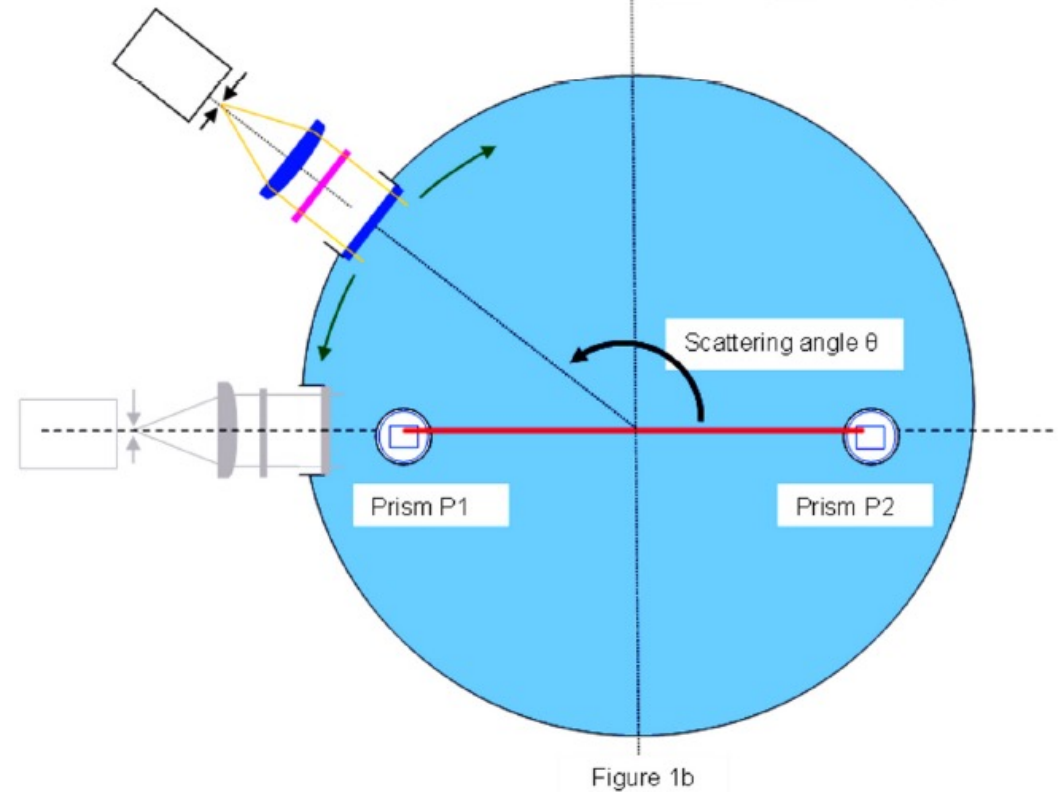
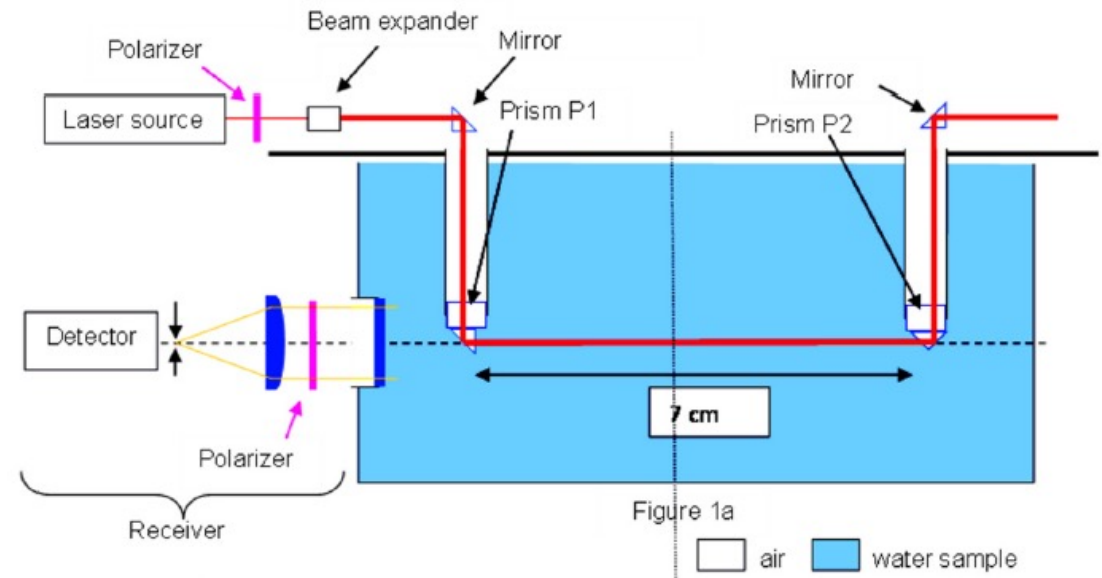


Lee and Lewis (2003)

# POLVSM (LOV)

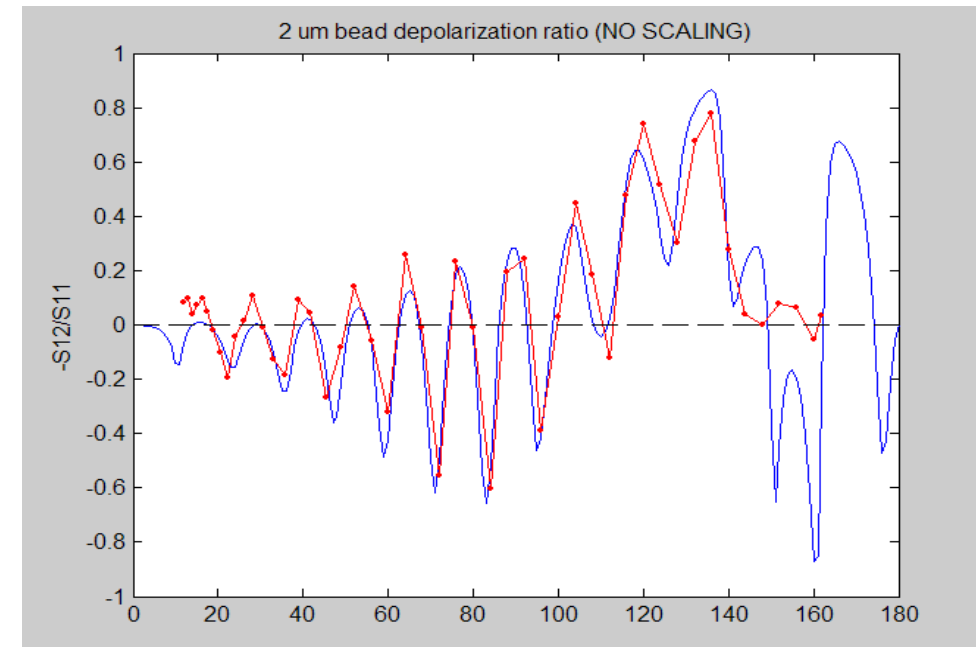
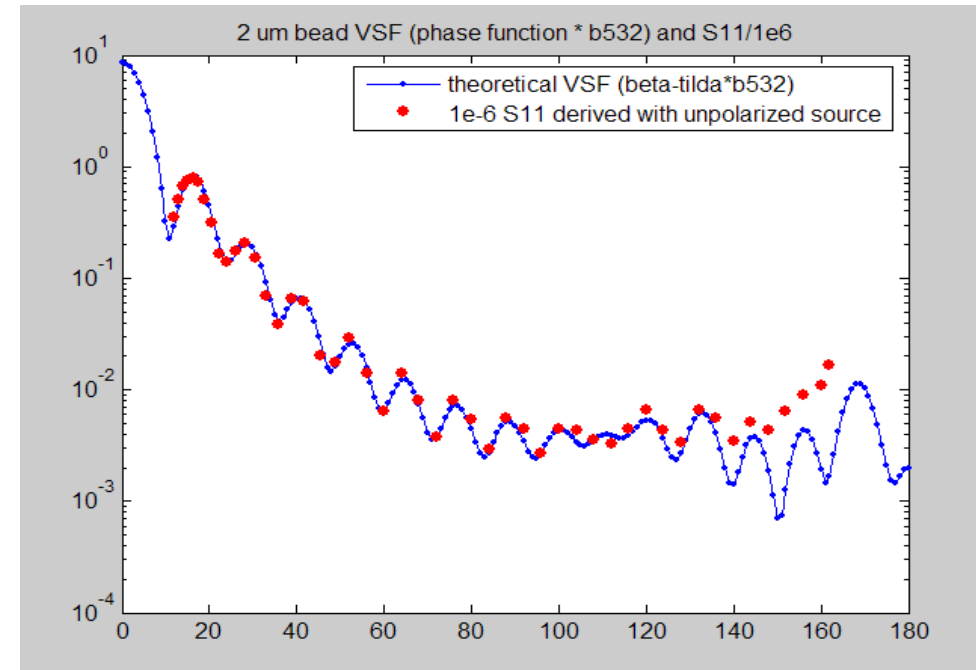


Chami et al. (2014)  
Harmel et al. (2015)

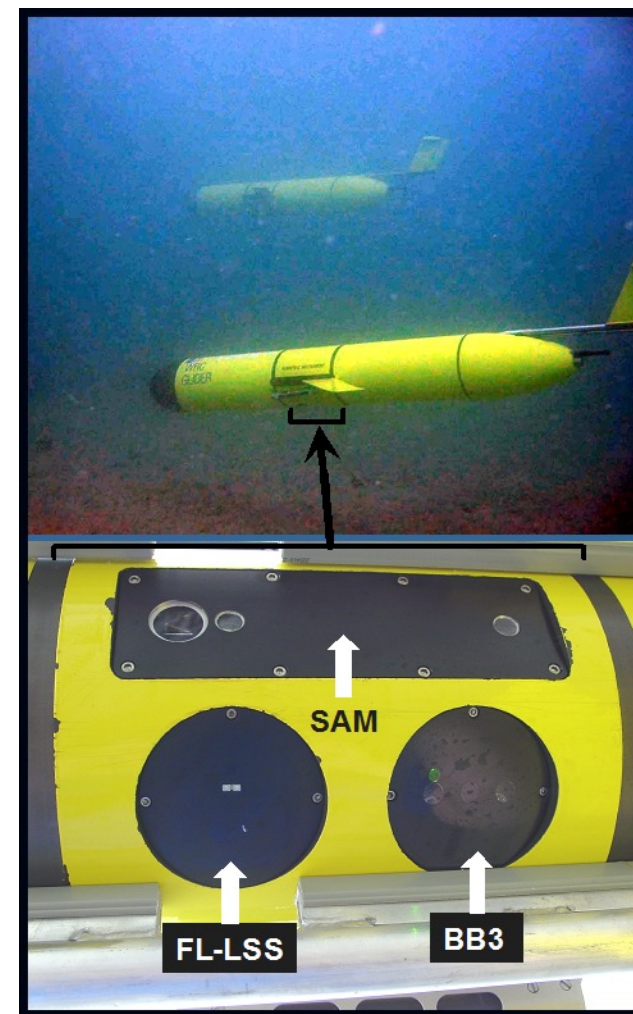
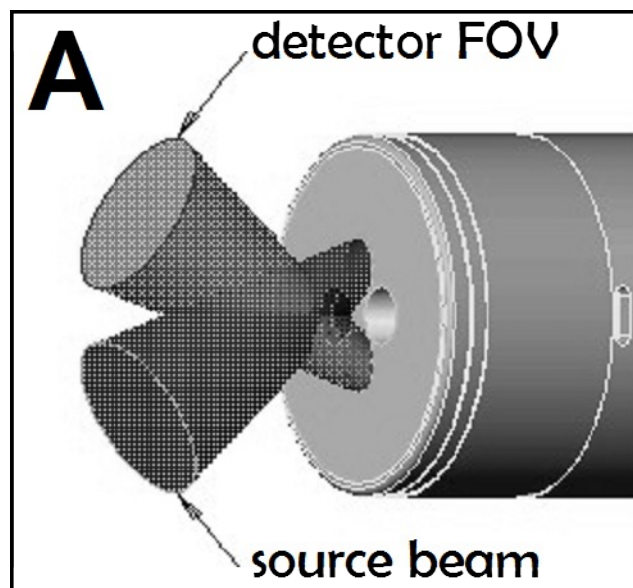




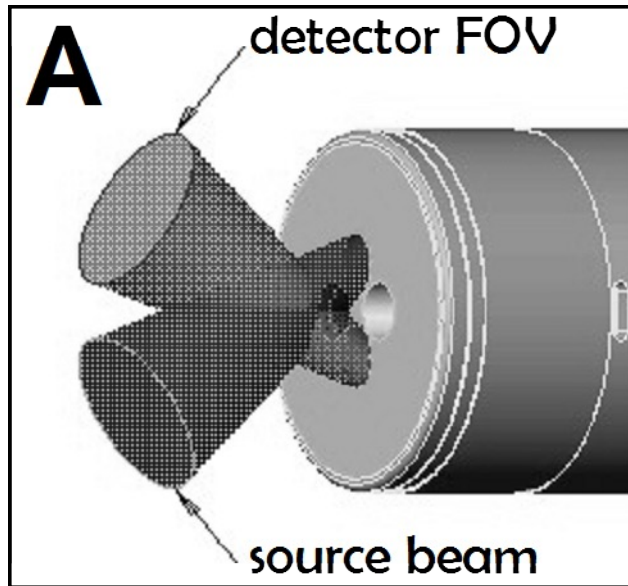
# BI-200 Goniometer (Brookhaven)



# WET Labs (SeaBird) ECOs



# IMO-SC6



6 wavelengths, centroid angle  $\sim 120$  deg

**Huge dynamic range – best choice for very turbid waters**

# Obtaining backscattering coefficients with $\beta$ at limited $\theta$

With a single  $\beta(\theta)$  in the backward hemisphere

$$b_{bp} = \chi(\theta)2\pi\beta_p(\theta)$$

Past discussion over which  $\theta$  and which  $\chi$  are best:

- Oishi (1990): **120°**
- Maffione and Dana (1997): **140 °**
- Boss and Pegau (2001): **117 °**
- Sullivan and Twardowski (2009): **118 °**



But all  $\beta$  measurements are made over an angular range

For most accurate current protocols, see Sullivan et al. (2013)



# What is “Turbidity” ? “NTUs”?

- Typically a measurement of scattering  $\sim 90^\circ$  but many sensors use angles  $> 90^\circ$
- Spectral characteristics vary (“white light,” 880 nm, etc.)
- Angular weighting ( $\Delta\theta$ ) varies
- Calibrated to formazin particles (phase function looks nothing like that of the real ocean)

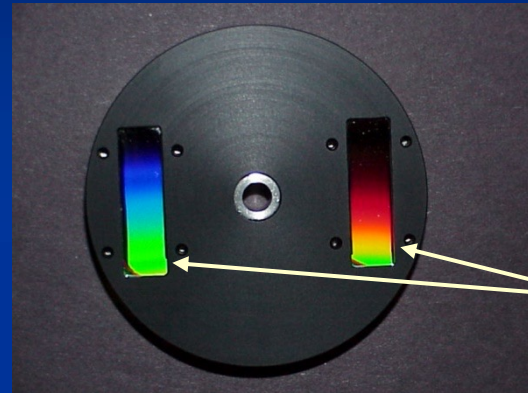
## So what does this mean?

- Every turbidity measurement, and NTU, is different!
- Turbidity is generally not a rigorous optical property
- Turbidity is not “water clarity” ( $c$  is best for estimating this).
- Signal may be correlated with backscattering.

# Measuring total scattering ( $b$ )

Typically derived from  $a$  and  $c$ : WET Labs ac-9 and ac-s

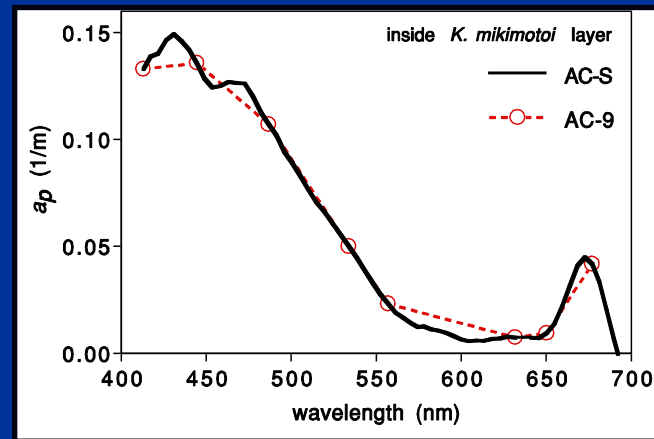
ac-s



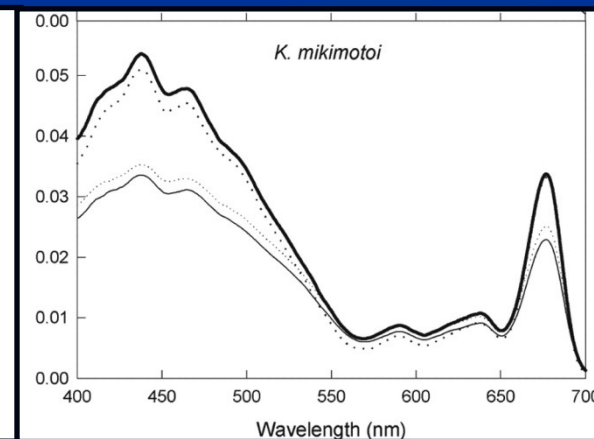
filter wheel

ac-9 has 9 individual interference filters

Linear Variable Filters (LVFs)

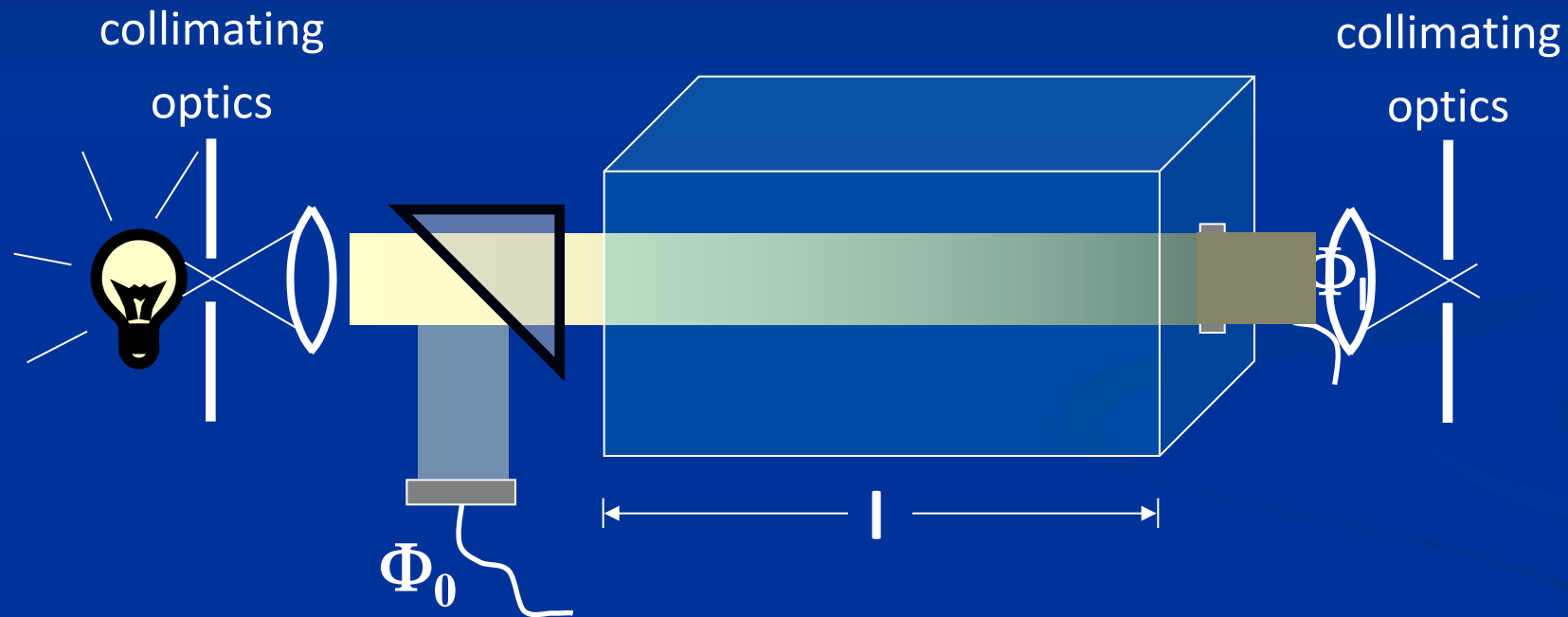


Sullivan and Donaghay (2004)  
Irish fjord



Stahr and Cullen (2003)  
In culture

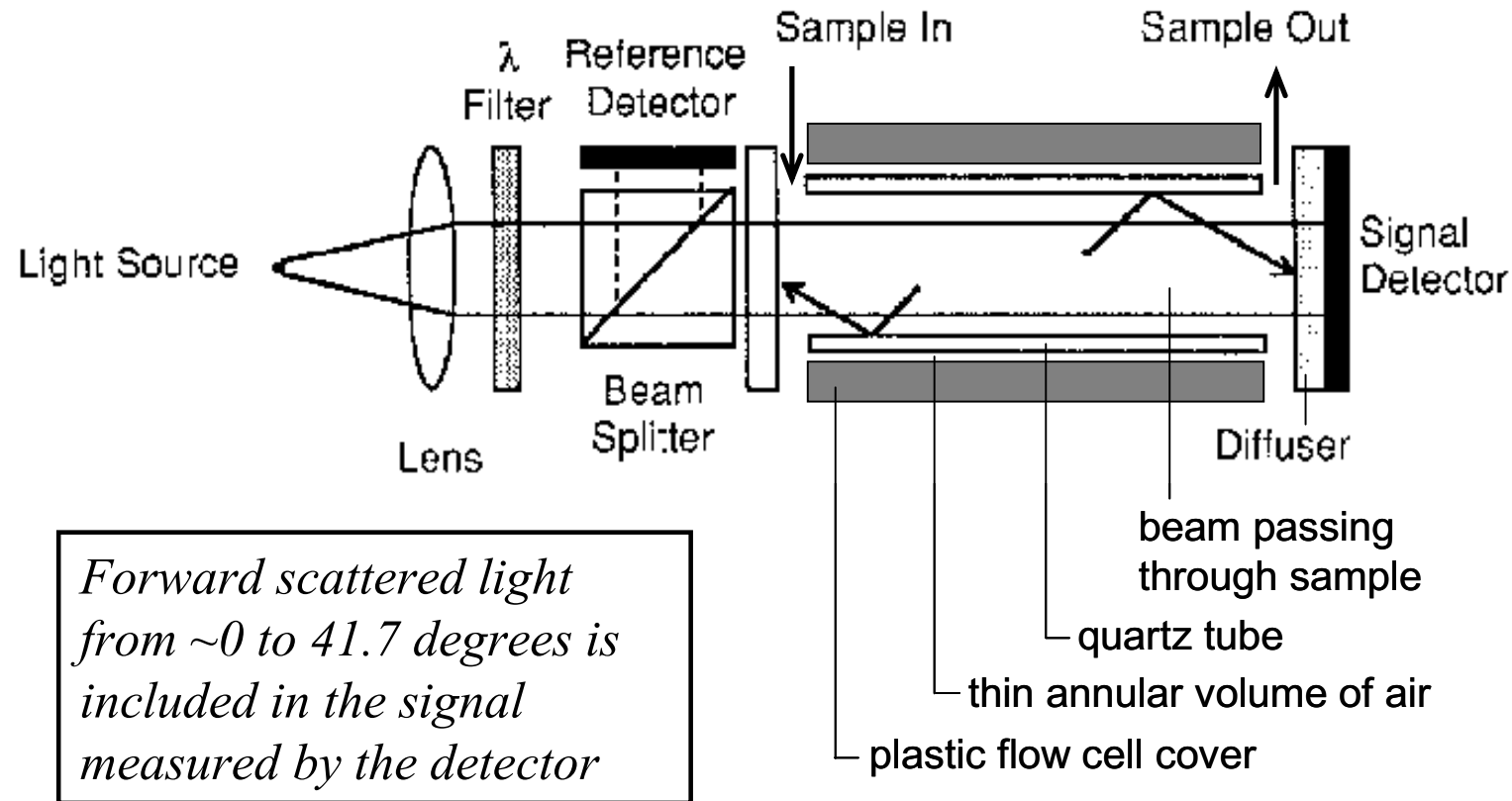
# Anatomy of a beam attenuation meter (transmissometer)



Problem: some scattered light also reaching detector  
The theoretically ideal attenuation meter has an acceptance angle of  $\sim 0^\circ$  but at  $0^\circ$  no light is received – need to compromise

*\*\*Optimal accuracy reached when  $l \sim 1/c$*

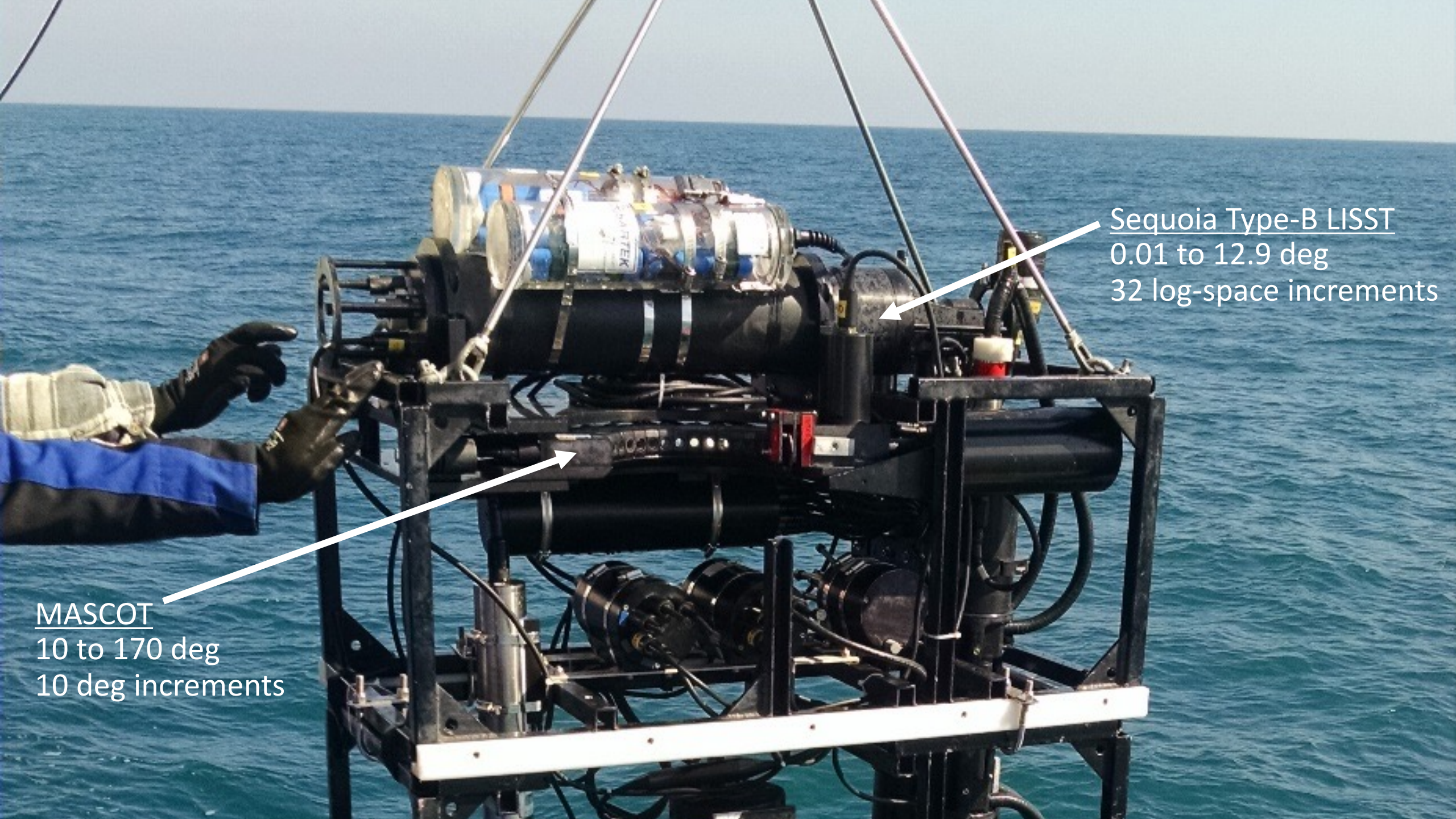
# Reflective tube method for absorption



Light scattered at angles  $> 41.7$  deg is not measured by detector and requires correction....

from Zaneveld et al. (1992)



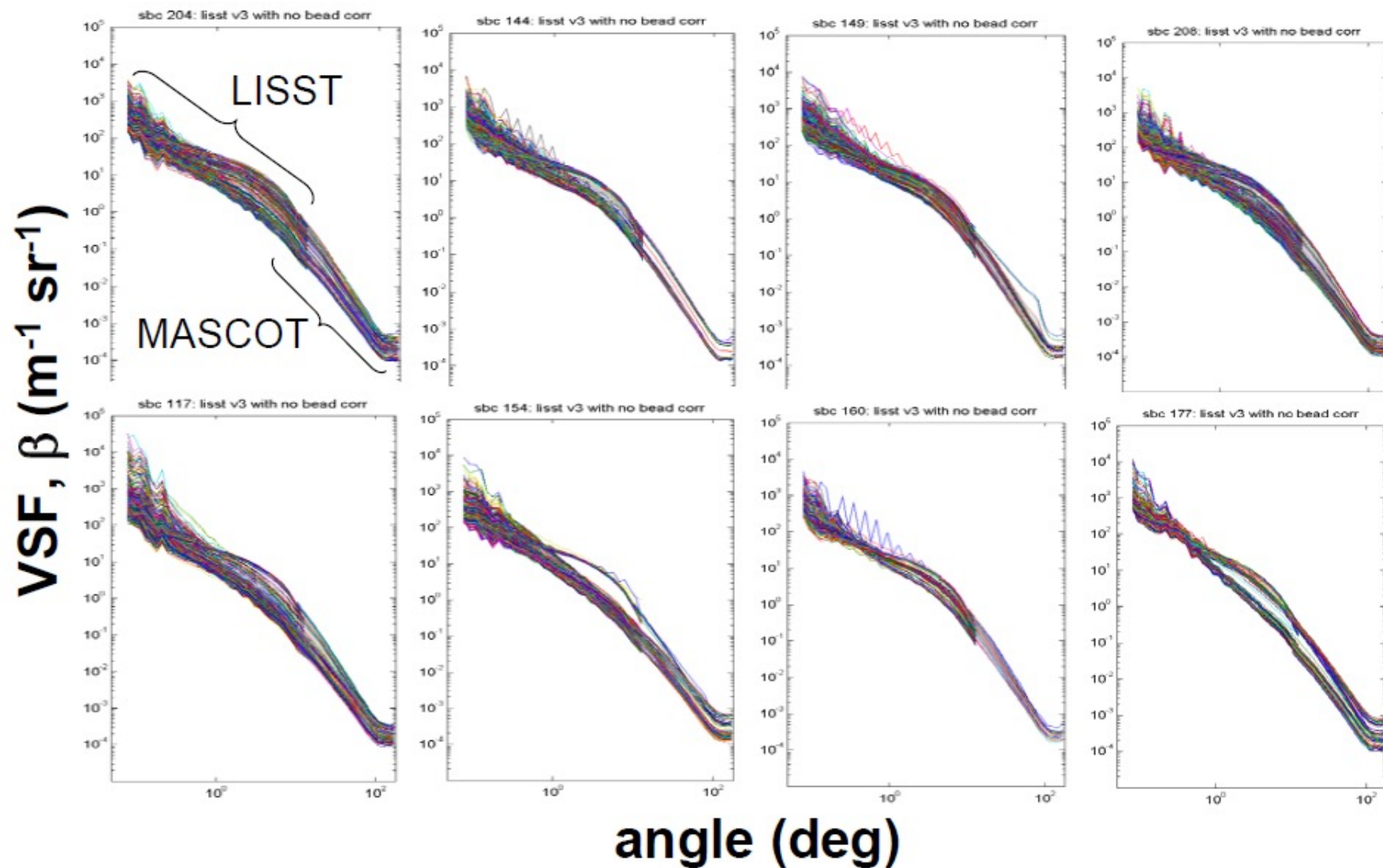


Sequoia Type-B LISST  
0.01 to 12.9 deg  
32 log-space increments

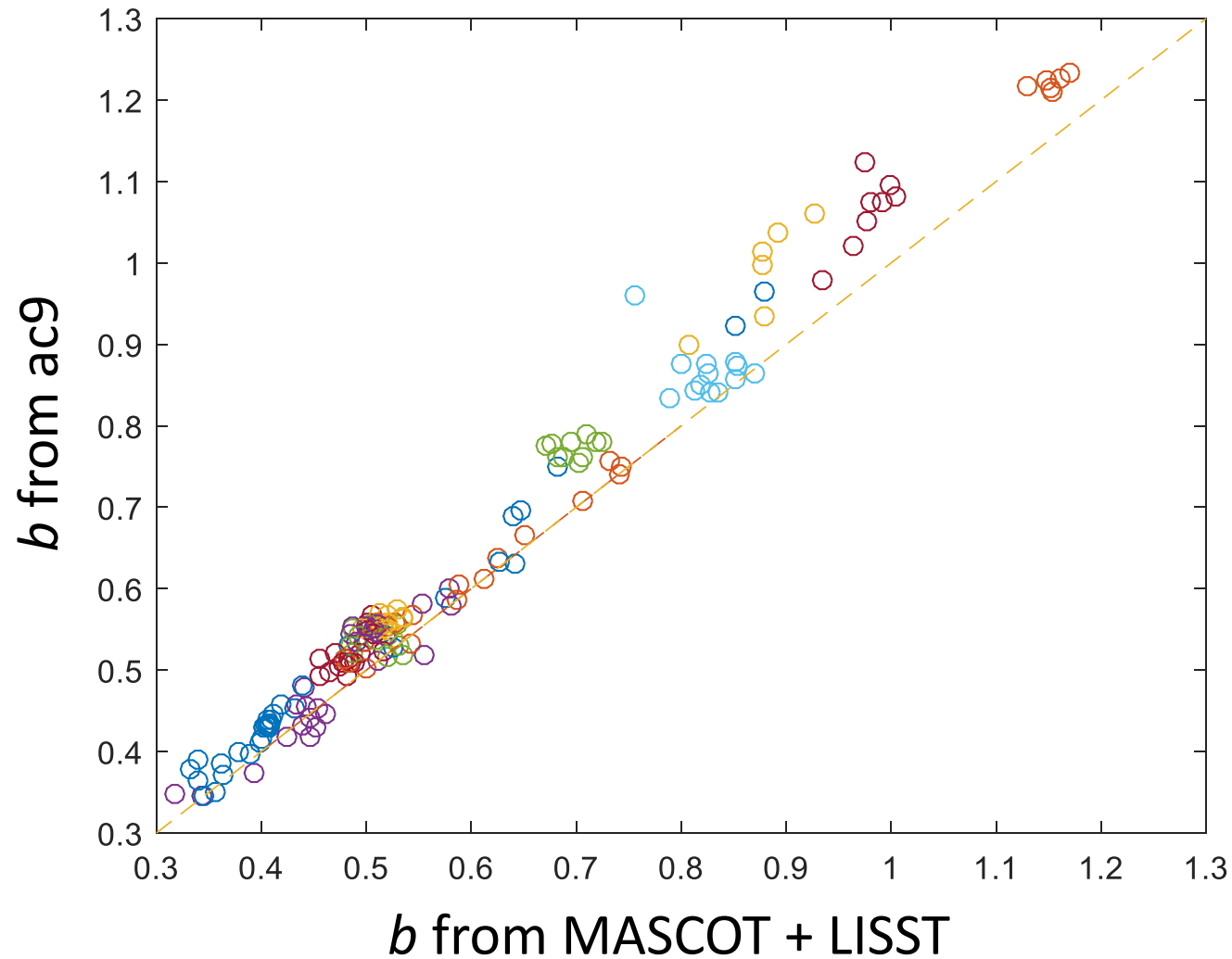
MASCOT  
10 to 170 deg  
10 deg increments



# VSF profile data

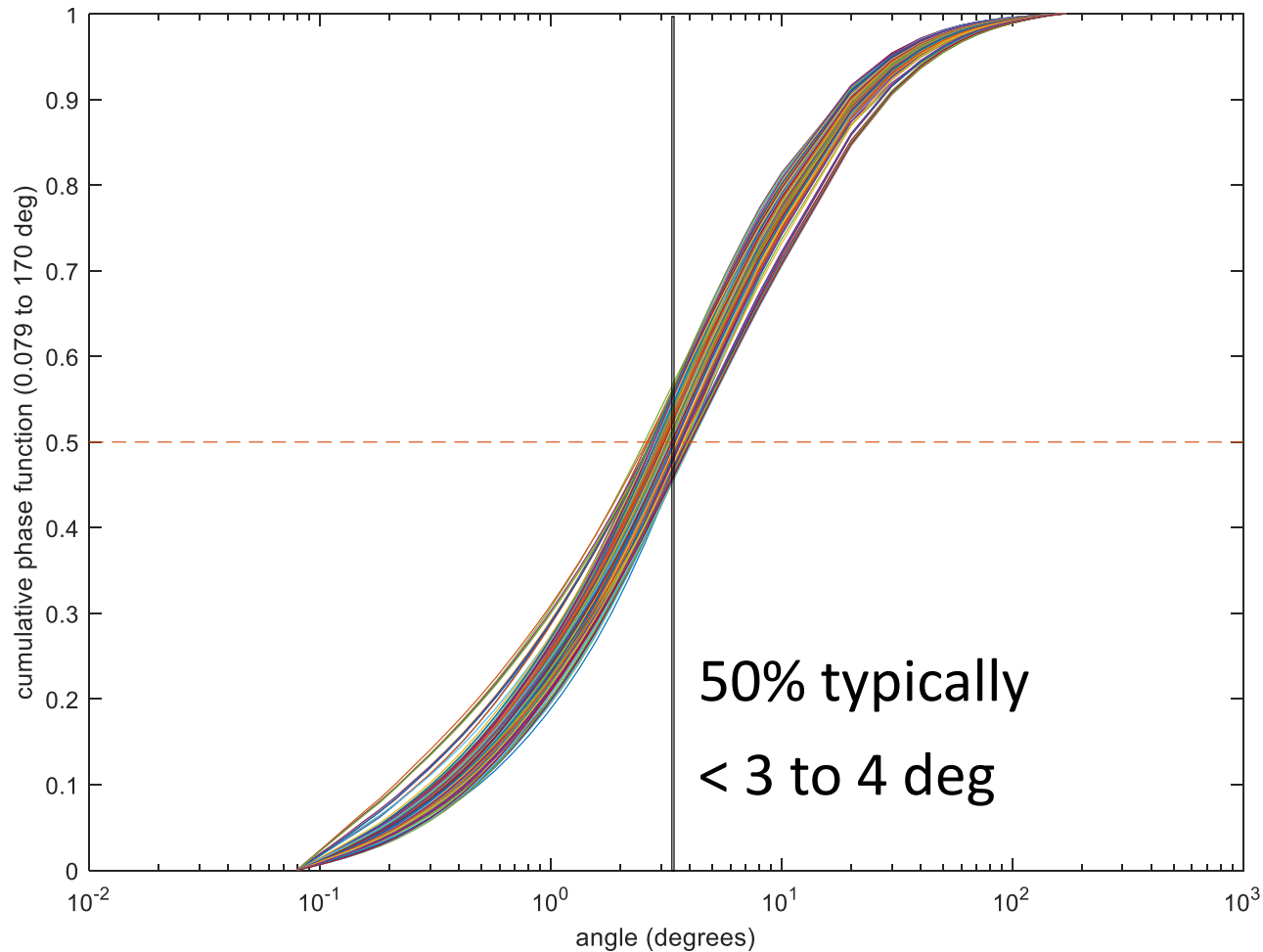


# Integrating the VSF: testing closure between sensors



$$b_{ac9} = 2\pi \int_{0.93}^{180} \sin(\theta) \beta(\theta) d\theta$$

# Cumulative scattering contribution

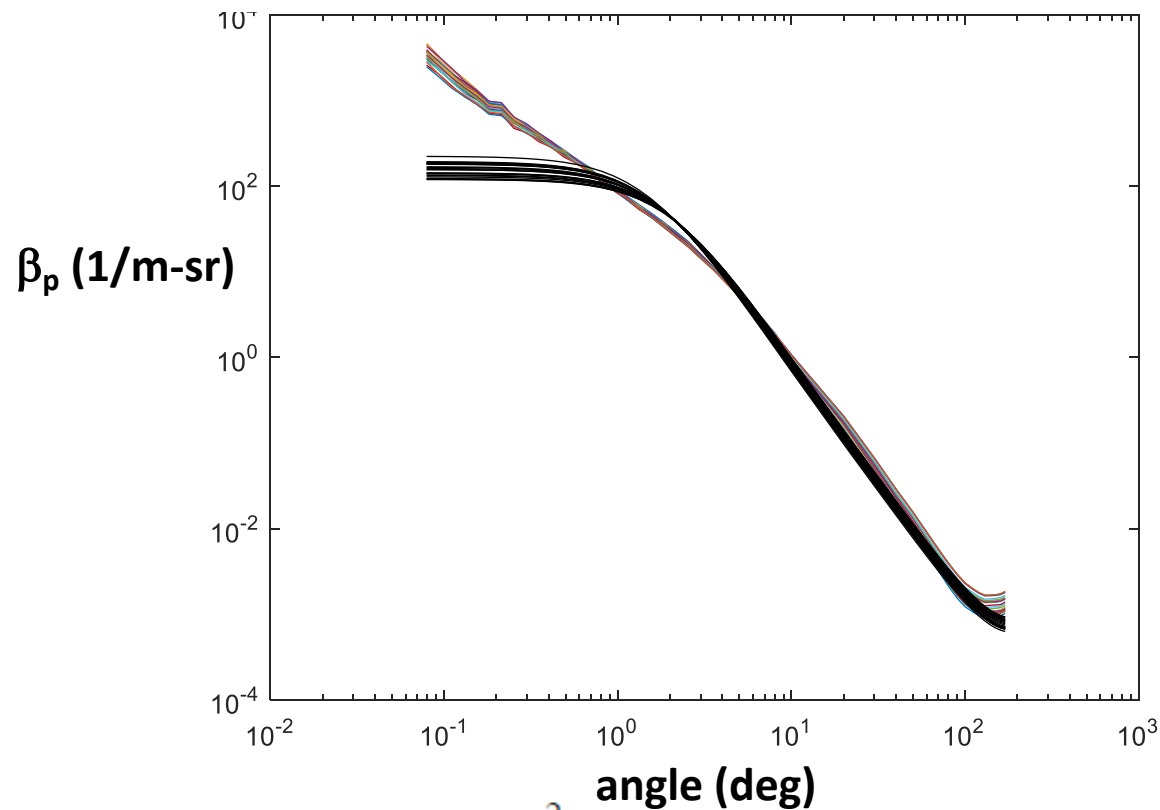


$$b_x = \frac{2\pi \int_i^j \sin(\theta) \beta(\theta) d\theta}{b}$$

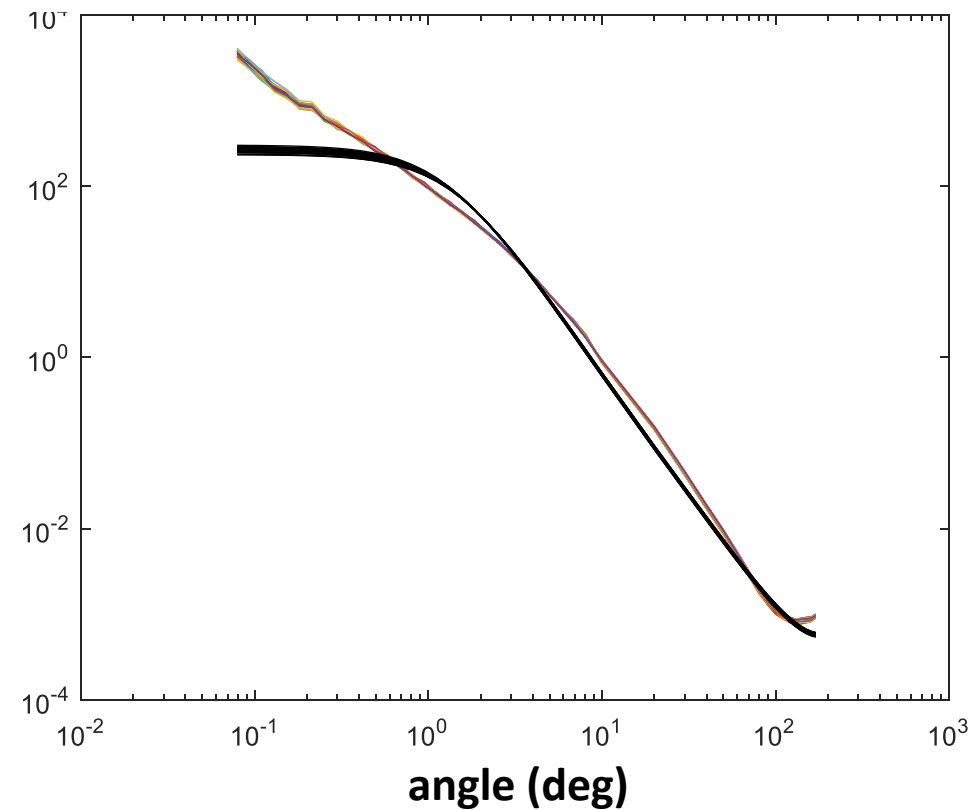


Analytical models of the VSF

# Analytical modeling: fitted Kattawar-Haltrin 2-term, 1-parameter Henyey-Greenstein



$$p_{HG}(\mu, g) = \frac{1 - g^2}{(1 - 2g\mu + g^2)^{3/2}}, \quad \mu = \cos \vartheta,$$



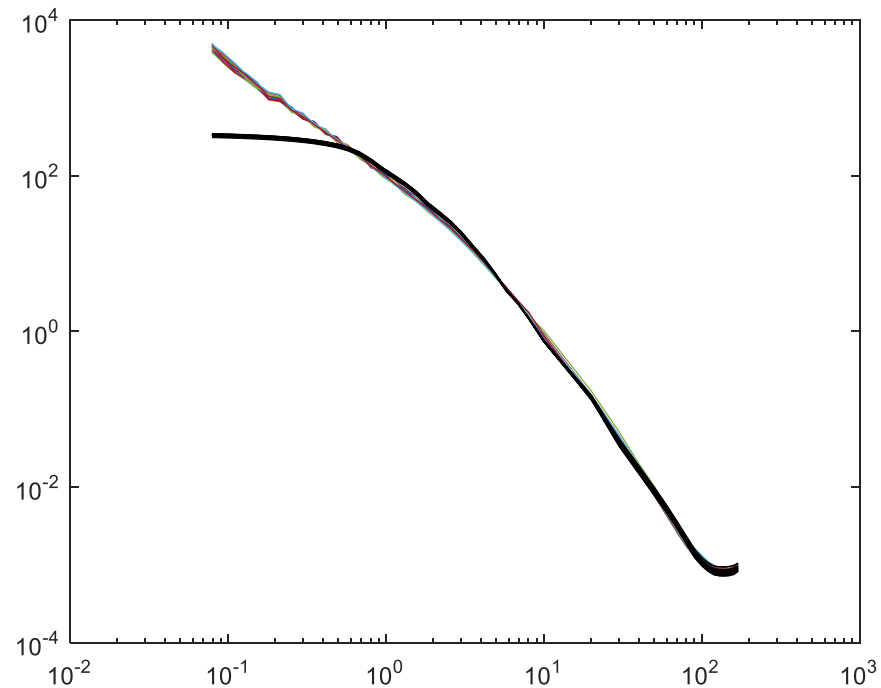
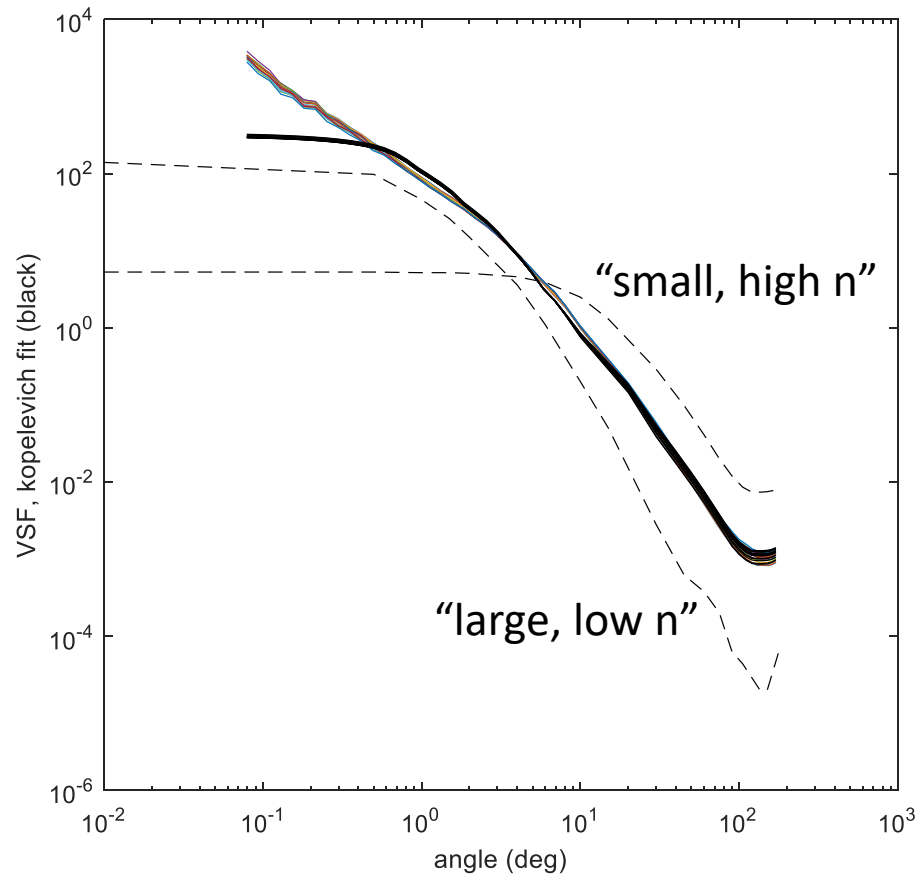
$$p_{TTHG}(\mu, \alpha, g, h) = \alpha p_{HG}(\mu, g) + (1 - \alpha) p_{HG}(\mu, -h)$$

$h(g)$  and  $\alpha(g)$

$0 \leq \alpha, g, h \leq 1.$

# Analytical modeling: fitted Kopelevich

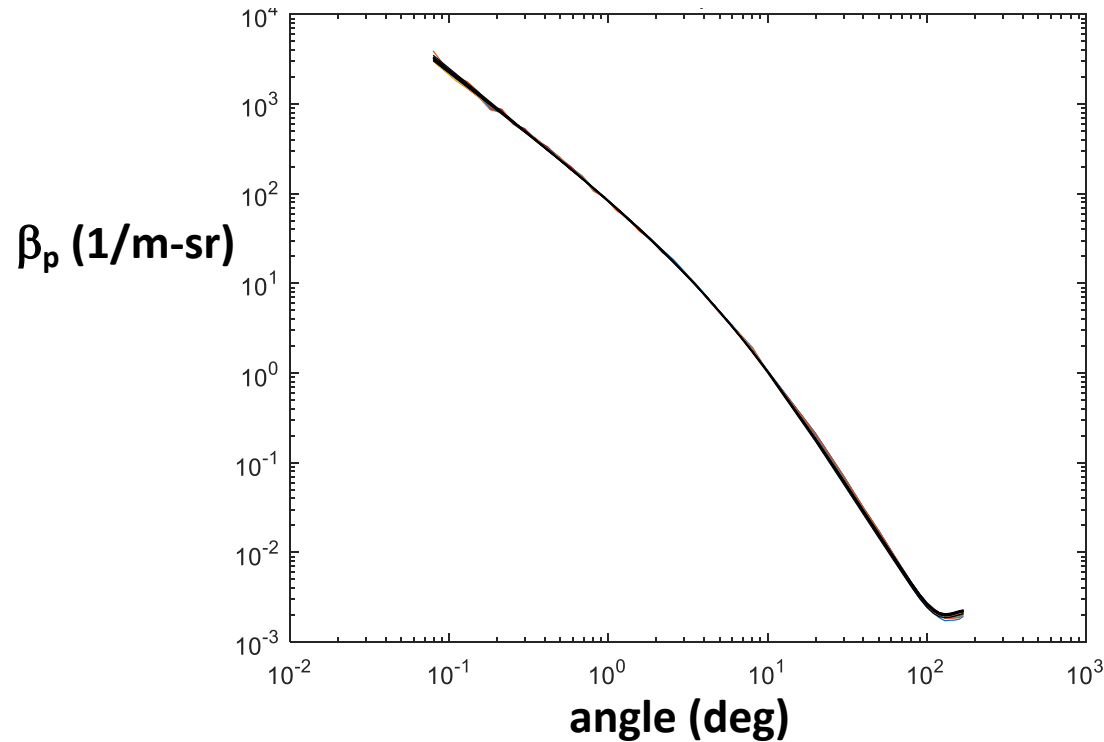
Fit 2 basis vectors recommended by Kopelevich (1983)



good results  $> \sim 0.6$  deg  
(as noted by Berthon et al. 2007)

# Analytical modeling: fitted Fournier-Forand (1994, 1999)

see Jonasz and Fournier (2007, with erratum)



$$\tilde{\beta}(\theta) = \frac{1}{4\pi} \frac{1}{(1-\delta)^2 \delta^v} \left( [v(1-\delta) - (1-\delta^v)] + \frac{4}{u^2} [\delta(1-\delta^v) - v(1-\delta)] \right)$$

$$v = \frac{3-\mu}{2} \quad , \quad \delta = \frac{u^2}{3(n-1)^2} \quad , \quad u = 2 \sin(\theta / 2)$$

INPUTS:

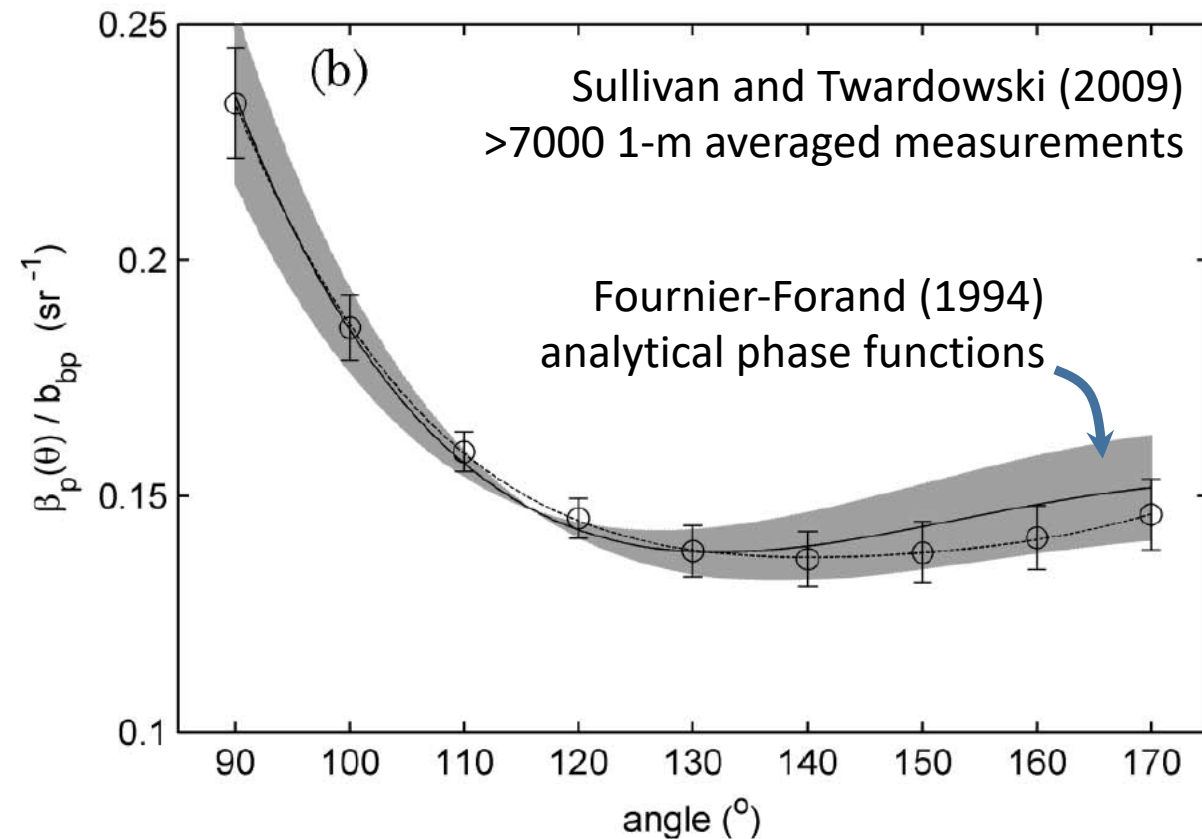
$\mu$  = power law slope for particle size distribution

$n$  = relative refractive index of particles

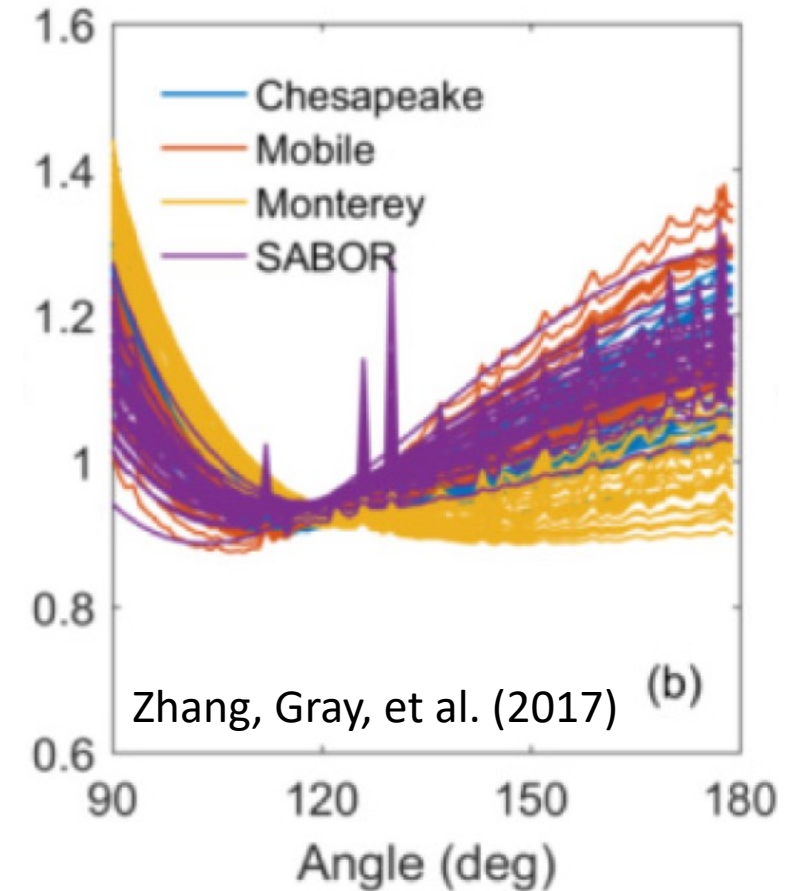
Excellent fits for entire angular range (0.079 to 180 deg)



# Backward phase function (i.e., backward VSF shape)



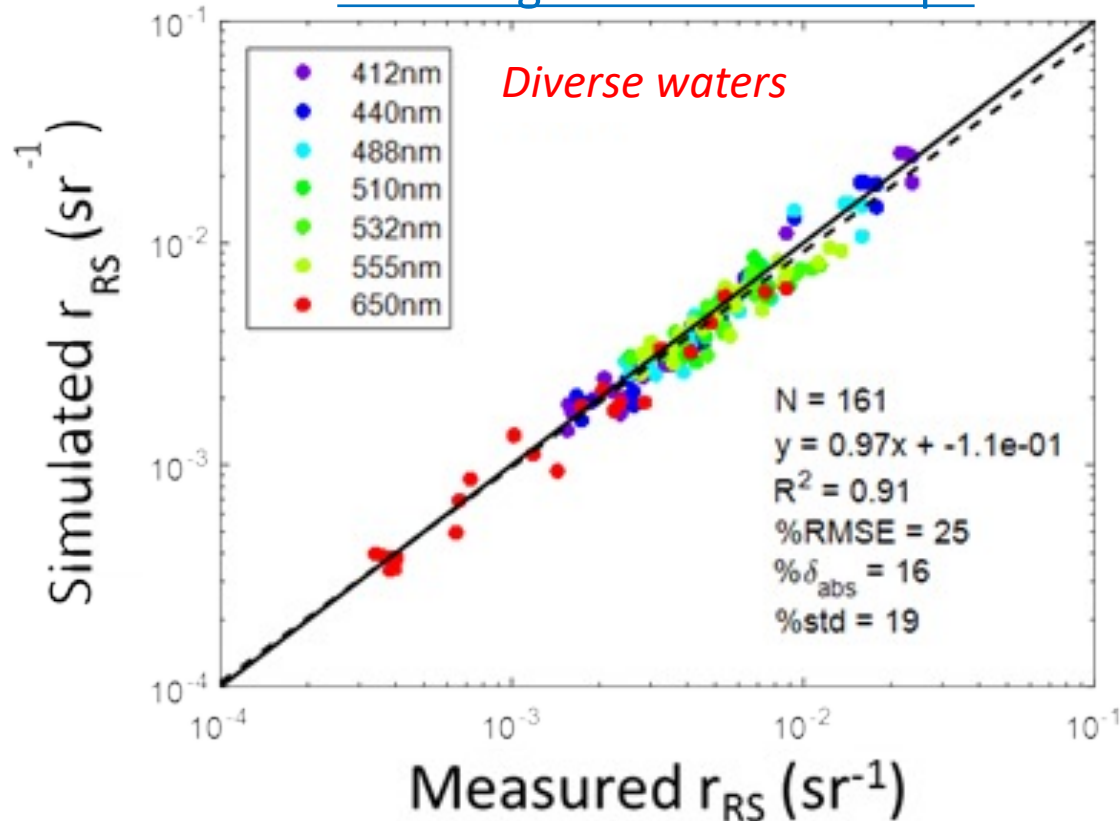
Remarkably consistent shape...  
Important implications for ocean color remote sensing



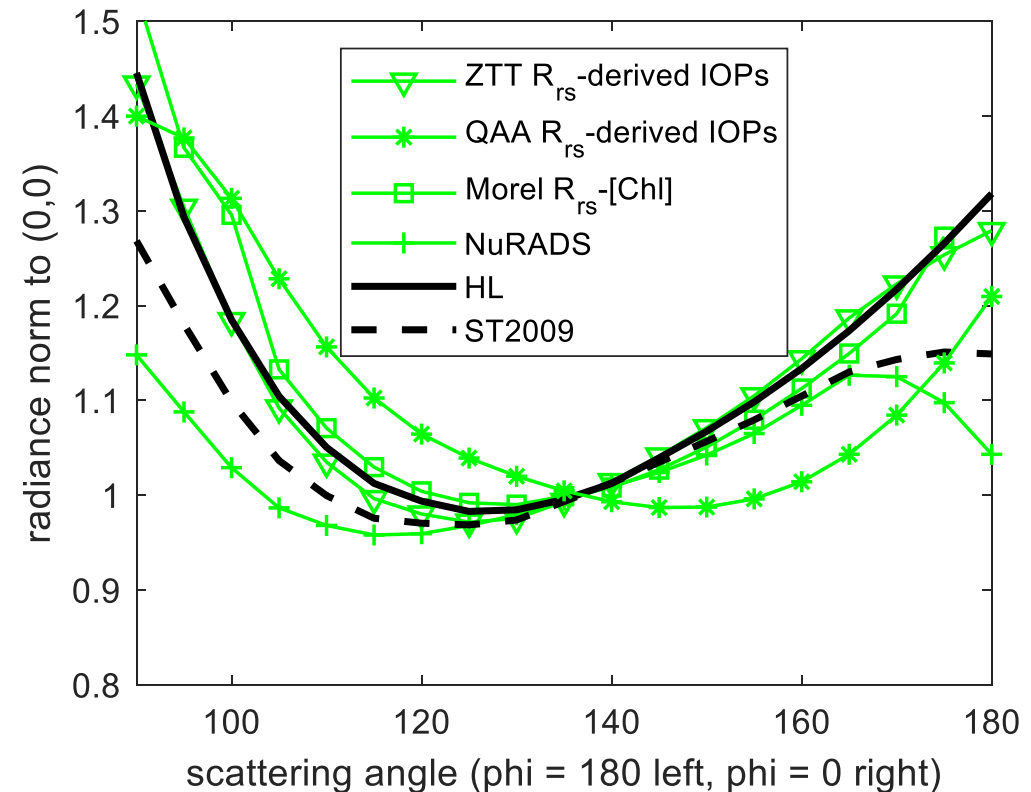
However, some inconsistency  
in current literature...

# Constant backward VSF shape appears realistic...

Radiative transfer simulations  
assuming constant VSF shape



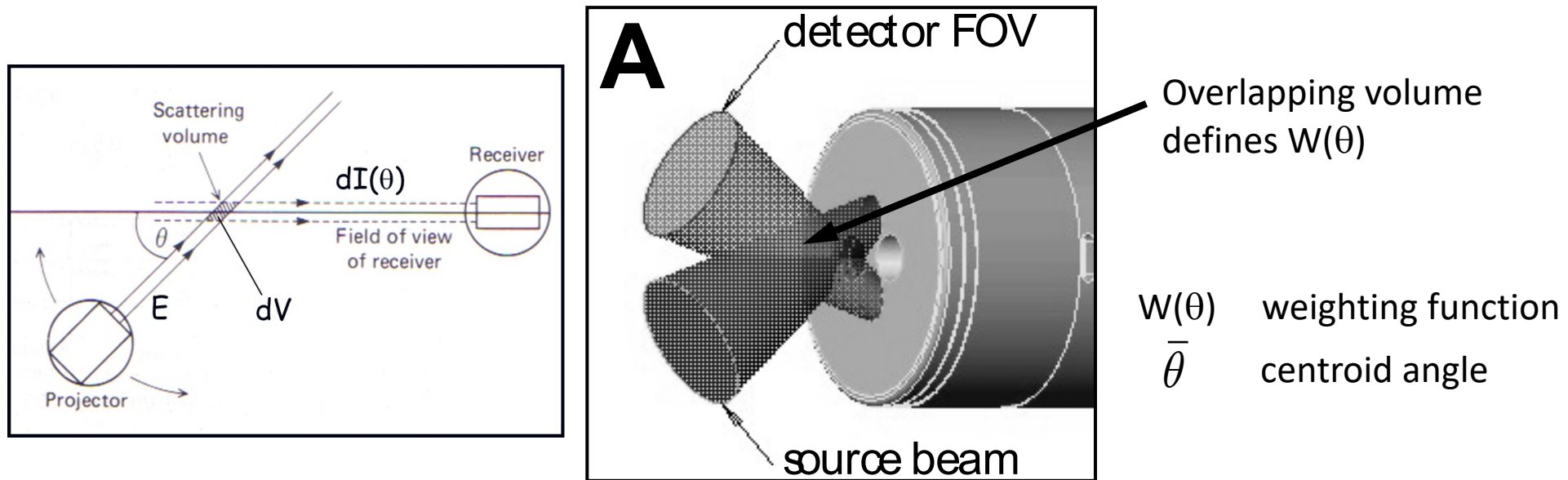
Bidirectional Reflectance Distribution Function  
assuming constant VSF shape



Results are equivalent or better to simulations using measured VSFs

# VSF measurement and calibration

$\beta(\theta)$  measurements are always resolved over a range of angles



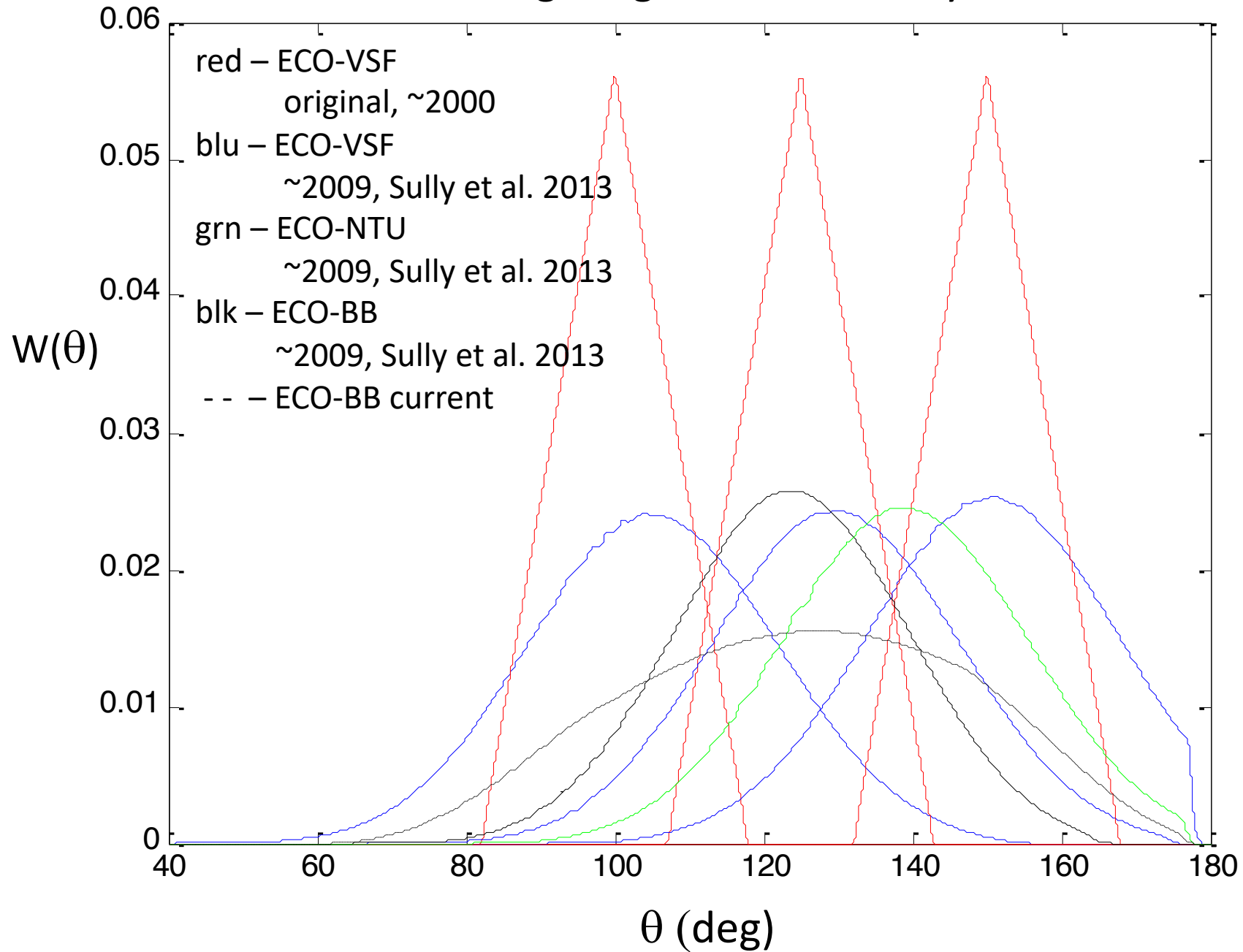
$$\bar{\beta}(\bar{\theta}, \Delta\theta) = \int_0^\pi \beta(\theta) W(\theta) d\theta$$

*See Sullivan et al. (2013) for detailed calibration methodology*





# ECO weighting function history



# Primary scattering components in water

- Pure seawater (molecular)
- Turbulence (i.e., refractive index discontinuities)
- Particles
- Bubbles

# Scattering by pure seawater

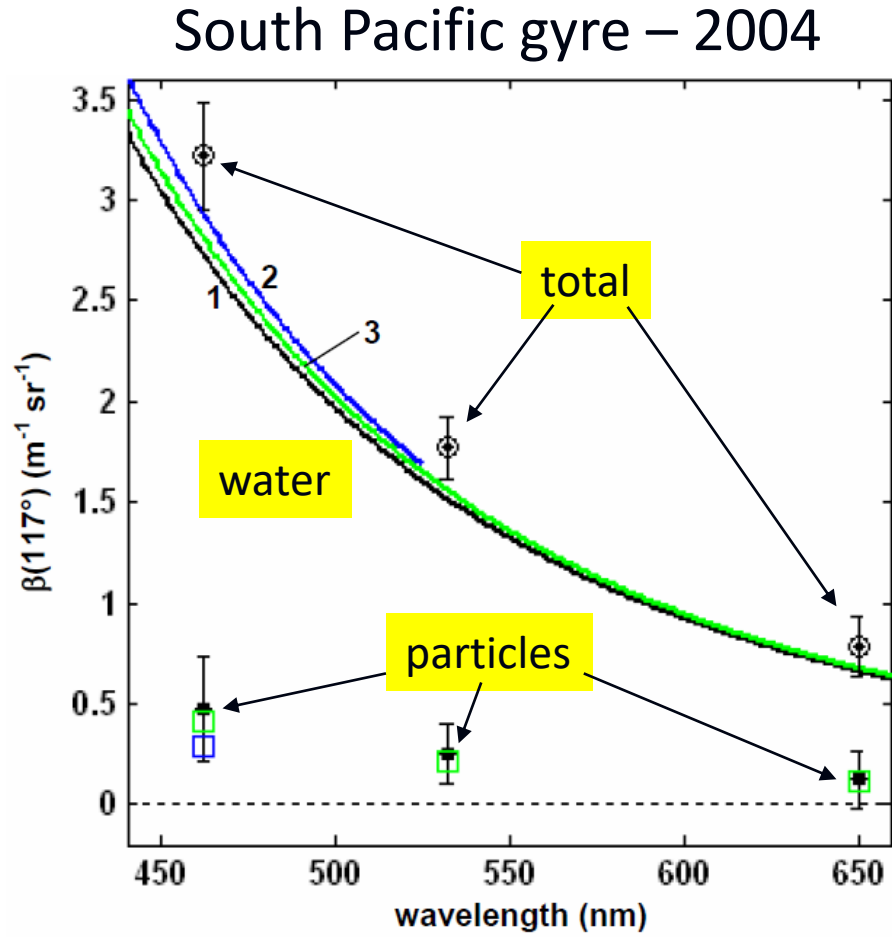
Zhang and Hu (2009); Zhang et al. (2009); Zhang et al. (2019)

Review: Zhang (2012)

- Uses Einstein-Smoluchowsky theory for refractive index fluctuations with updated constants
- The depolarization ratio used is 0.039, also after Farinato and Rowell (1974)
  - Experimentally verified in Zhang et al. (2019)
- Agrees well with experimental work of Morel (1968)

For backscattering by seawater, divide  $b_w$  by 2.

# Scattering by clearest natural waters

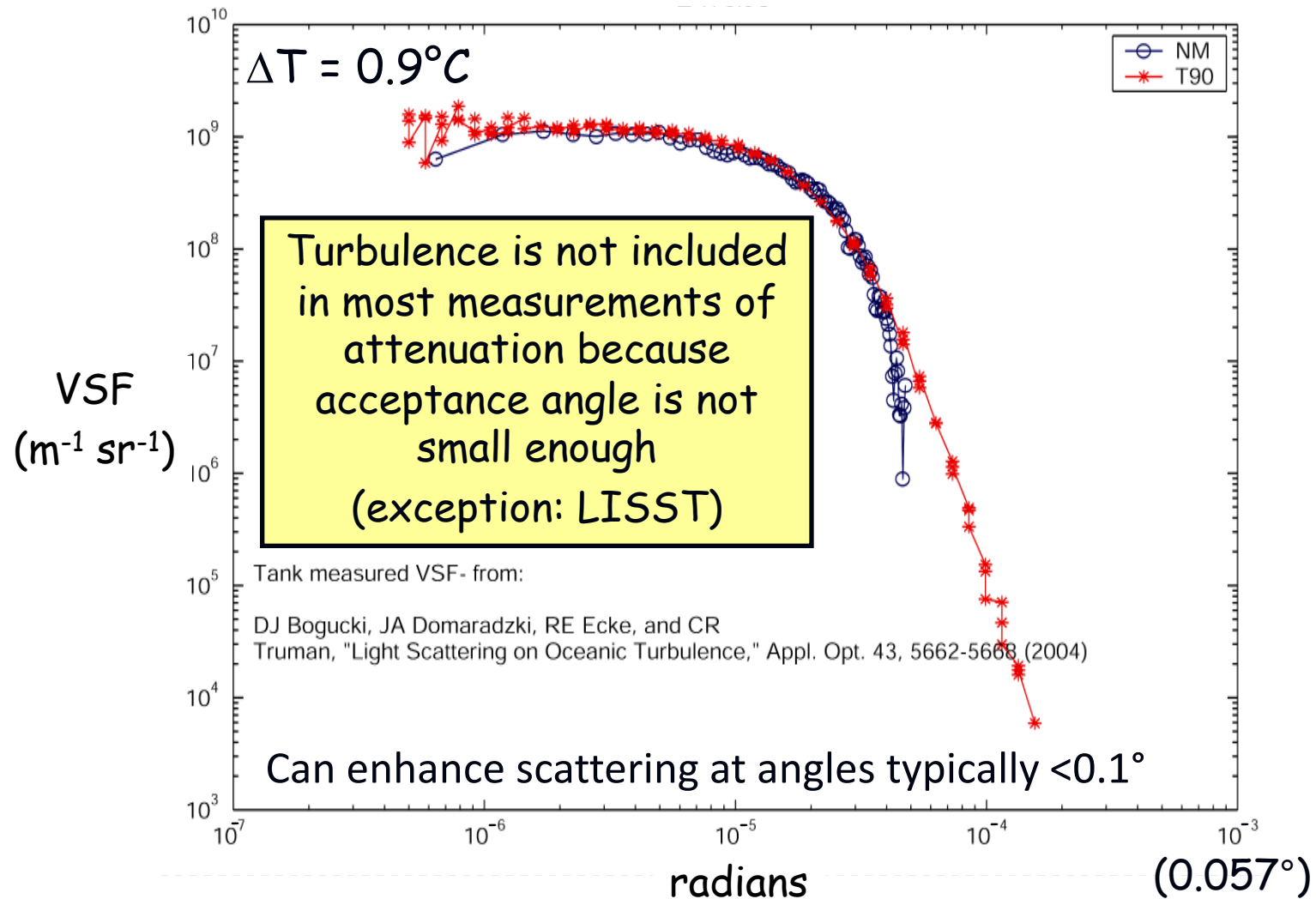


Backscattering by seawater can be 90+% of total  $b_b$  in the very clear ocean.

*Accuracy is very important if we are interested in  $b_{bp}$*

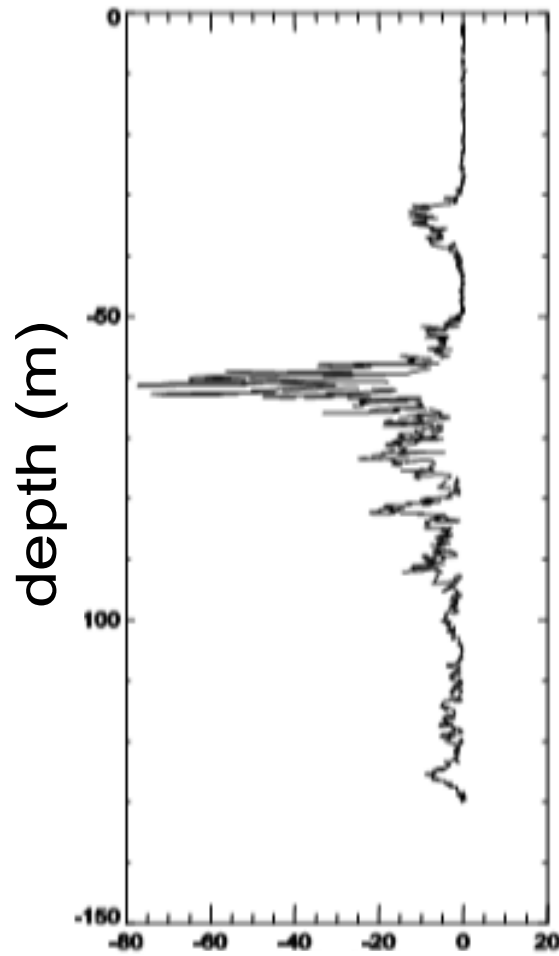
$$\lambda^{-4.28}$$

# Turbulence (refractive index discontinuities)

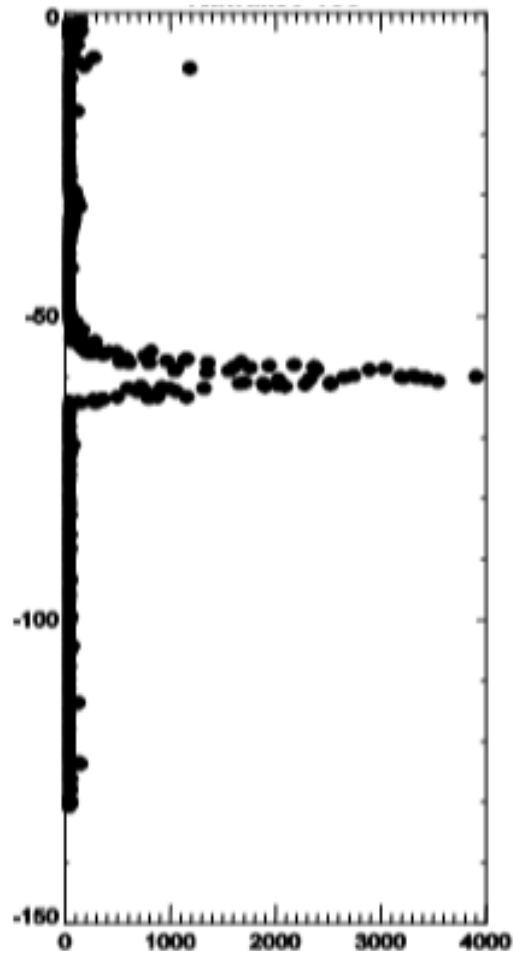




# Turbulence measurement with LISST-100X

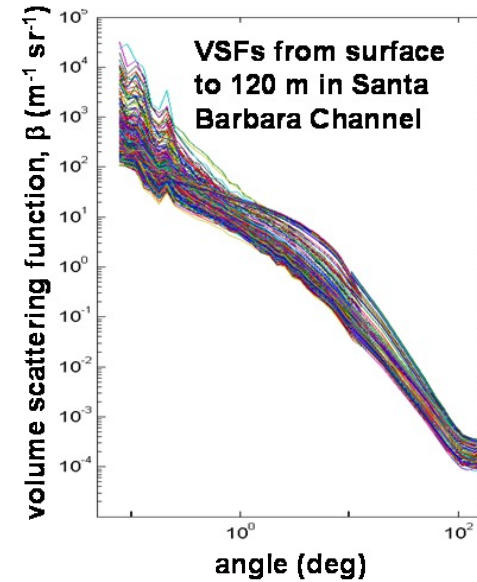
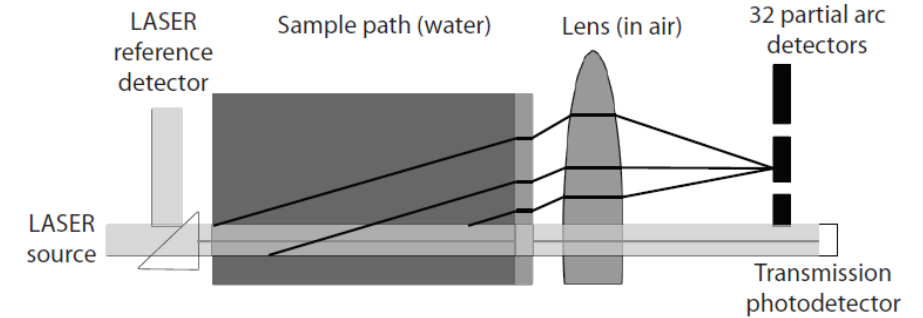


$dn/dt$   
from T&S

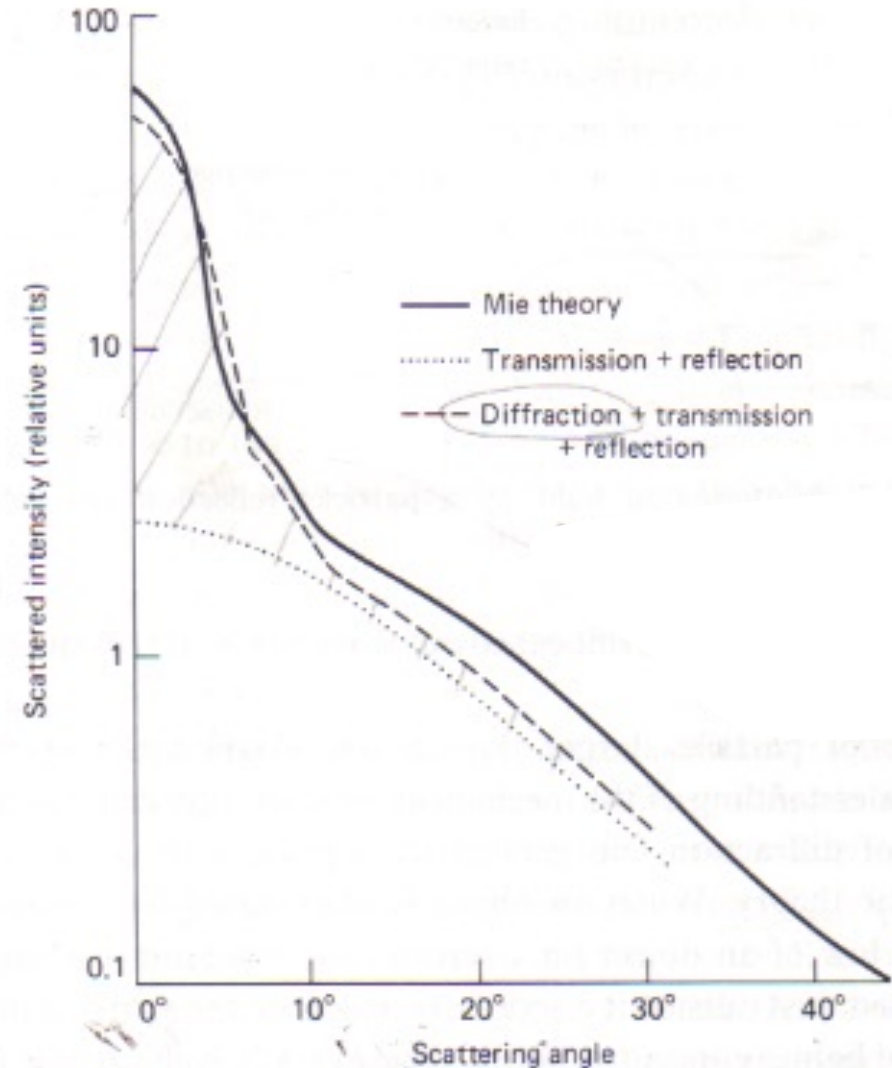
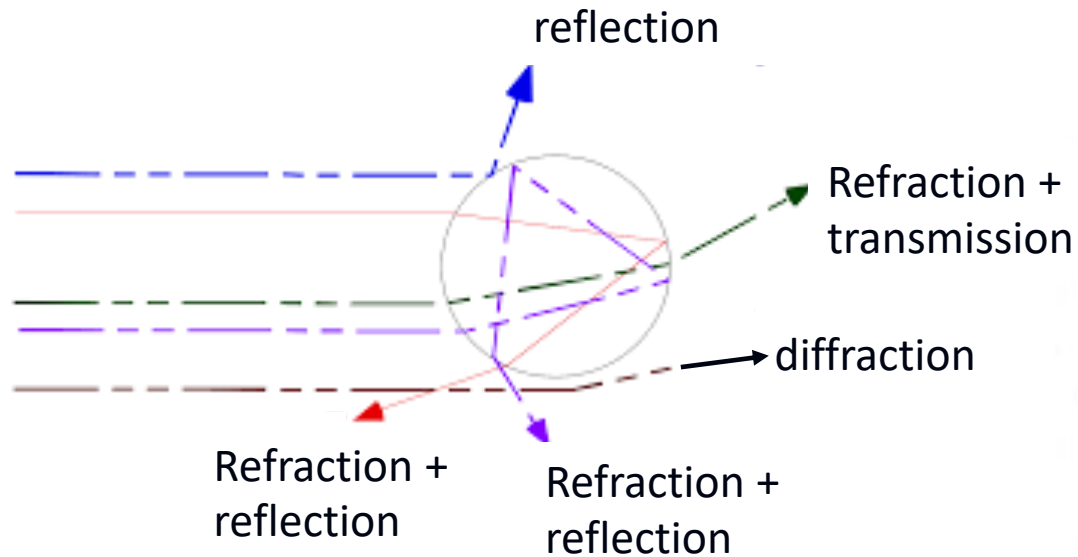


turbulence indicator  
from LISST VSF

Hawaii  
09/2009



# Particle scattering



Kirk 1994

Fig. 4.1. Angular distribution of scattered intensity from transparent spheres calculated from Mie theory (Ashley & Cobb, 1958) or on the basis of transmission and reflection, or diffraction, transmission and reflection (Hodkinson & Greenleaves, 1963). The particles have a refractive index (relative to the surrounding medium) of 1.20, and have diameters 5–12 times the wavelength of the light. After Hodkinson & Greenleaves (1963).

*“...our present-day interpretation and detailed understanding of major sources of backscattering and its variability in the ocean are uncertain and controversial.”*

Stramski, D., E. Boss, D. Bogucki, and K. J. Voss, 2004. The role of seawater constituents in light backscattering in the ocean. Progress in Oceanography, 61(1), 27-55.

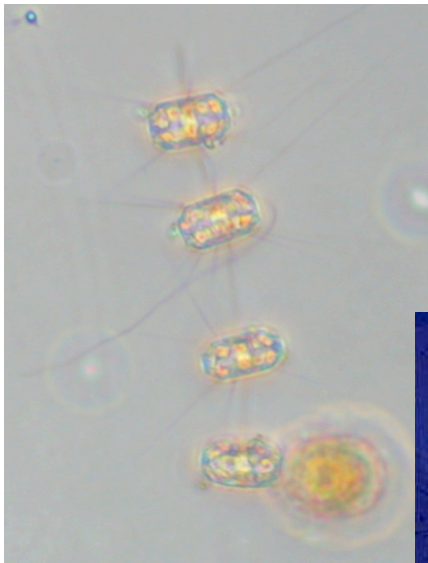
# The Enigma of Phytoplankton Backscattering...

Modeling phytoplankton as homogeneous spheres results in backscattering levels too low (only a few percent contribution) to be consistent with their influence on remote sensing reflectance ( $R_{RS}$ ).

*Stramski and Kiefer 1991; Stramski et al. 2001*

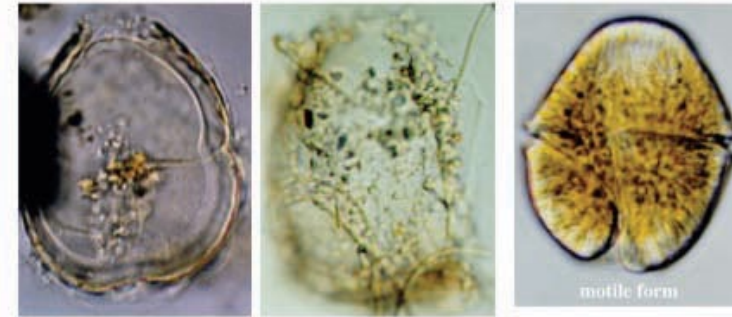
# Testing the “Complex Particle” Hypothesis

*Thalassiosira weissflogii*



~25  $\mu\text{m}$  diameter

*Gyrodinium instriatum*



photomicrographs by K. Matsuoka and Y. Fukuyo

~50 mm diameter



*Chaetoceros socialis*

~10  $\mu\text{m}$  cell diameter  
Up to 1 mm colonies

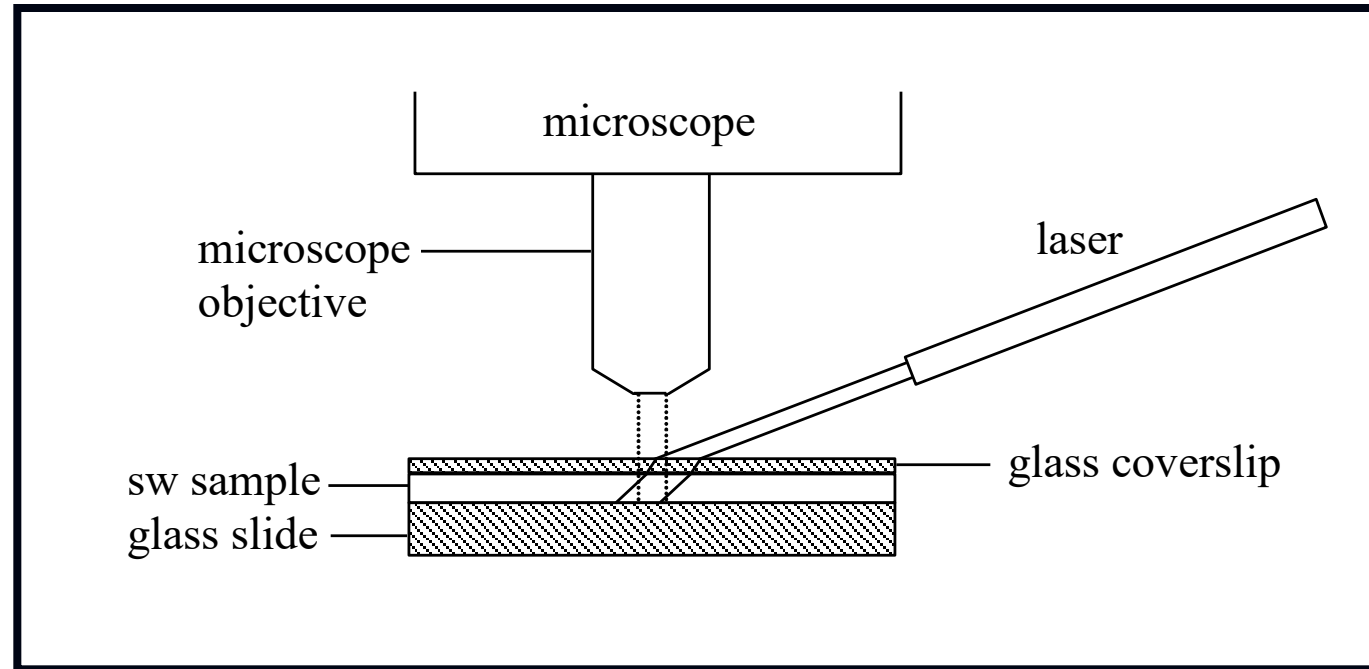


# Phytoplankton scattering: measurements and modeling

$$b_{bp}/b_p$$

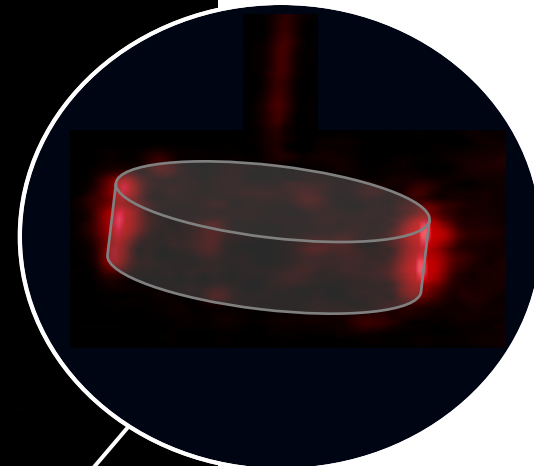
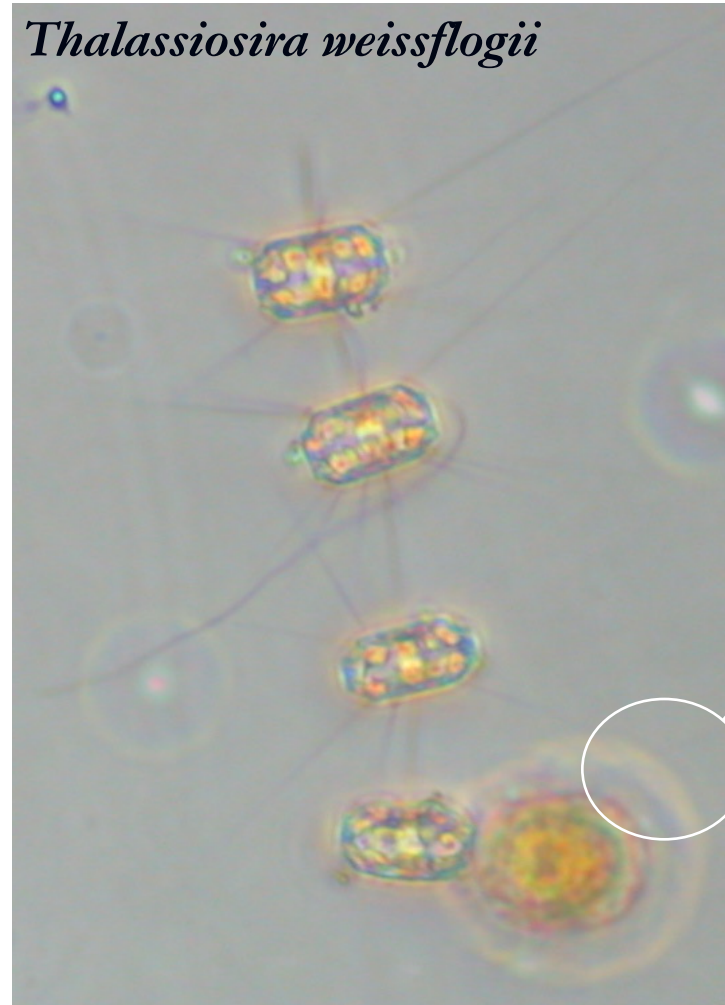
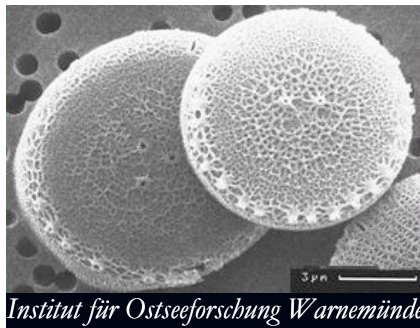
	Measured	Mie theory	Coated Mie theory
<i>Thalassiosira</i> cells	<b>0.013</b>	0.006	<b>0.013</b>
<i>Gyrodinium</i> cells	<b>0.006</b>	0.003	<b>0.007</b>
<i>C. socialis</i> cells	<b>0.004</b>	0.0006	0.0237
<i>C. socialis</i> <sup>1</sup> cell $Q_{bb}$ <sup>2</sup> colony $Q_b$	<b>0.004</b>	<b>0.004</b>	

# Imaging Particle Backscattering



Backscattering imaged at  $\sim 140^\circ$

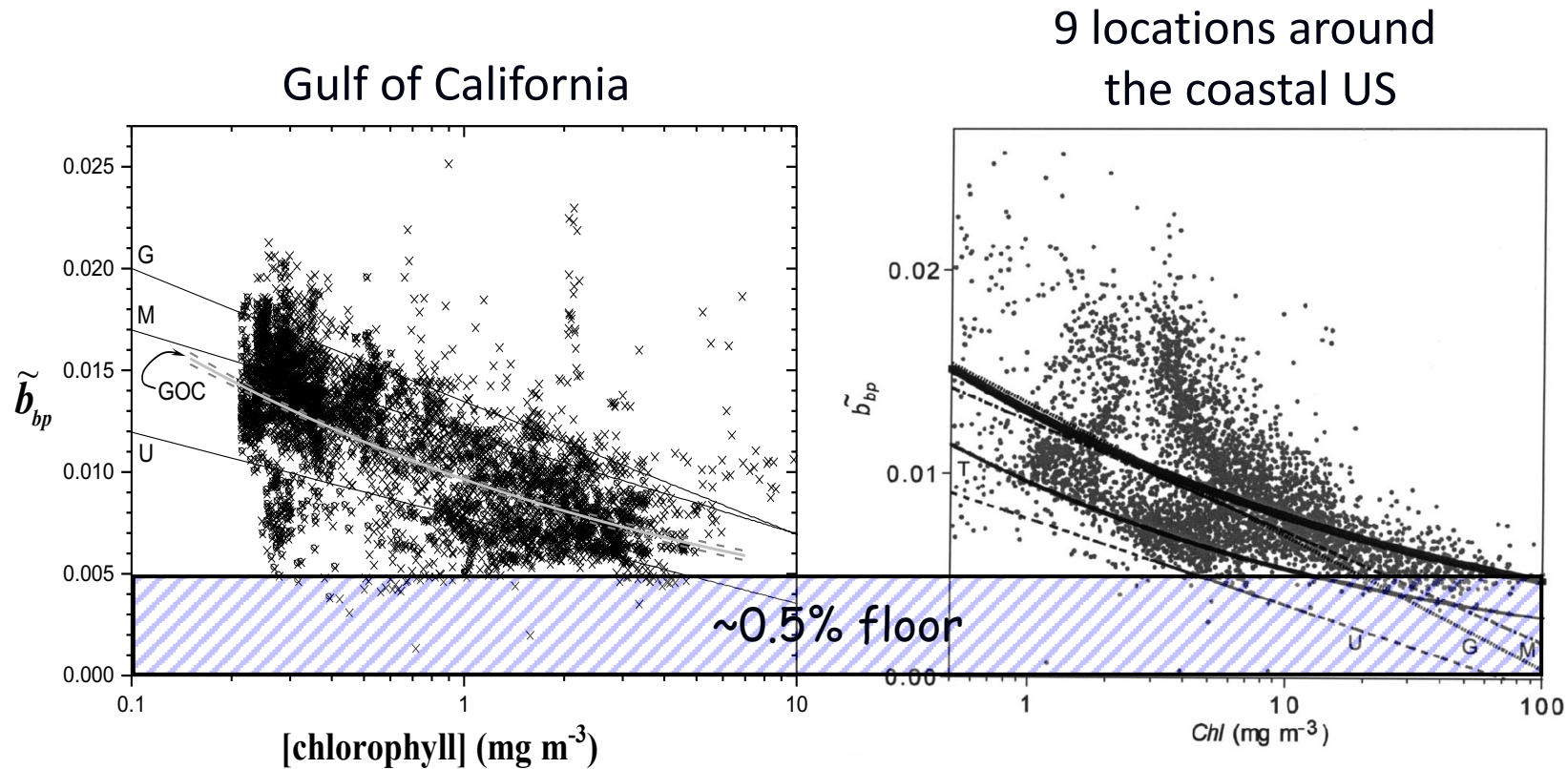
# Imaging Particle Backscattering



Need hi  
refractive  
index  
difference  
( $n_p - n_m$ )

er direction  
g image

# Backscattering ratio and chlorophyll

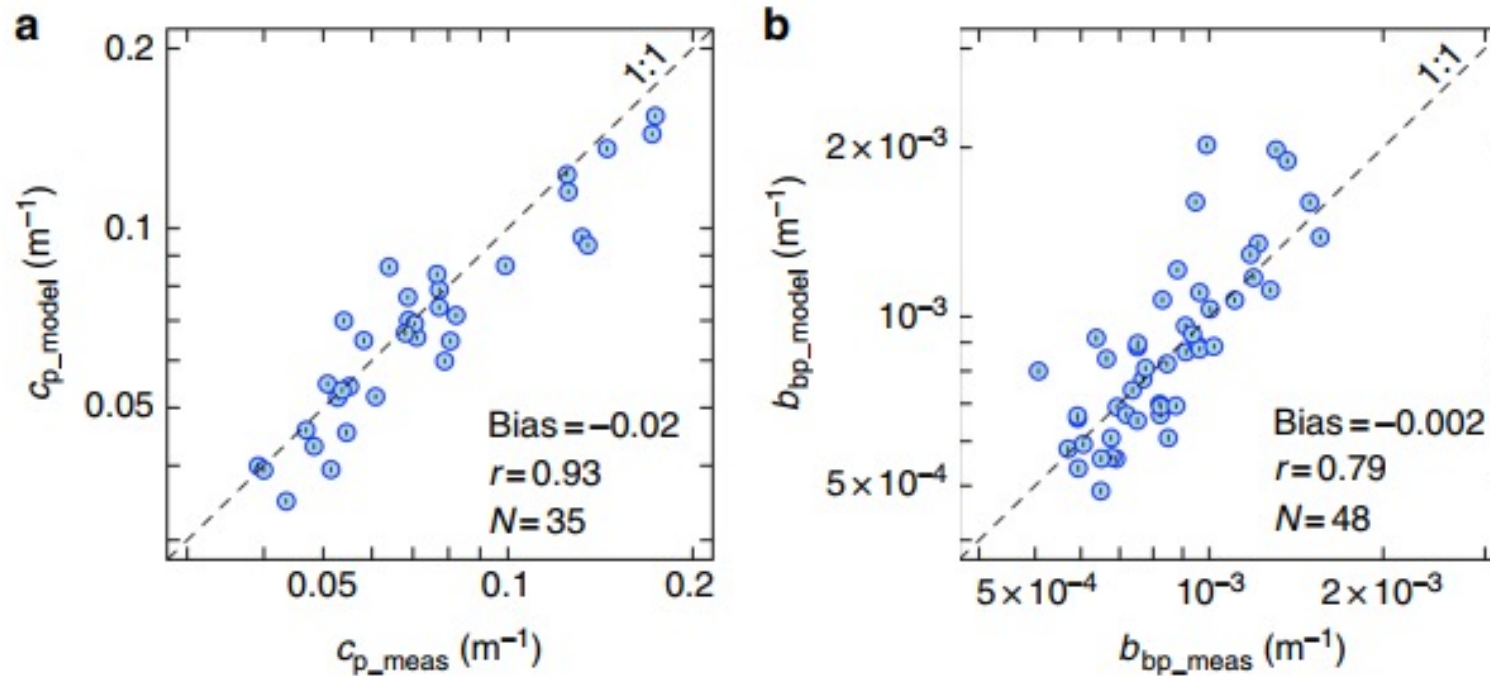


*Twardowski et al. 2001*

*Sullivan et al. 2005*

Even in phytoplankton dominated waters,  $b_{bp}/b_p$  does not fall below ~0.5%  
Phytoplankton likely do make a significant direct contribution to  $b_{bp}$

# Coated sphere model is a good first approximation



Organelli et al. (2018)

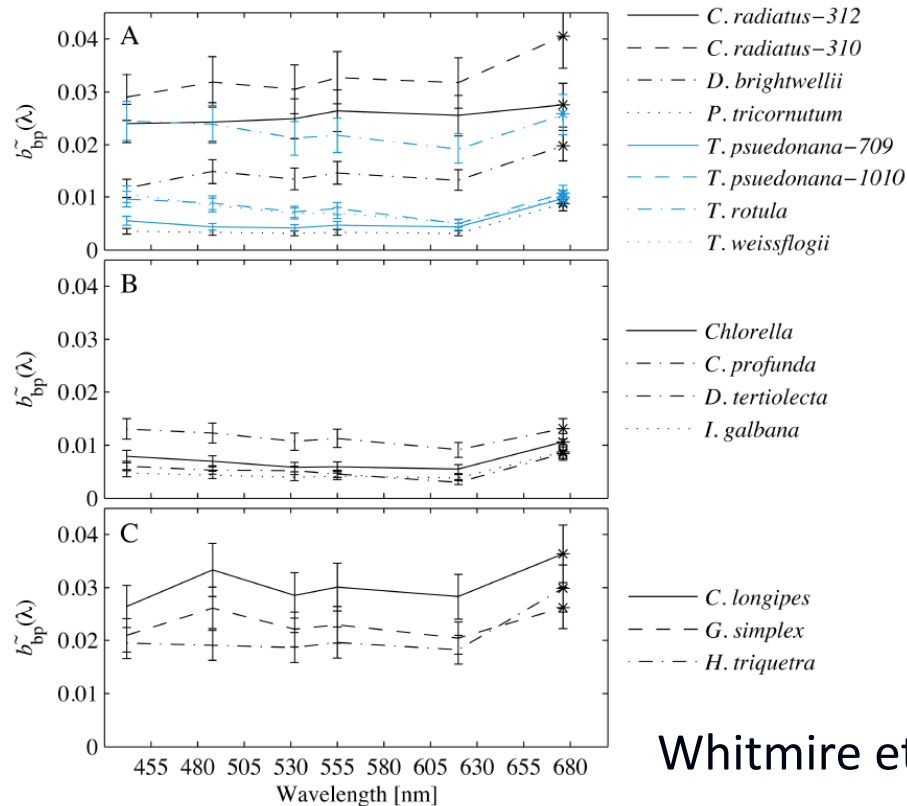
- Coated sphere model could reproduce both particulate attenuation and backscattering
- Homogeneous sphere model could not



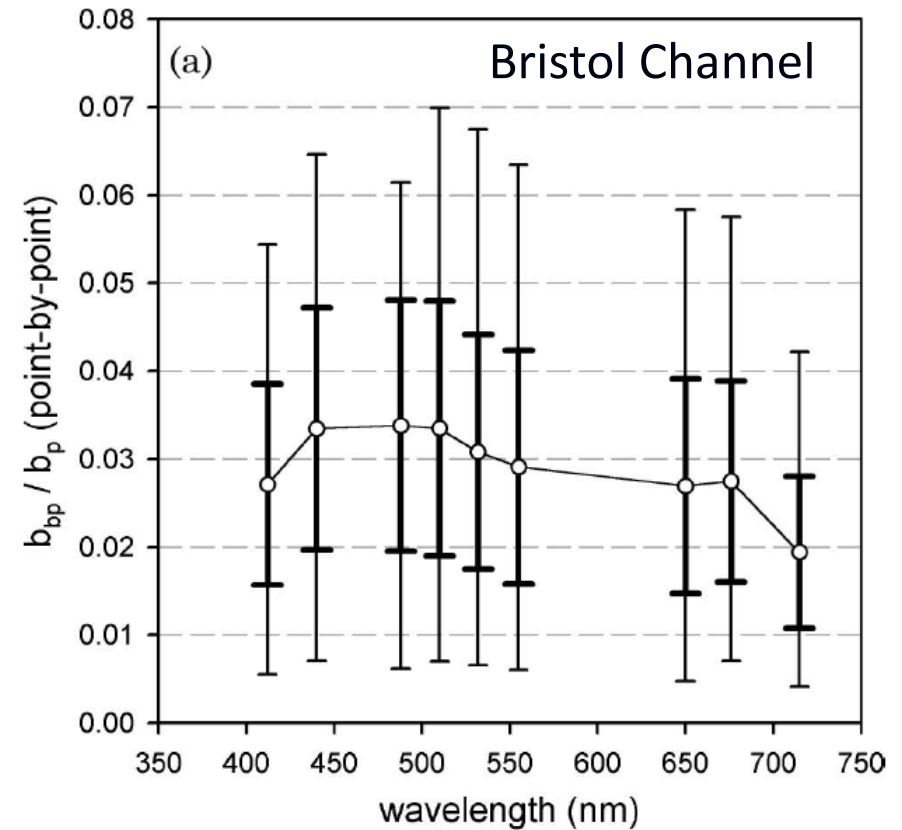
Additional considerations with  
particle scattering....

# Spectral backscattering ratio by particles

For size distribution described by power law,  
with relatively low absorption, theory predicts  
spectrally independent  $b_{bp}/b_p$ ....  
(e.g. Morel 1973; Twardowski et al. 2001)



Whitmire et al. 2009



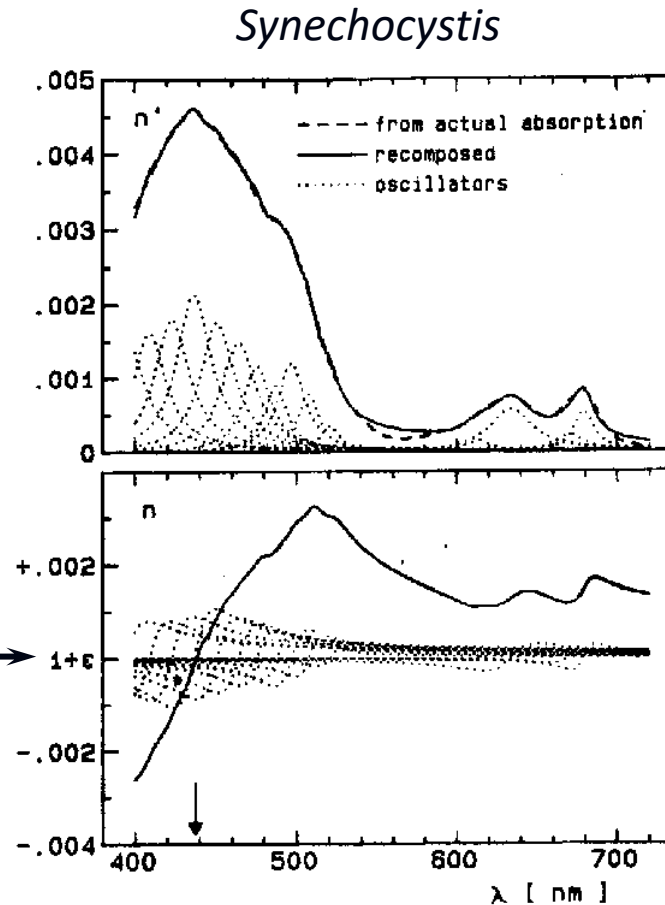
McKee et al. 2009

# Anomalous dispersion

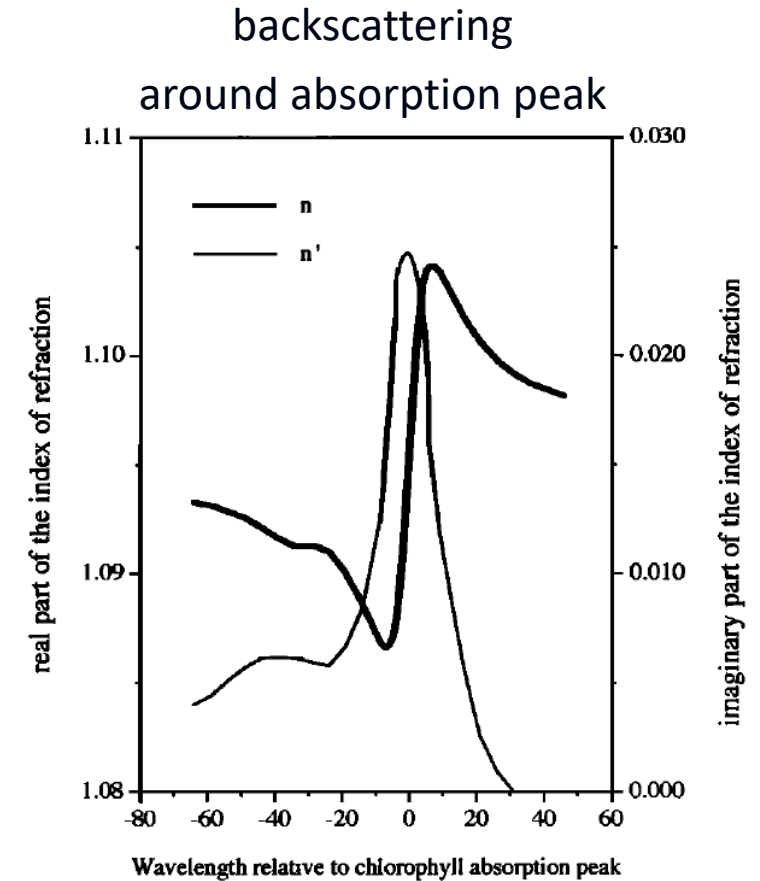
Spectral and angular scattering intensity of a particle is principally dependent on:

- size relative to  $\lambda$
- complex refractive index relative to the medium ( $n - in'$ )

Anomalous dispersion describes how particle absorption alters the refractive index spectrum, i.e., if you change  $a_p$ , you will change  $b_p$ ,  $b_{bp}$



Stramski et al. 1988



Zaneveld and Kitchen 1995

# Near $\beta(180)$ , coherent scattering – the “glory”

Phases interact in a constructive way to enhance scattering near 180 deg

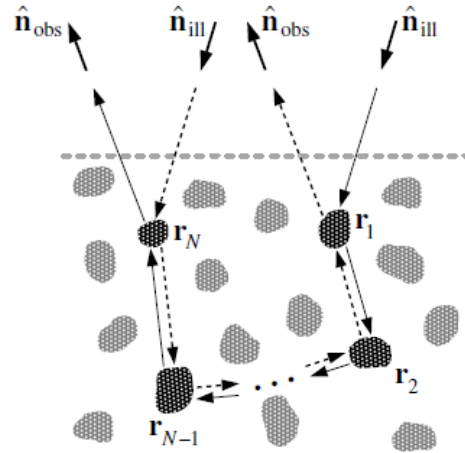


**Figure 3.3.** Schematic explanation of coherent backscattering.

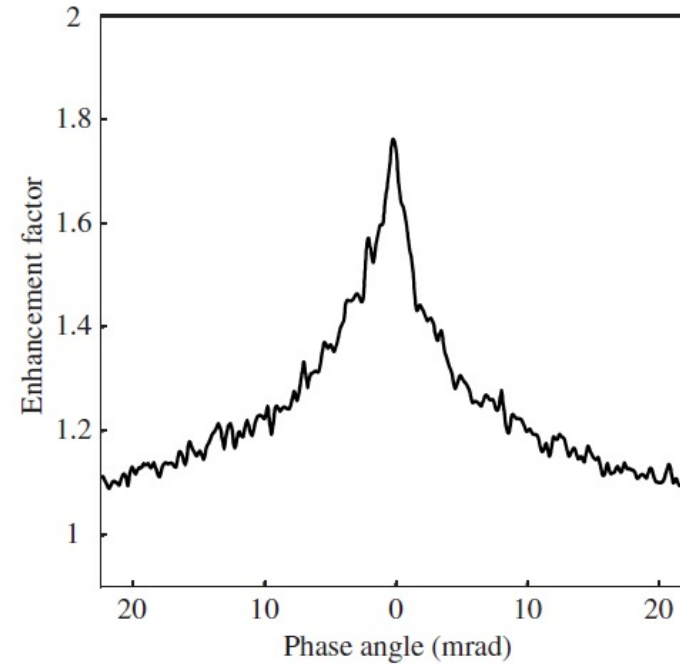


**Figure 3.5.** Angular profile of the coherent backscattering peak produced by a 1500- $\mu\text{m}$ -thick slab of 9.6 vol% of 0.215- $\mu\text{m}$ -diameter polystyrene spheres suspended in water. The slab was illuminated by a linearly polarized laser beam ( $\lambda_1 = 633 \text{ nm}$ ) incident normally to the slab surface. The scattering plane (i.e., the plane through the vectors  $\hat{n}_{\text{ill}}$  and  $\hat{n}_{\text{obs}}$ , Fig. 3.3) was fixed in such a way that the electric vector of the incident beam vibrated in this plane. The detector measured the component of the backscattered intensity polarized parallel to the scattering plane. The curve shows the profile of the backscattered intensity normalized by the intensity of the incoherent background as a function of the phase angle. The latter is defined as the angle between the vectors  $\hat{n}_{\text{obs}}$  and  $-\hat{n}_{\text{ill}}$ . (After van Albada *et al.* 1987.)

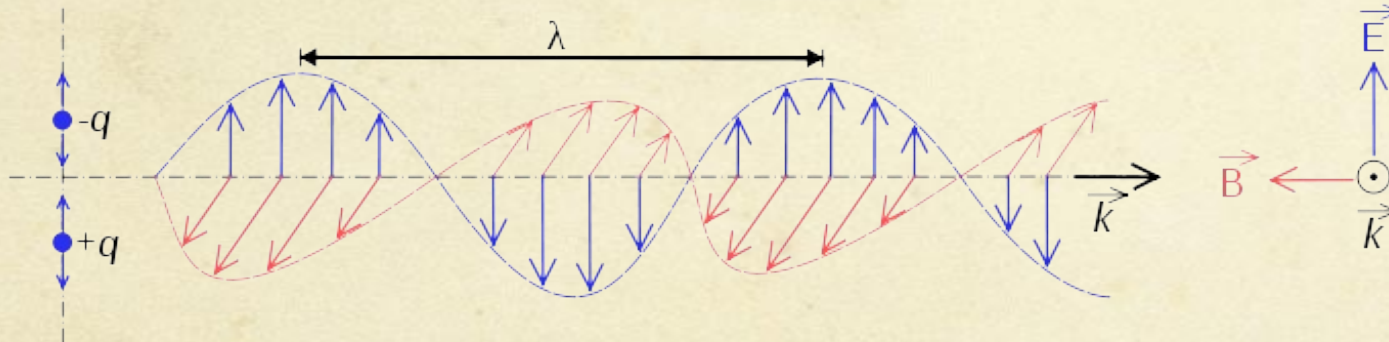
# Polarized Scattering



In 1864, Maxwell wrote "*A dynamical theory of the electromagnetic field*", where he first proposed that light was in fact undulations in the same medium that is the cause of electric and magnetic phenomena.

Maxwell derived a wave form of the electric and magnetic equations, revealing the wave-like nature of electric and magnetic fields, and their symmetry. His work in producing a unified model of electromagnetism is considered to be one of the greatest advances in physics.

And then there was light...



Polarization of light is defined by E only



# 4-component Stokes vector and polarization parameters

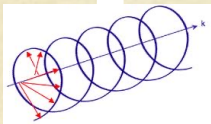
I is the radiance intensity (this is what the human eye sees)



Q is the amount of radiation that is polarized in the 0/90° orientation



U is the amount of radiation polarized in the +/-45° orientation



V is the amount of radiation that is right or left circularly polarized

$$\text{DOP} = \text{Degree of polarization} = \sqrt{Q^2 + U^2 + V^2} / I$$

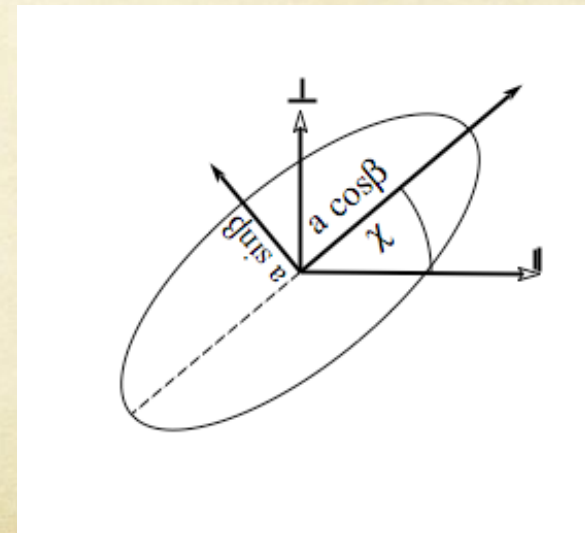
$$\text{DOLP} = \text{Degree of linear polarization} = \sqrt{Q^2 + U^2} / I$$

$$\text{DOCP} = \text{Degree of circular polarization} = |V| / I$$

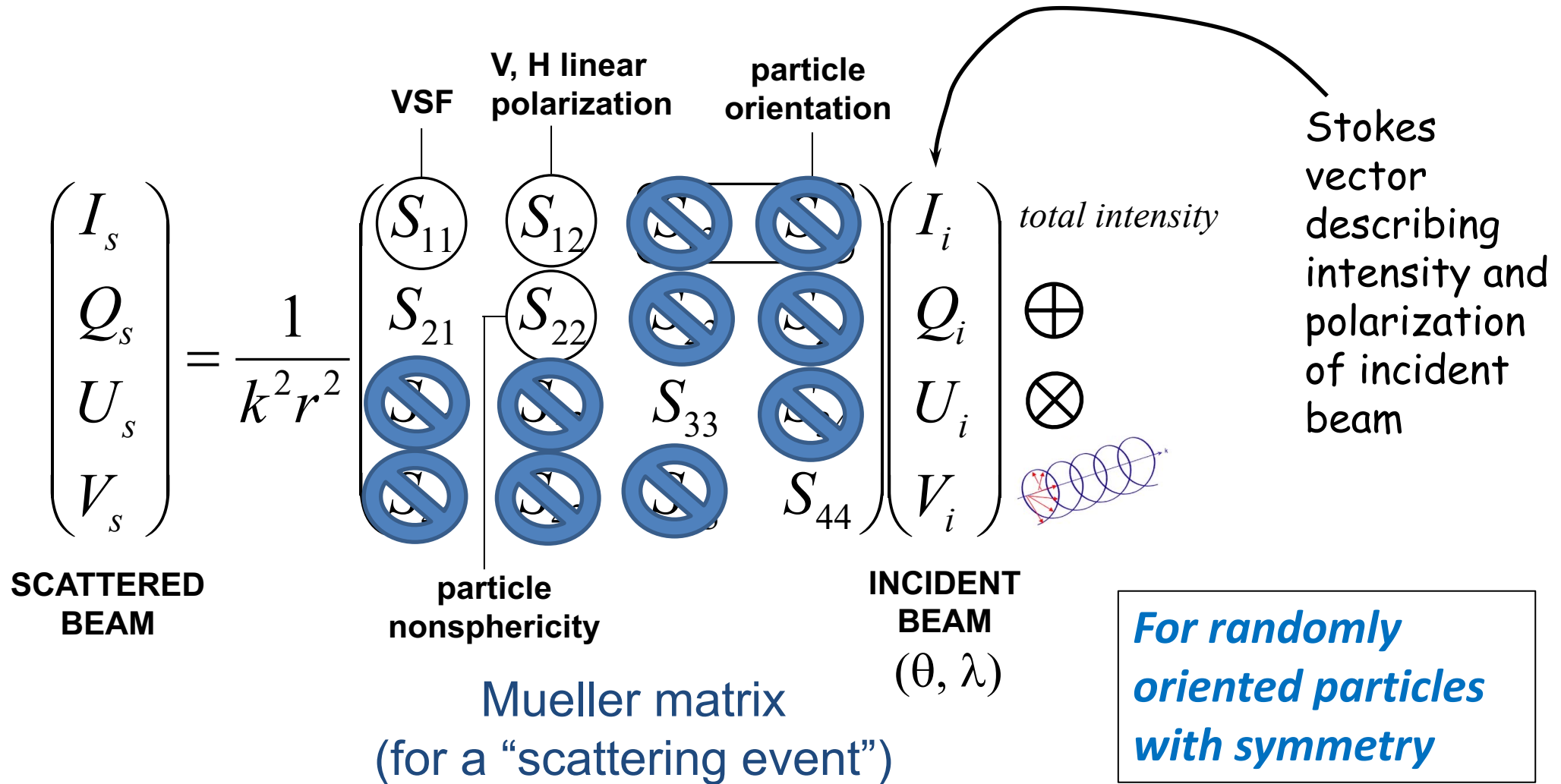
$$\text{Orientation of plane of polarization} = \chi = \tan^{-1}(U/Q)/2$$

*The four components of the Stokes vector are all real numbers and satisfy the relation:*

$$I^2 = Q^2 + U^2 + V^2$$



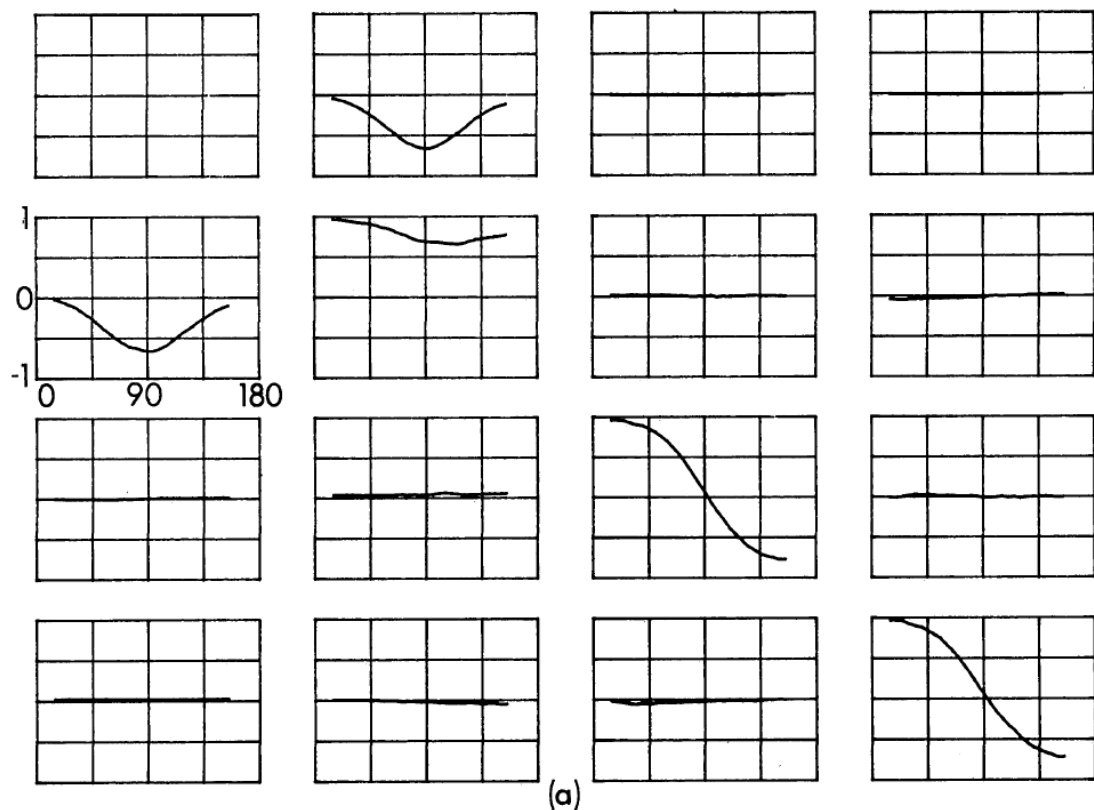
# Polarized scattering – Mueller matrix



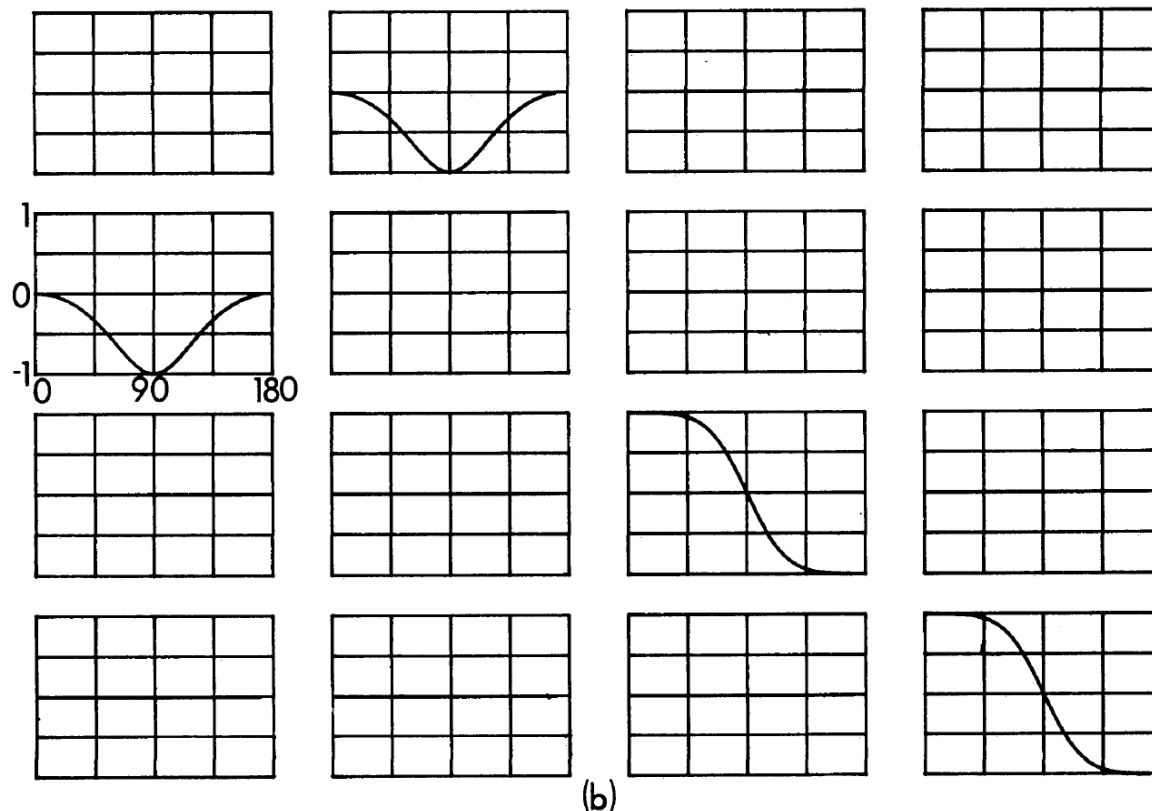
*Every element has wavelength and angular dependencies*

# Mueller matrix: Voss and Fry (1984)

All normalized to  $S_{11}$



Modeled for very small particles (Rayleigh)

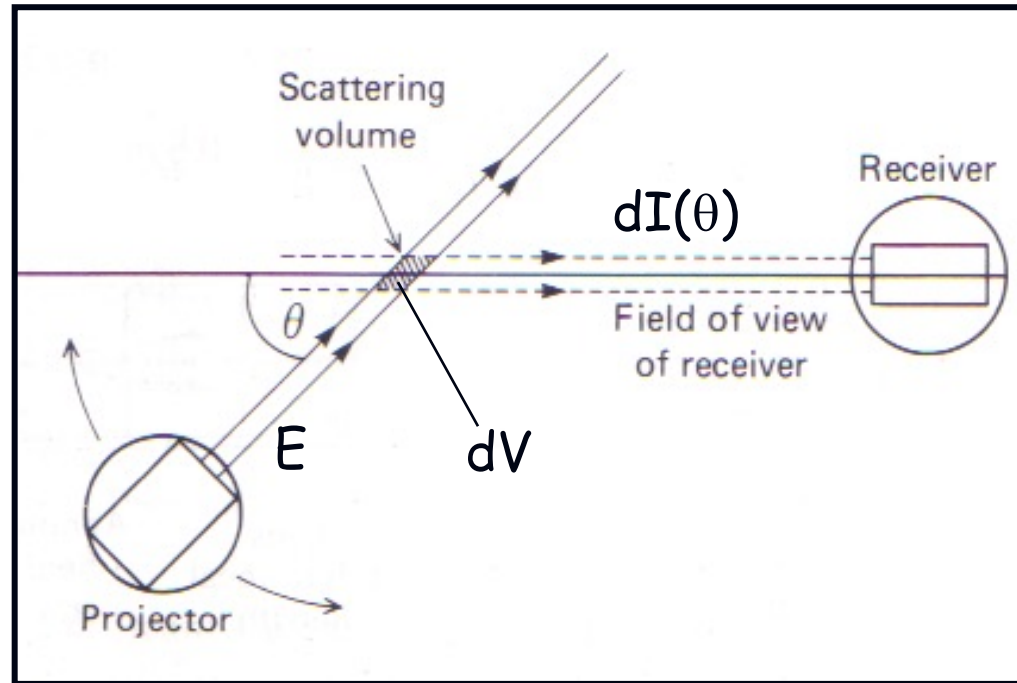


Averaged from Atlantic and Pacific Oceans

> 60 samples



# Polarization: Measuring the Mueller matrix



Bohren and Huffman 1983

Table 13.1 Combinations of Scattering Matrix Elements That Result from Measurements with a Polarizer  $P_s$  Forward of the Scattering Medium and an Analyzer  $A_s$  aft<sup>a</sup>

$U$	$U$	$S_{11}$	$P_{\perp}$	$U$	$\frac{1}{2}(S_{11} - S_{12})$
$U$	$A_{\parallel}$	$\frac{1}{2}(S_{11} + S_{21})$	$P_{\perp}$	$A_{\parallel}$	$\frac{1}{4}(S_{11} - S_{12} + S_{21} - S_{22})$
$U$	$A_{\perp}$	$\frac{1}{2}(S_{11} - S_{21})$	$P_{\perp}$	$A_{\perp}$	$\frac{1}{4}(S_{11} - S_{12} - S_{21} + S_{22})$
$U$	$A_{+}$	$\frac{1}{2}(S_{11} + S_{31})$	$P_{\perp}$	$A_{+}$	$\frac{1}{4}(S_{11} - S_{12} + S_{31} - S_{32})$
$U$	$A_{-}$	$\frac{1}{2}(S_{11} - S_{31})$	$P_{\perp}$	$A_{-}$	$\frac{1}{4}(S_{11} - S_{12} - S_{31} + S_{32})$
$U$	$A_R$	$\frac{1}{2}(S_{11} - S_{41})$	$P_{\perp}$	$A_R$	$\frac{1}{4}(S_{11} - S_{12} - S_{41} + S_{42})$
$U$	$A_L$	$\frac{1}{2}(S_{11} + S_{41})$	$P_{\perp}$	$A_L$	$\frac{1}{4}(S_{11} - S_{12} + S_{41} - S_{42})$
$P_{\parallel}$	$U$	$\frac{1}{2}(S_{11} + S_{12})$	$P_{+}$	$U$	$\frac{1}{2}(S_{11} + S_{13})$
$P_{\parallel}$	$A_{\parallel}$	$\frac{1}{4}(S_{11} + S_{12} + S_{21} + S_{22})$	$P_{+}$	$A_{\parallel}$	$\frac{1}{4}(S_{11} + S_{13} + S_{21} + S_{23})$
$P_{\parallel}$	$A_{\perp}$	$\frac{1}{4}(S_{11} + S_{12} - S_{21} - S_{22})$	$P_{+}$	$A_{\perp}$	$\frac{1}{4}(S_{11} + S_{13} - S_{21} - S_{23})$
$P_{\parallel}$	$A_{+}$	$\frac{1}{4}(S_{11} + S_{12} + S_{31} + S_{32})$	$P_{+}$	$A_{+}$	$\frac{1}{4}(S_{11} + S_{13} + S_{31} + S_{33})$
$P_{\parallel}$	$A_{-}$	$\frac{1}{4}(S_{11} + S_{12} - S_{31} - S_{32})$	$P_{+}$	$A_{-}$	$\frac{1}{4}(S_{11} + S_{13} - S_{31} - S_{33})$
$P_{\parallel}$	$A_R$	$\frac{1}{4}(S_{11} + S_{12} - S_{41} - S_{42})$	$P_{+}$	$A_R$	$\frac{1}{4}(S_{11} + S_{13} - S_{41} - S_{43})$
$P_{\parallel}$	$A_L$	$\frac{1}{4}(S_{11} + S_{12} + S_{41} + S_{42})$	$P_{+}$	$A_L$	$\frac{1}{4}(S_{11} + S_{13} + S_{41} + S_{43})$
$P_{-}$	$U$	$\frac{1}{2}(S_{11} - S_{13})$	$P_L$	$U$	$\frac{1}{2}(S_{11} - S_{14})$
$P_{-}$	$A_{\parallel}$	$\frac{1}{4}(S_{11} - S_{13} + S_{21} - S_{23})$	$P_L$	$A_{\parallel}$	$\frac{1}{4}(S_{11} - S_{14} + S_{21} - S_{24})$
$P_{-}$	$A_{\perp}$	$\frac{1}{4}(S_{11} - S_{13} - S_{21} + S_{23})$	$P_L$	$A_{\perp}$	$\frac{1}{4}(S_{11} - S_{14} - S_{21} + S_{24})$
$P_{-}$	$A_{+}$	$\frac{1}{4}(S_{11} - S_{13} + S_{31} - S_{33})$	$P_L$	$A_{+}$	$\frac{1}{4}(S_{11} - S_{14} + S_{31} - S_{34})$
$P_{-}$	$A_{-}$	$\frac{1}{4}(S_{11} - S_{13} - S_{31} + S_{33})$	$P_L$	$A_{-}$	$\frac{1}{4}(S_{11} - S_{14} - S_{31} + S_{34})$
$P_{-}$	$A_R$	$\frac{1}{4}(S_{11} - S_{13} - S_{41} + S_{43})$	$P_L$	$A_R$	$\frac{1}{4}(S_{11} - S_{14} - S_{41} + S_{44})$
$P_{-}$	$A_L$	$\frac{1}{4}(S_{11} - S_{13} + S_{41} - S_{43})$	$P_L$	$A_L$	$\frac{1}{4}(S_{11} - S_{14} + S_{41} - S_{44})$
$P_R$	$U$	$\frac{1}{2}(S_{11} + S_{14})$			
$P_R$	$A_{\parallel}$	$\frac{1}{4}(S_{11} + S_{14} + S_{21} + S_{24})$			
$P_R$	$A_{\perp}$	$\frac{1}{4}(S_{11} + S_{14} - S_{21} - S_{24})$			
$P_R$	$A_{+}$	$\frac{1}{4}(S_{11} + S_{14} + S_{31} + S_{34})$			
$P_R$	$A_{-}$	$\frac{1}{4}(S_{11} + S_{14} - S_{31} - S_{34})$			
$P_R$	$A_R$	$\frac{1}{4}(S_{11} + S_{14} - S_{41} - S_{44})$			
$P_R$	$A_L$	$\frac{1}{4}(S_{11} + S_{14} + S_{41} + S_{44})$			

<sup>a</sup> $U$  indicates the absence of a polarizer or analyzer.



# Voss and Fry (1984) Polarimeter matrix

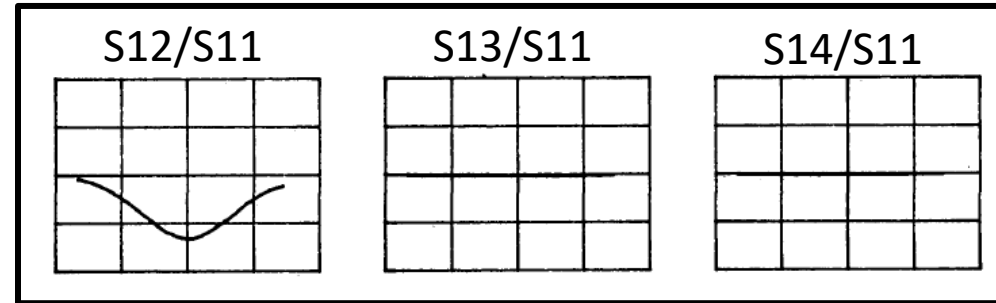
Degree of Linear  
Polarization

$$\text{DoLP} = -S_{12} / S_{11}$$

$$= -(H-V)/(H+V)$$

$$H = \frac{1}{2}(S_{11} + S_{12})$$

$$V = \frac{1}{2}(S_{11} - S_{12})$$



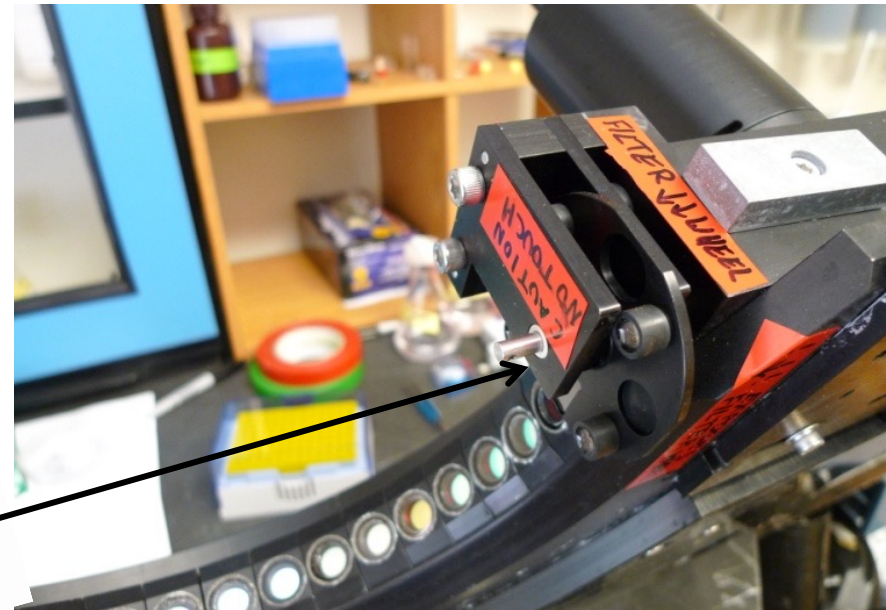
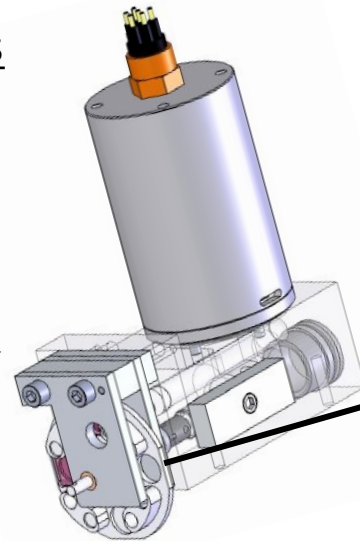
4 positions

1 - OPEN

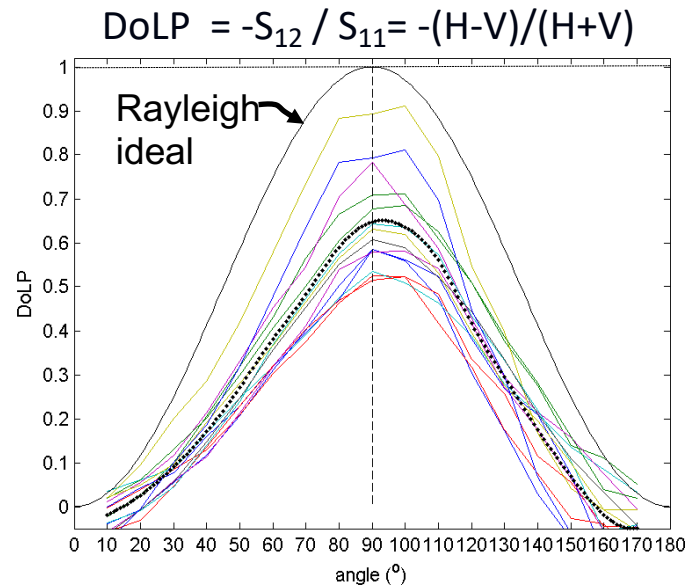
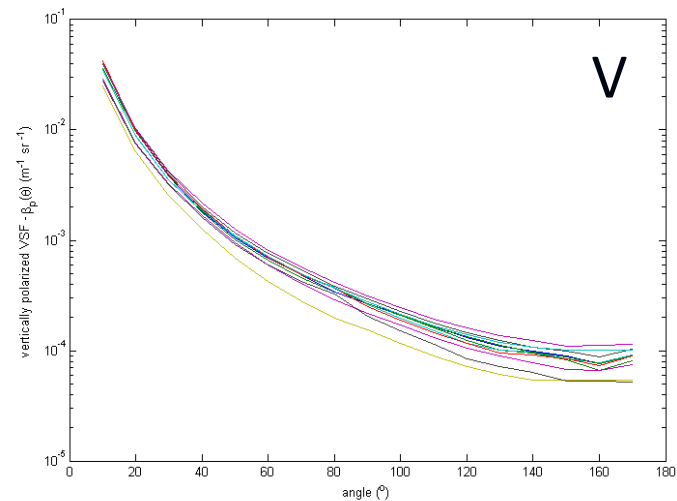
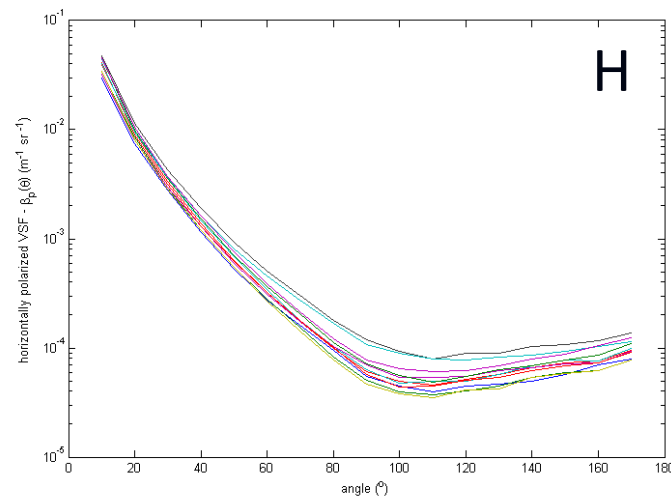
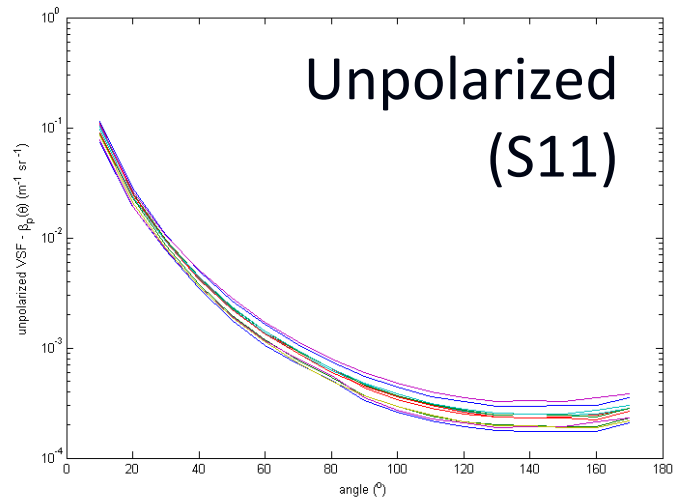
2 - DARK

3 - H  $\longleftrightarrow$

4 - V  $\updownarrow$



# Curaçao, 2012: single vertical profile

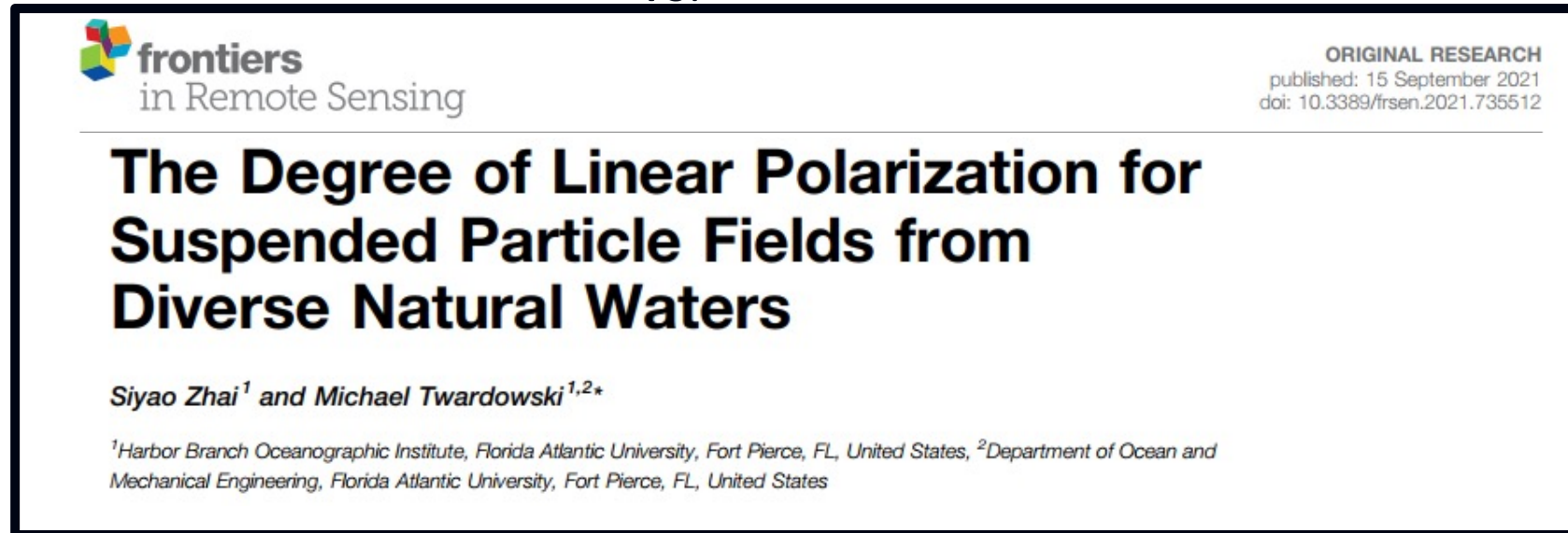


## Cruise locations with MASCOT polarization measurements (since 2008)

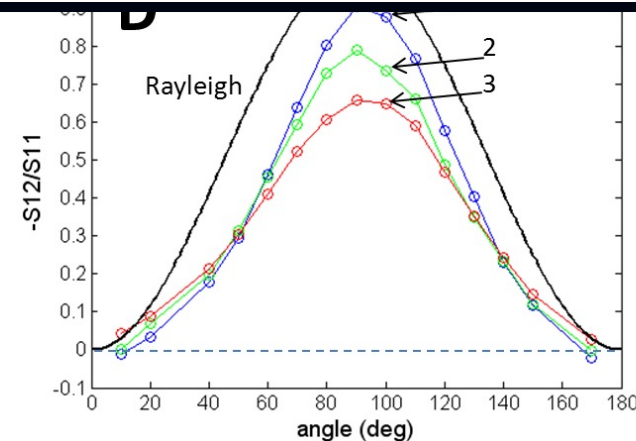
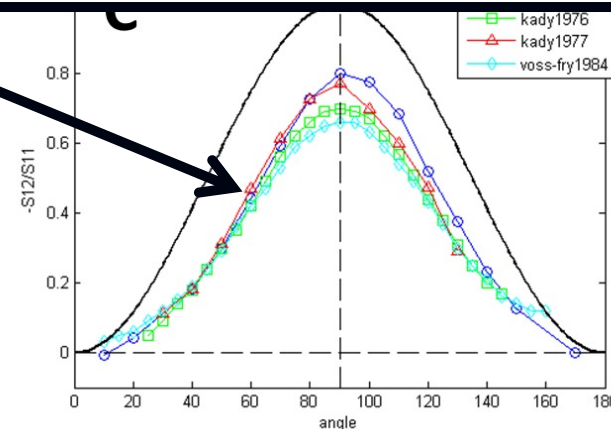
- Ligurian Sea (S13 and S14 also)
- NY bight
- Santa Barbara Channel
- Gulf of Mexico
- Port Aransas, TX
- Florida Keys (2X)
- Curacao
- East Sound, WA
- Florida, Indian lagoon
- N. Lake Michigan

# Polarized scattering measurements

VSF



As of 2020, there were only 3 other measurements of  $S_{12}/S_{11}$  for ocean water in the literature!



$S_{12}/S_{11}$ :  
degree of  
linear polarization  
(DOLP)

Santa Barbara Channel, September 2008

# Polarized scattering

## phytoplankton species

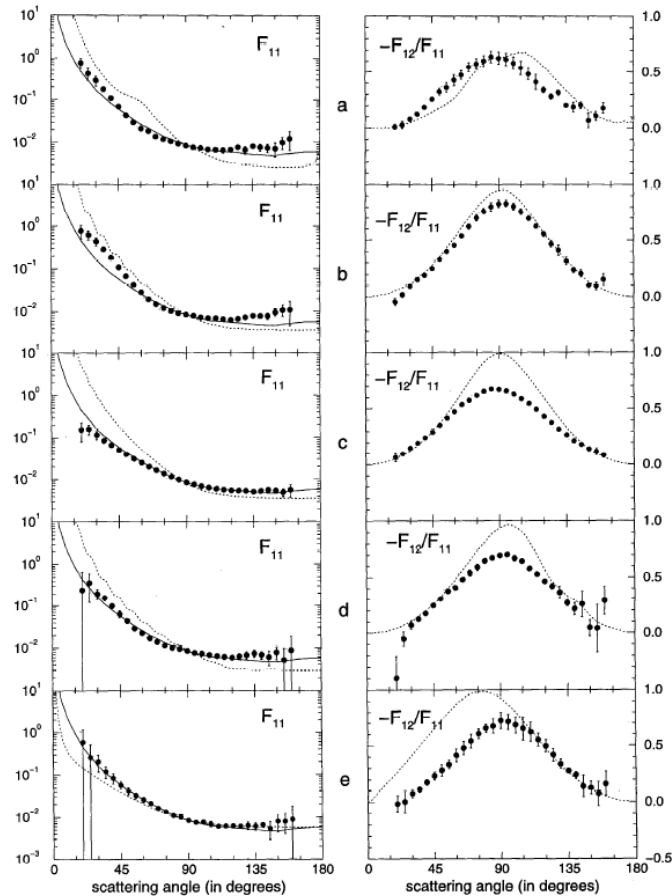


Fig. 6. The measured scattering functions,  $F_{11}$ , and ratios  $-F_{12}/F_{11}$  are shown in the left and right panels, respectively (filled circles) for (a) *Microcystis aeruginosa* without gas vacuoles, (b) *Microcystis aeruginosa* with gas vacuoles, (c) *Microcystis* sp., (d) *Phaeocystis*, and (e) *Volvox aureus*. Also plotted are the scattering function for San Diego Harbor (solid, left panels) and the results of Mie calculations (dashed, left and right panels). The  $F_{11}(\theta)$  functions are scaled at 90° to the scattering function of San Diego Harbor. Errors are smaller than symbols if no error bar is indicated.

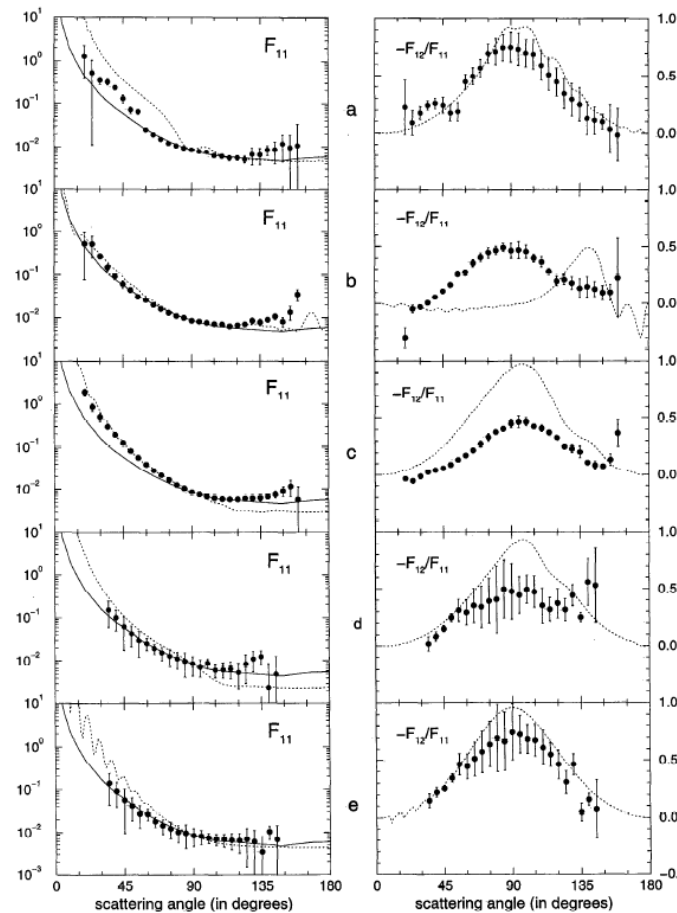


Fig. 8. Same as Fig. 6 for (a) *Astrionella formosa*, (b) *Selenastrum capricornutum*, (c) *Phaeodactylum*, (d) *Emiliania huxleyi* with coccoliths, and (e) *Emiliania huxleyi* without coccoliths.

## sediment samples

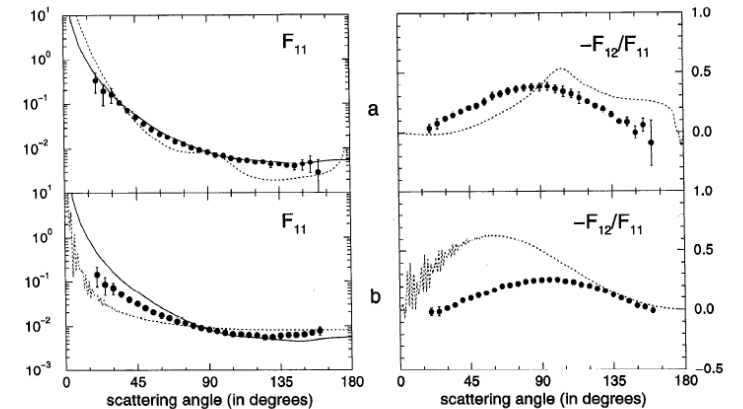
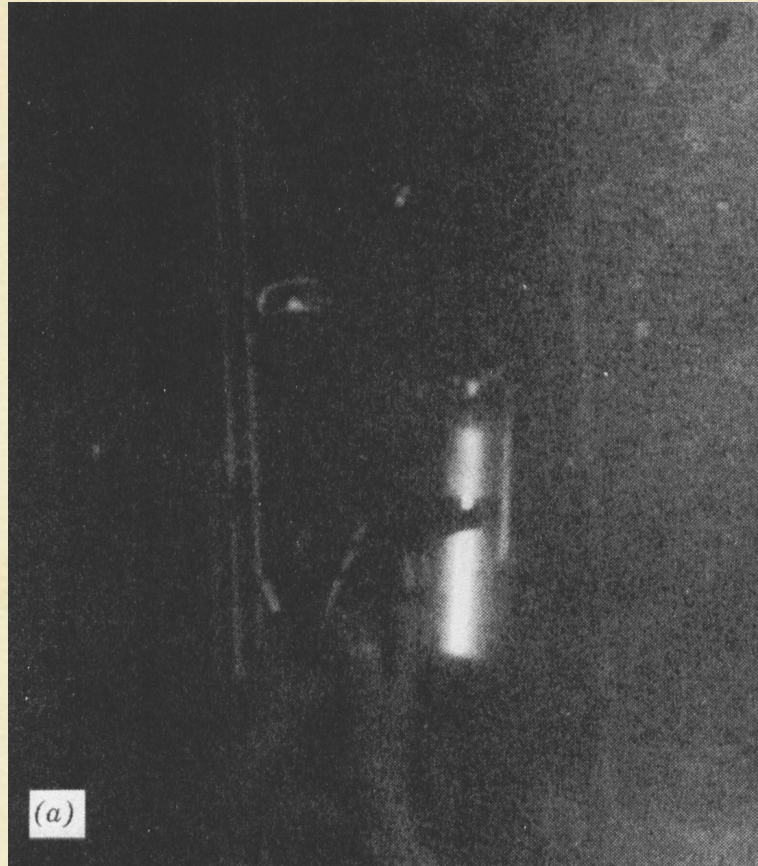


Fig. 9. Same as Fig. 6 for (a) Westerschelde silt with diameters ranging between 3 and 5  $\mu\text{m}$ , and (b) Westerschelde silt with diameters ranging between 5 and 12  $\mu\text{m}$ .

**Included reflection  
corrections**



# Contrast enhancement using polarization



No polarization optics

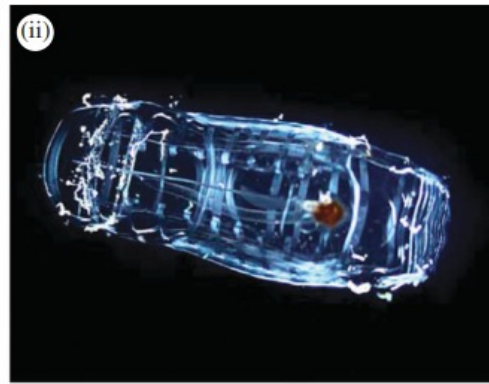
*Seeing a target underwater is a function of*

- character of incident light
- scattering properties of target
- capabilities of viewer
- contrast relative to background

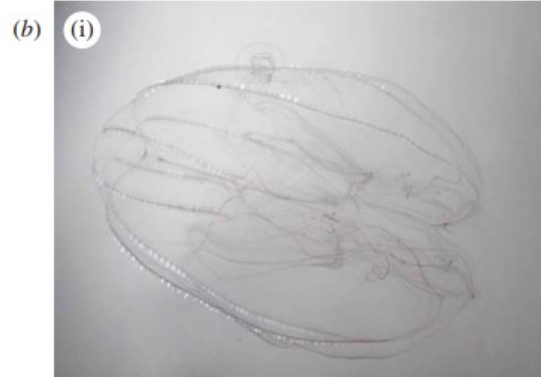


Circular polarized light for illumination, circular analyzer for viewing

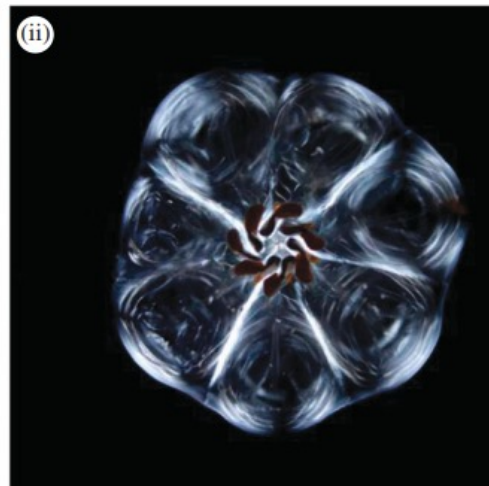
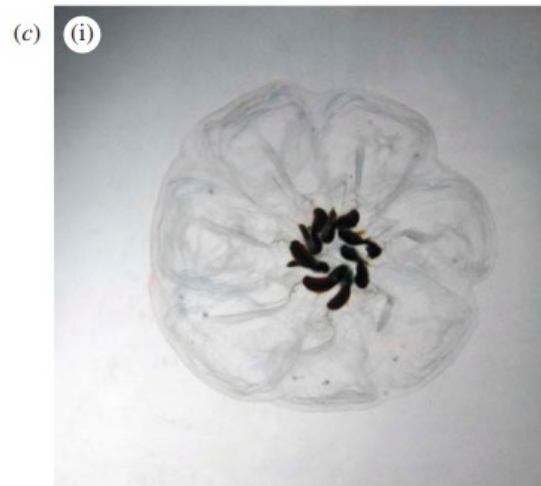




salp



ctenophore



salp

Between parallel  
polarizers

Between cross  
polarizers

# Interpreting polarized scattering of particles

The angular and spectral characteristics of the Mueller scattering matrix parameters are a function of several properties of the particle population, including:

- Refractive index ( $n$ ) composition
- Size distribution
- Particle shape
- Particle orientation

*Much to be done!*

*New polarimeters will be on PACE!*

# Modeling scattering

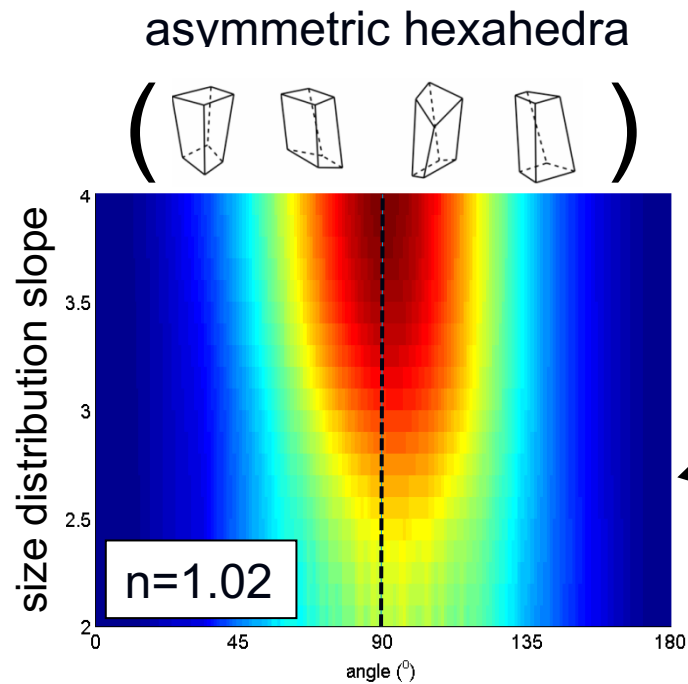
# Models for computing particle scattering

- Rayleigh
  - Lorenz-Mie (also coated sphere, multi-layer sphere versions)
  - van de Hulst anomalous diffraction approximation
  - Geometric optics (IGOM, RBR)
  - Discrete dipole approximation (DDA)
  - Finite difference, time-domain (FDTD)
  - Pseudo-spectral time-domain (PSTD)
  - T-matrix (invariant imbedding, multiple sphere, extended boundary condition, many body iterative...)
  - Surface roughness models....
- Combination pioneered by Yang, Kattawar for nonspherical particles

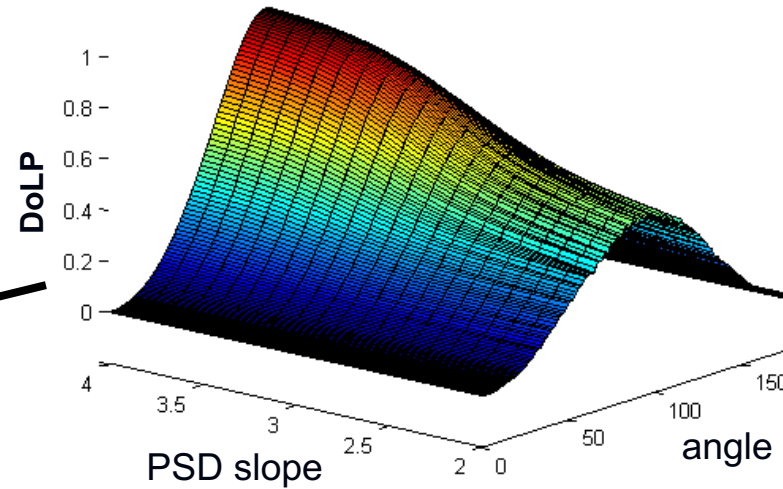
Each has restrictions: size ranges,  $n$ , shape and symmetries

# Why model particle scattering?

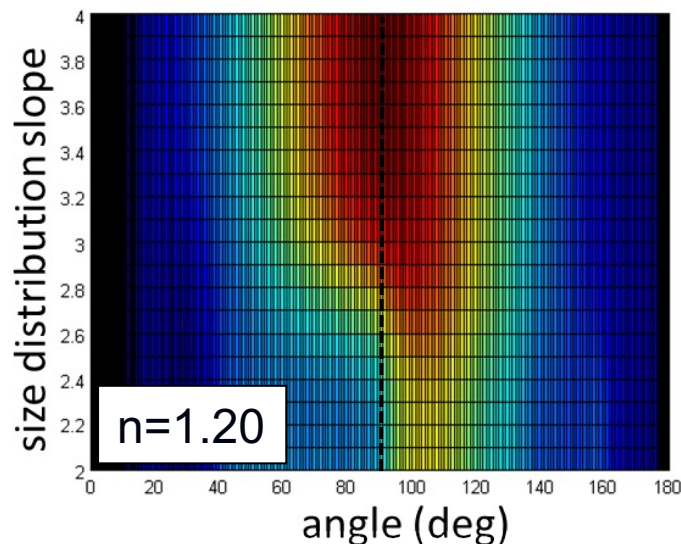
- Models can help qualitatively interpret scattering measurements in terms of particle characteristics
- Sometimes this can be done explicitly, which is known as an inversion



## Degree of Linear Polarization



another  
view



- **Increasing nonsphericity** lowers DoLP and shifts the DoLP peak to larger angles
- **Increasing refractive index** lowers DoLP, particularly for populations with relatively flat size distributions
- **As size distributions become increasingly flat**, the DoLP decreases and the maximum shifts to larger angles



# Interpretation and Application for Biogeochemical Properties

# Scattering as a proxy for biogeochemical properties

## EMPIRICAL

A common example → Beer's Law:  $IOP = \varepsilon[\text{conc}]$

### Some biogeochemical properties that influence scattering properties:

Chlorophyll and other phytoplankton pigments, particle size, particle density, particle composition, particle shape, particle concentration, total particle mass (TSM, SPM), POM/C, DOM/C, biomass, humic substances, hydrocarbons,  $\text{CaCO}_3$ ,...

However: pools of particulate and dissolved matter can be highly variable and complex in composition, especially in coastal regions, usually confounding simple relationships.

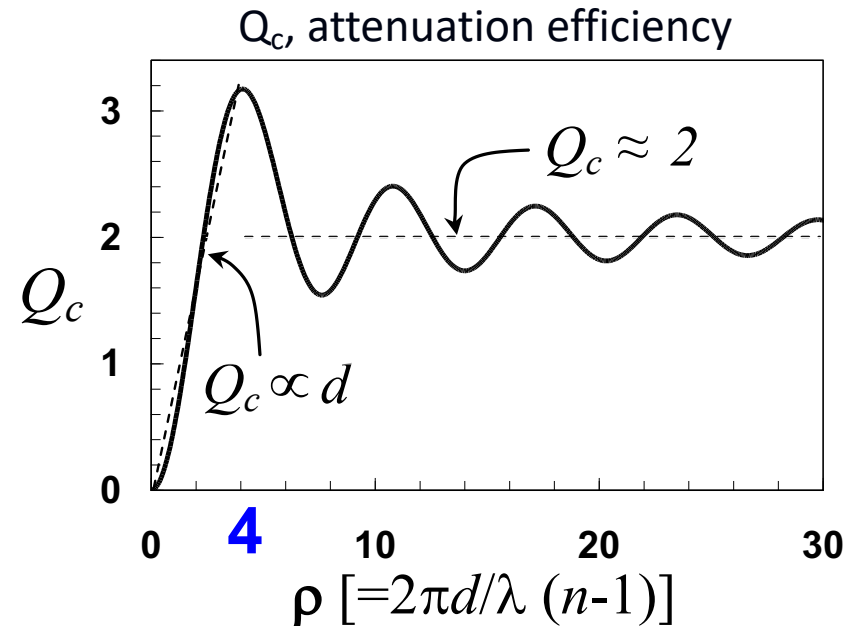
# How is $c_p$ (or $b_p$ or $b_{bp}$ ) directly linked to particles?

For population of spherical particles:

$$c_p = \pi \int_{r_{\min}}^{r_{\max}} Q_c(r, n) F(r) r^2 dr$$

- $Q_c$  is attenuation efficiency
- $F(r)$  is size distribution
- $n$  is refractive index
- $r$  is radius

Widely varying PSDs and particle  $n$  are the main reason why  $c_p$ -TSM,  $c_p$ -POC etc relationships vary



Can be modeled well for spheres with approximation from van de Hulst (1957, 1981)

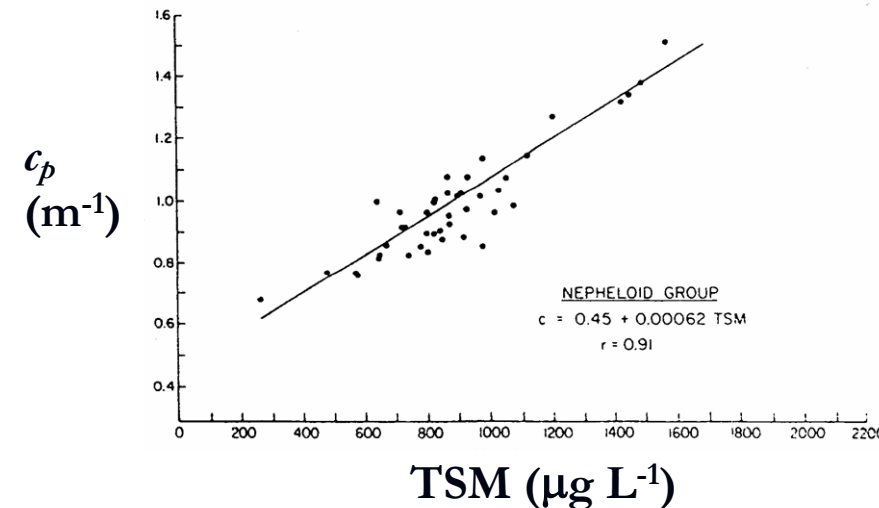
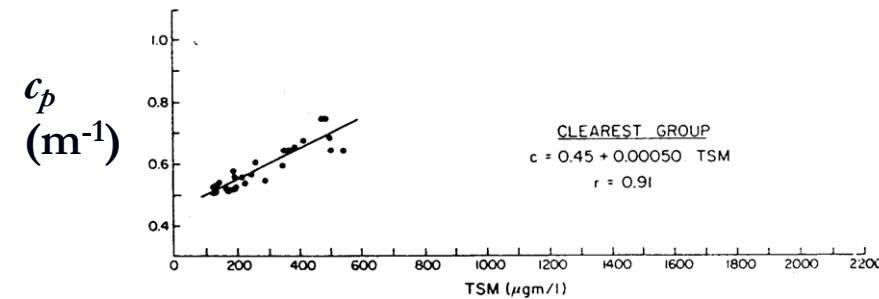
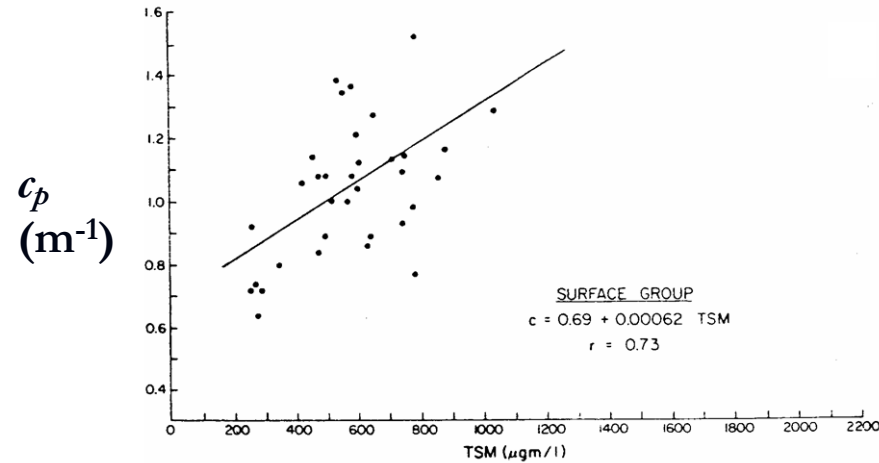
$$c_p \propto \begin{cases} \sum_{i=1}^N d_i^3, & \rho < 4 \xrightarrow{\propto} \text{total particle volume (TPV)} \\ \sum_{i=1}^N d_i^2, & \rho > 4 \xrightarrow{\propto} \text{total surface area (TSA) OR total cross-sectional area (\Sigma G)} \end{cases}$$

See reviews: Morel and Bricaud 1986 and Morel 1991

# Example: $c_p$ and TSM

Reasonable correlations  
for each regression, but  
slopes are different for  
different water masses

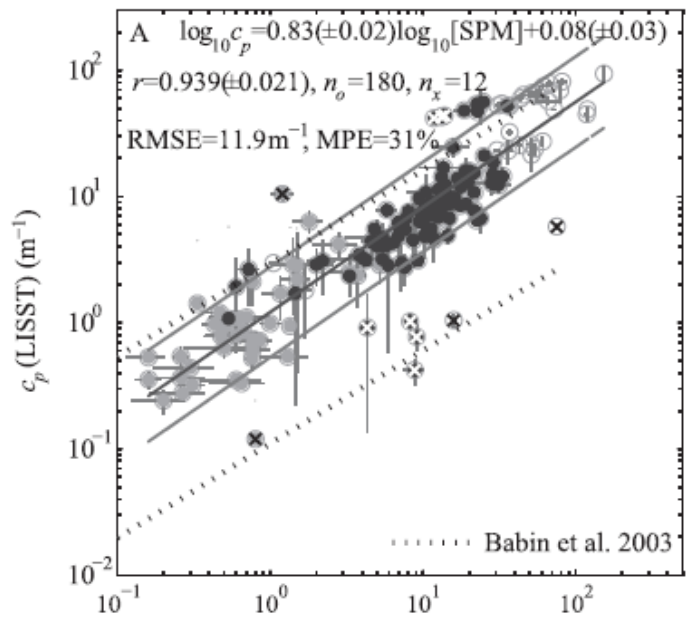
*EMPIRICAL*



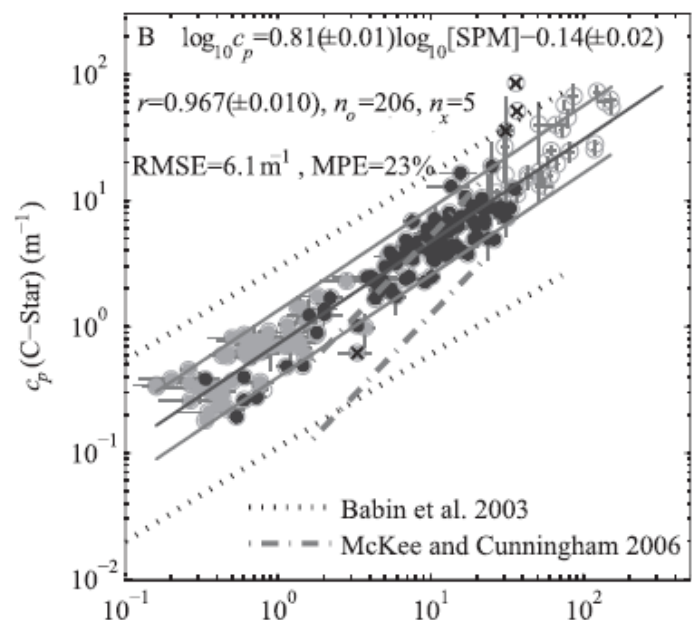
Peterson 1977

*Assessment with  
first modern  
transmissometer*

LISST

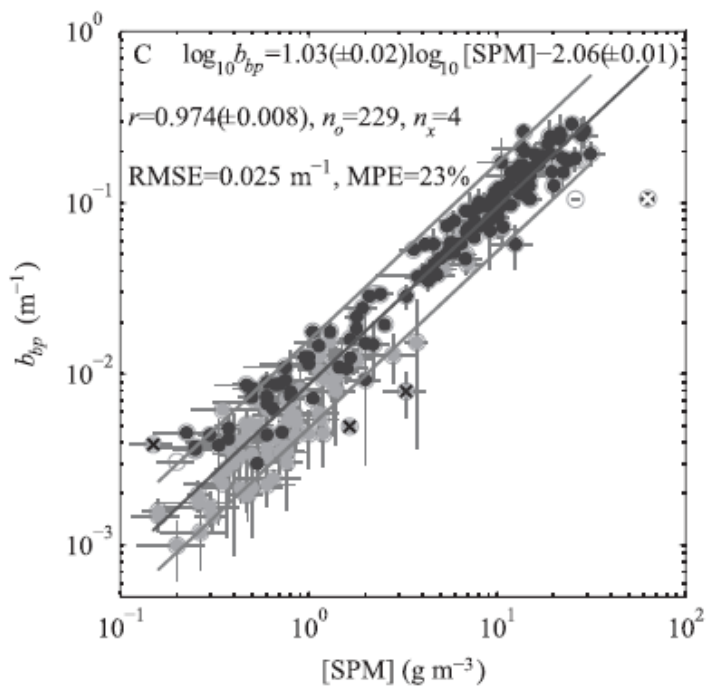


C-star

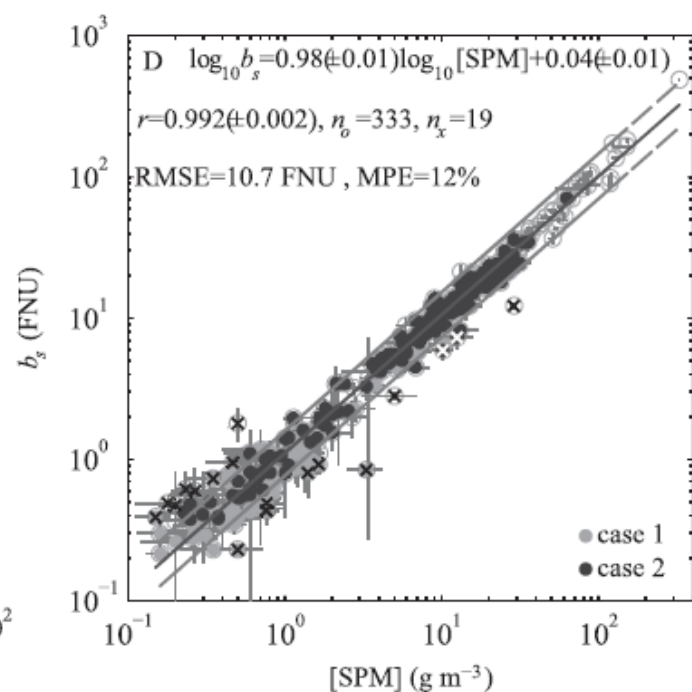


*EMPIRICAL*

ECO bb



NTU



# Published slopes for TSM- $c_p$ and POC- $c_p$

**Table 1.** Published biogeochemical-optical data.

reference	location	$\frac{\text{TSM}}{c_p^a}$ ( $\mu\text{g-m/L}$ )	$\frac{\text{POC}}{c_p^a}$ ( $\mu\text{g-m/L}$ )
Peterson (1977)	OR coast - nepheloid layer	1600	
	OR coast - clearest waters	2000	
	OR coast - surface	1600	
Mishonov et al. (2000)	Ross Sea		674
	NABE		319
	APFZ		455
Bishop et al. (1999)	N. Pacific		195
Gardner et al. (1992)	N. Atlantic	1020	378
Gardner et al. (2001)	NW Atlantic - pre-hurricane 1996, surface	1000	400
	NW Atlantic - pre-hurricane 1996, subsurface	1100	105
	NW Atlantic - post-hurricane 1996, surface	770	455
	NW Atlantic - post-hurricane 1996, subsurface	2500	135
	NW Atlantic - Spring 1997, surface	770	
	NW Atlantic - Spring 1997, subsurface	1700	
	NW Atlantic - Spring 1997, mid-water		1250
Walsh et al. (1995)	Eq. Pac April, 1992	451	
	Eq. Pac October, 1992	642	
Walsh (1990)	Gulf of Mexico	660	
Mishonov et al. (2003)	BATS		323
	NABE (revised from Mishonov et al. 2000)		303

<sup>a</sup> – wavelength typically 660 nm

TSM/ $c_p$  range:  
~450-2500

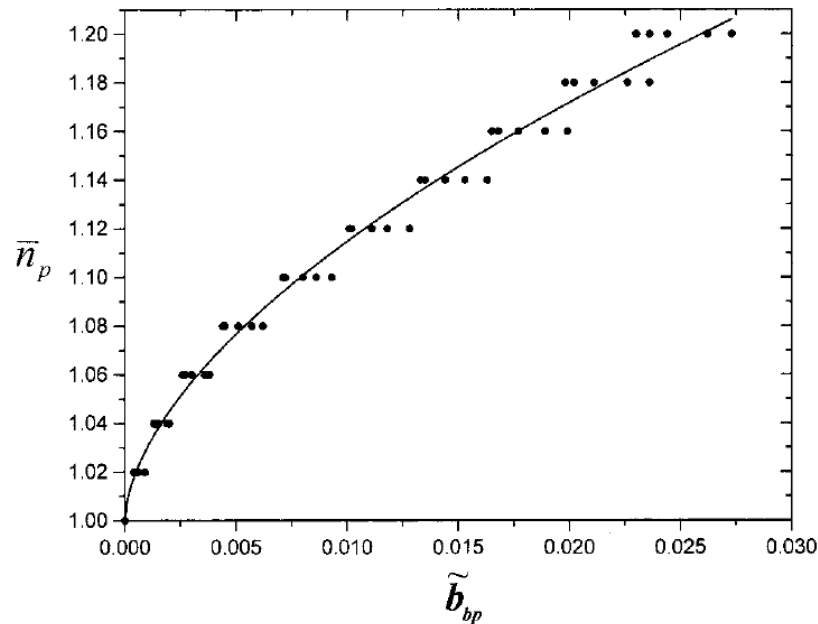
POC/ $c_p$  range:  
~100-1250

*EMPIRICAL*

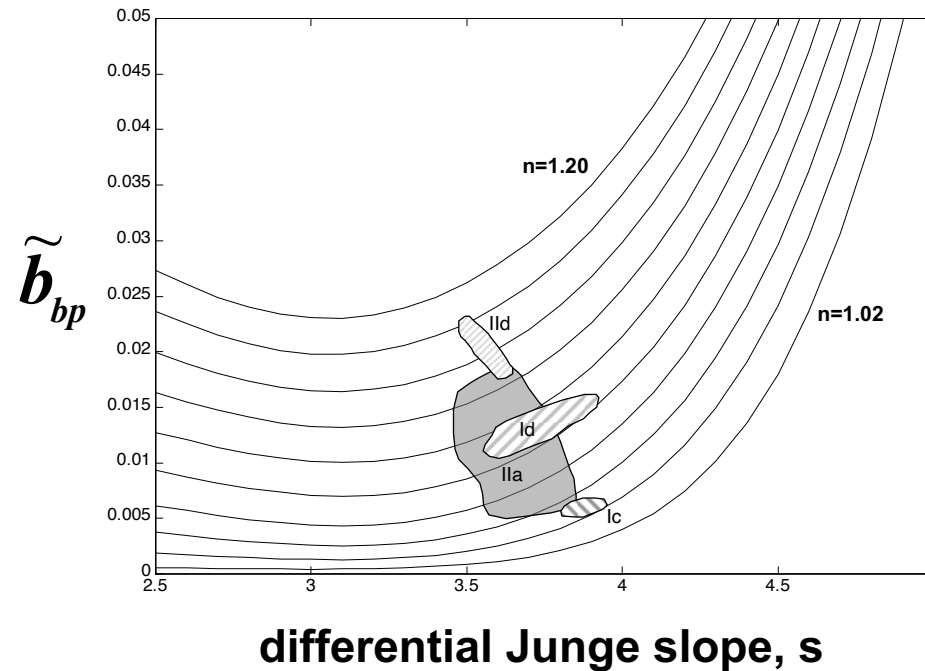


# Analytical inversion to solve for bulk particle refractive index

$$\hat{n}_p(\tilde{b}_{bp}, \gamma) = 1 + \tilde{b}_{bp}^{0.5377+0.4867(\gamma)^2} [1.4676 + 2.2950(\gamma)^2 + 2.3113(\gamma)^4].$$



Inputs:  $b_{bp}/b_p$ ,  $c(\lambda)$



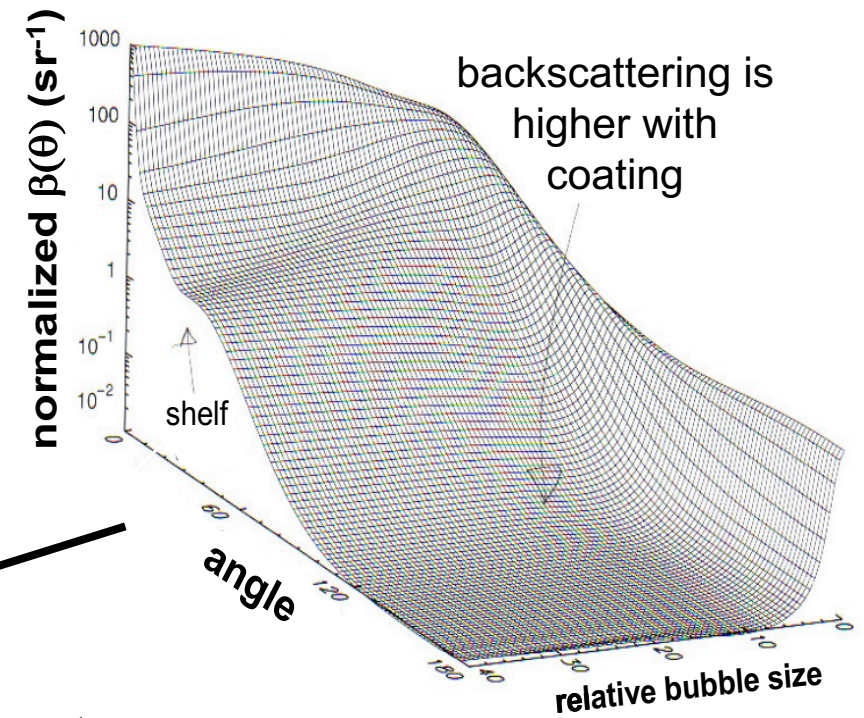
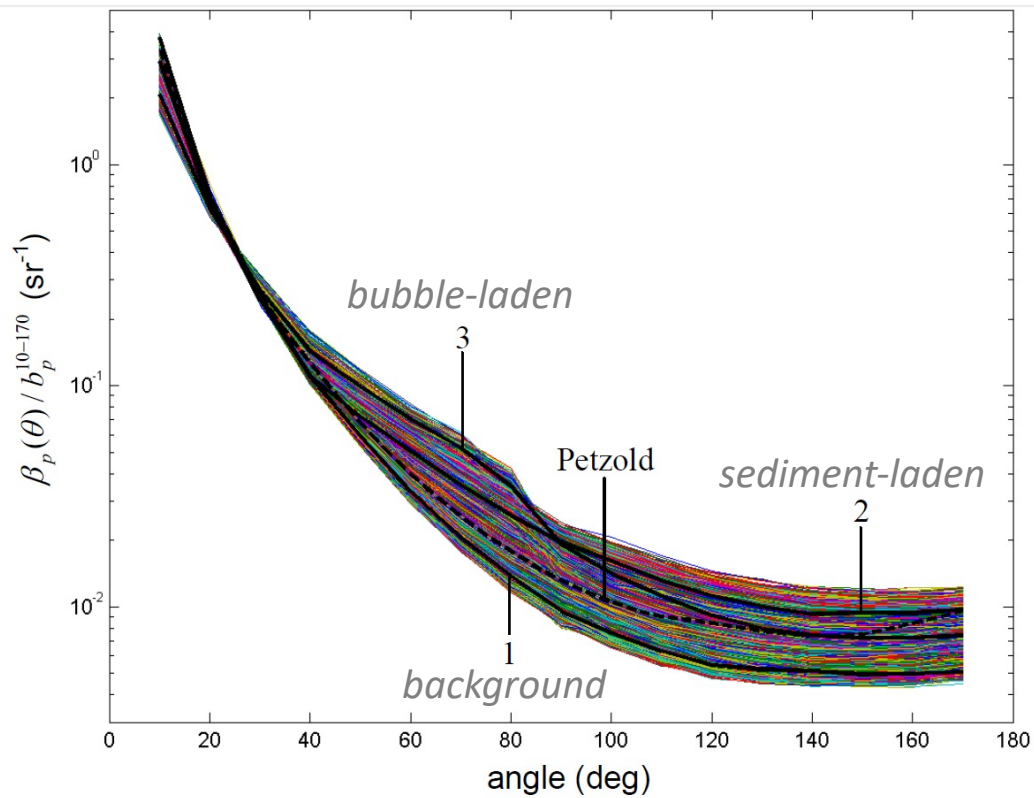
Based on Lorenz-Mie theory

Field data from Gulf of California

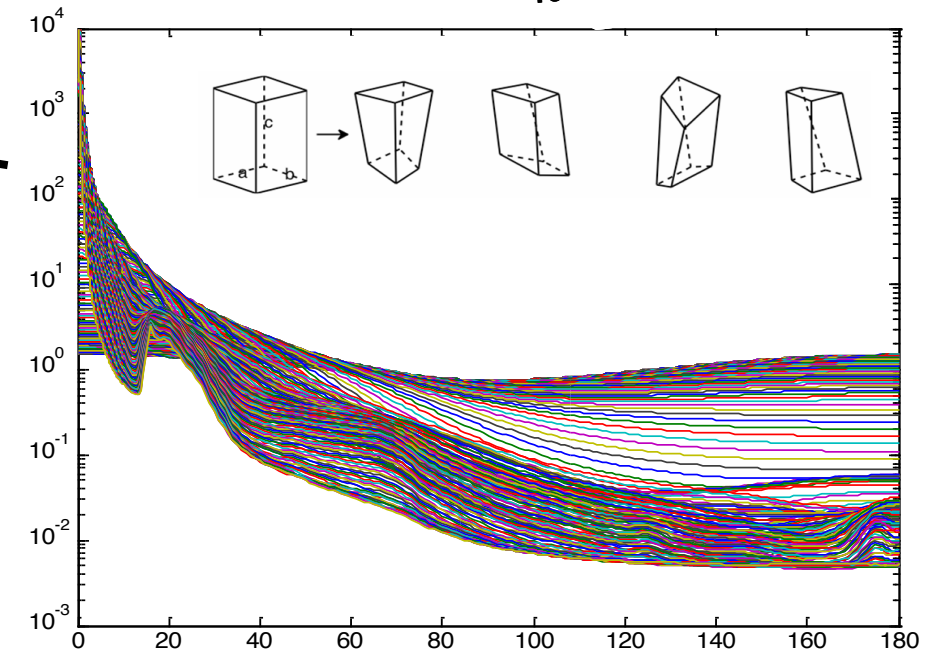
Typically gives reasonable values

# VSF inversion

Scripps Pier, 2008



Fit to  
measured  
VSFs



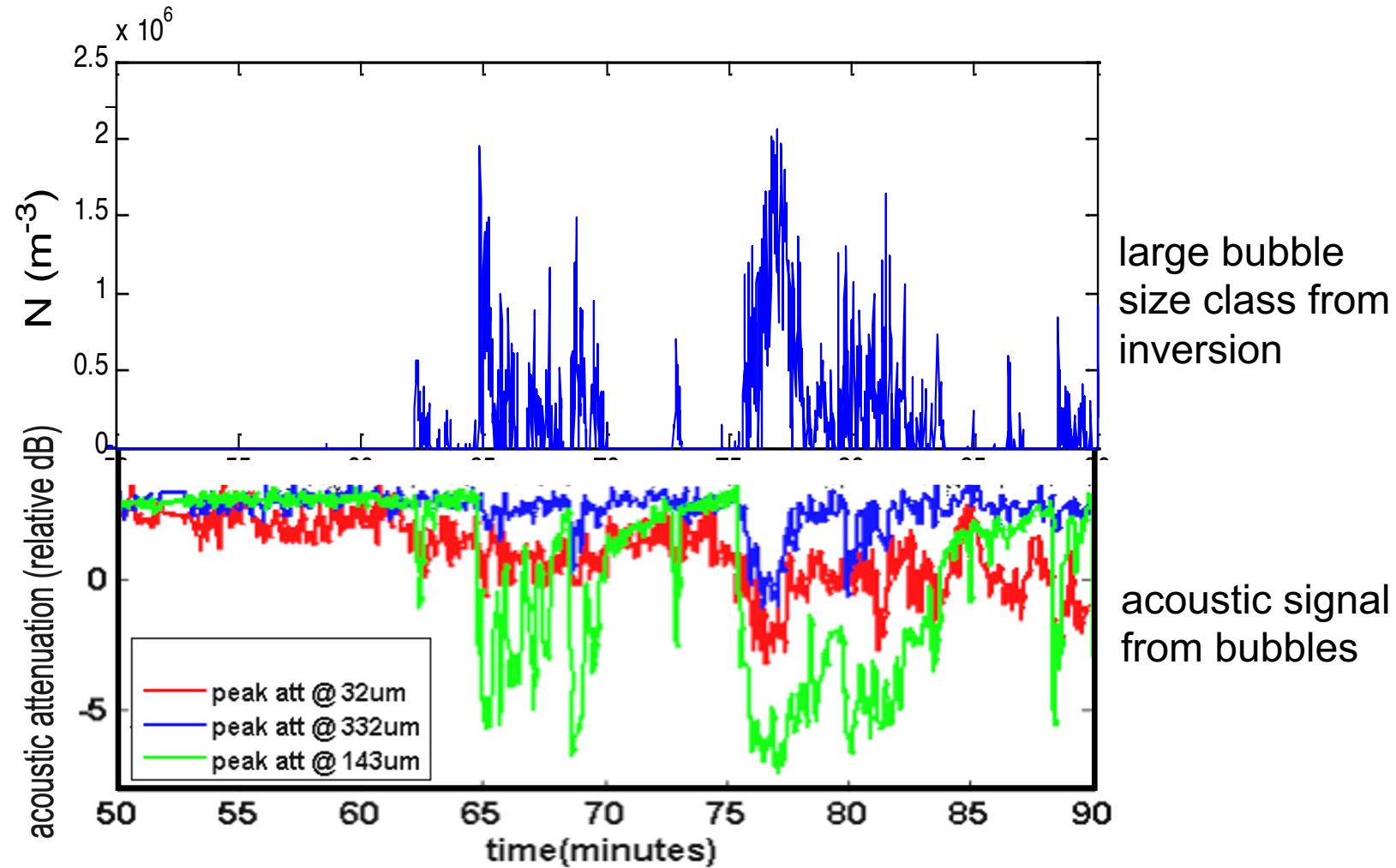
Twardowski et al. (2012)



**Scripps Pier**



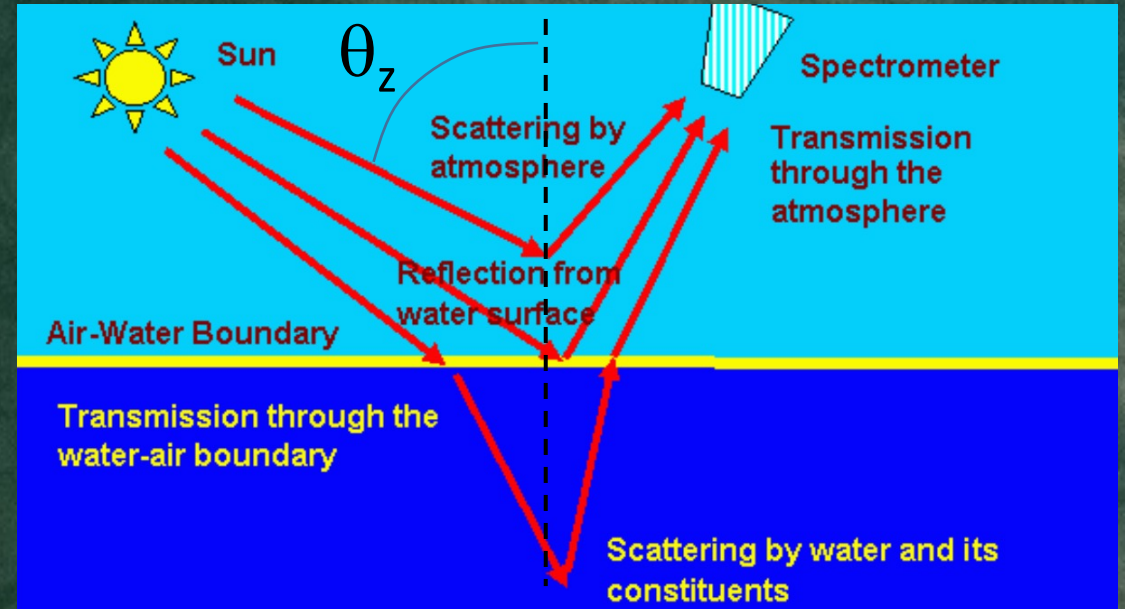
# Bubbles resolved with optics and acoustics



# Relevance of VSF to ocean color

$$R_{rs}(0^-) = \frac{L_u(0^-)}{E_d(0^-)} \cong \Psi \left( \frac{b_b}{a + b_b} \right)$$

Gordon (1975)  
Morel and Prieur (1975)



$$L_w(\theta, \phi, \theta_z) \xrightarrow[\text{BRDF}]{\text{1}} L_{wN}(\pi, \theta_z = 0)$$

Algorithms...

THIS IS CONTROLLED  
BY THE VSF



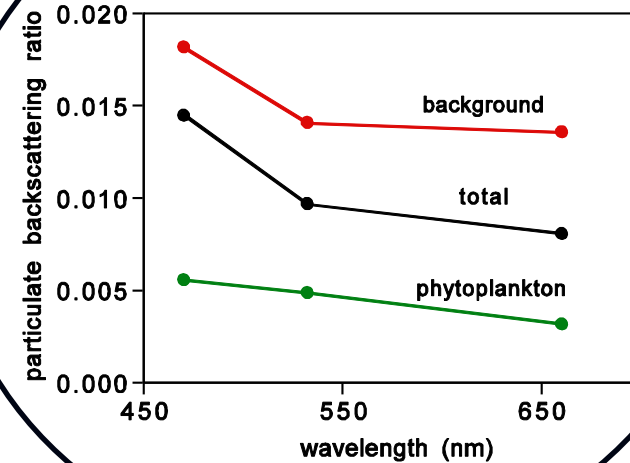
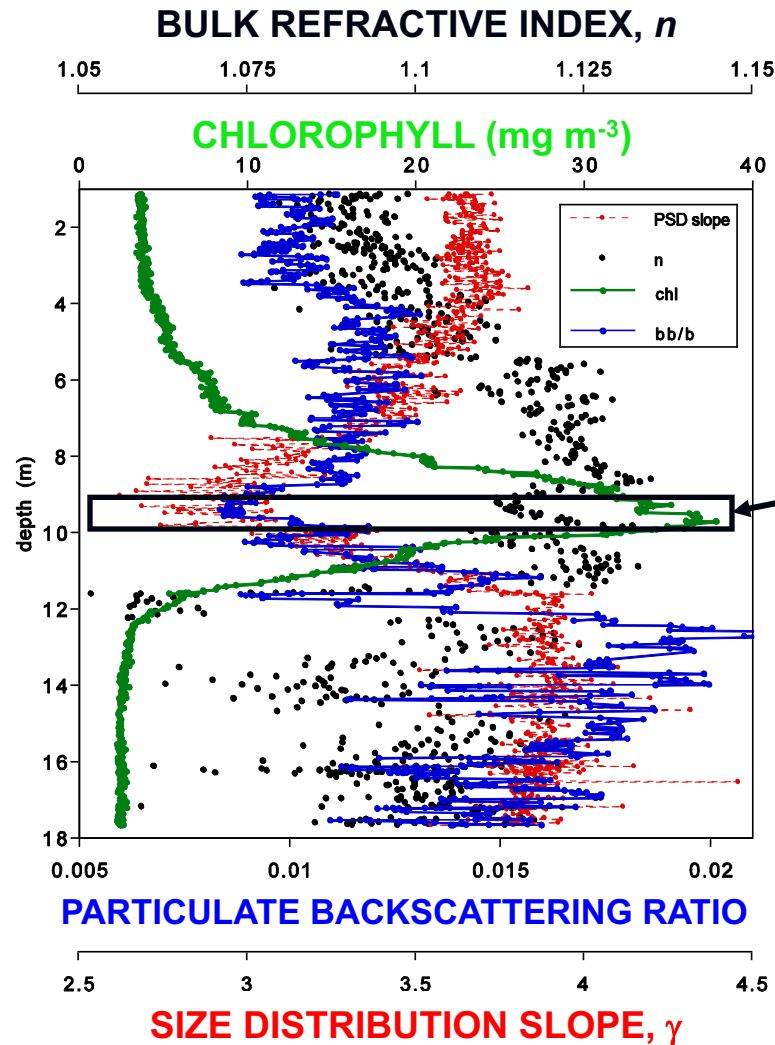
# SO MUCH TO DO...!

## For example:

- Spectral scattering:
  - hyperspectral bb
  - phase function shape
  - anomalous dispersion
- $\beta(180)$
- Scattering by nonspherical, complex particle populations
- Effect of scattering by nonrandomly oriented particles
- Anything to do with polarized scattering
- Remote algorithms from space including both ocean color and polarimetry that explicitly include VSF

**BACKUP**

# Akashiwo Layer in Monterey Bay

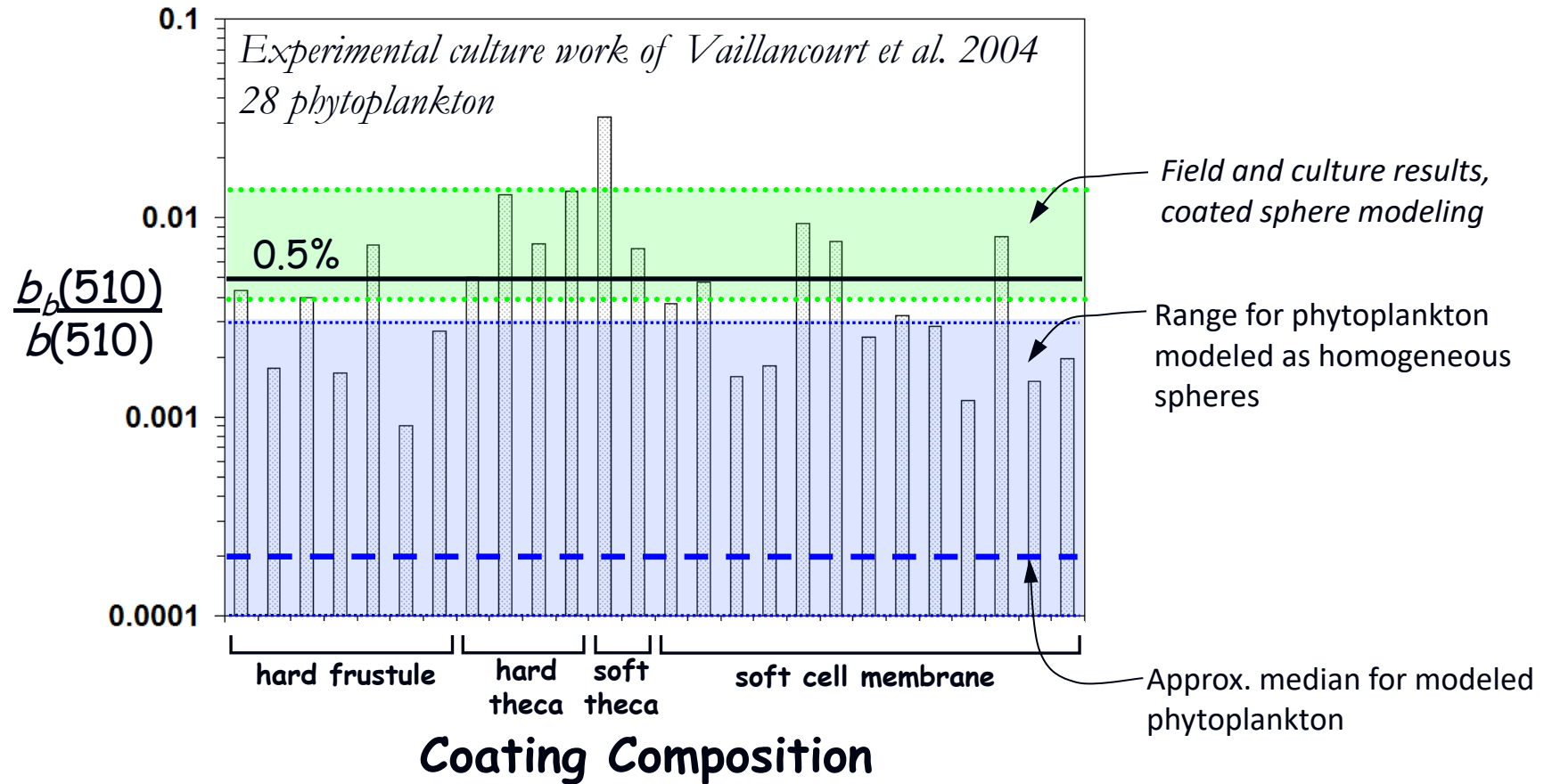


Akashiwo et al.

$$b_{bp}(532) / b_p(532) \approx \underline{0.005}$$

$\sim \underline{20\%}$  of  $b_{bp}(532)$

# Phytoplankton $b_b/b$



*Phytoplankton likely do make a significant direct contribution to  $b_{bp}$*

# Component decomposition of linear Polarization

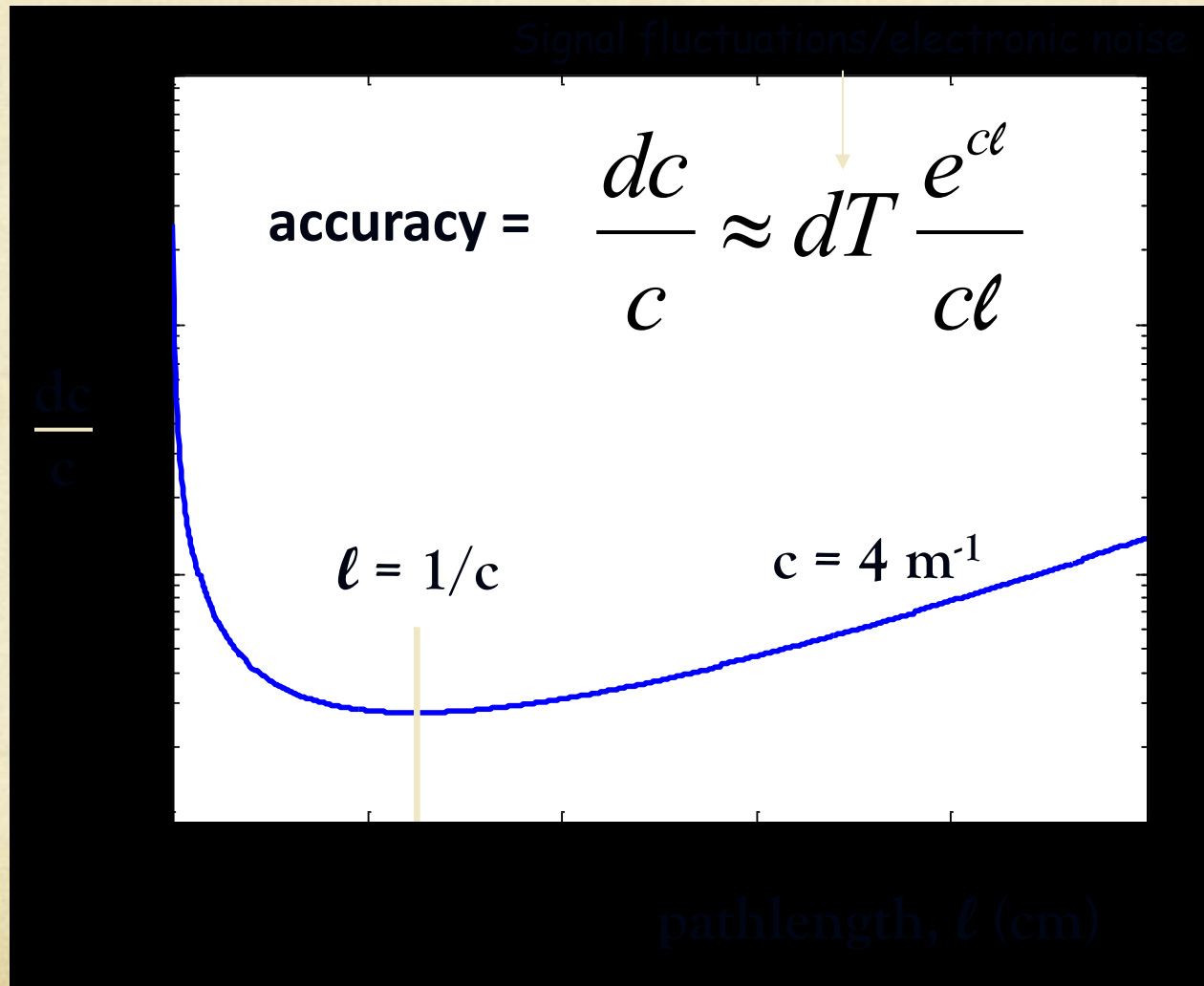




# Component decomposition of circular Polarization



# Accuracy



Accuracy is optimized when  $dc/c$  is minimized

Minimum occurs when  $c\ell \approx 1$

Choose pathlength accordingly...



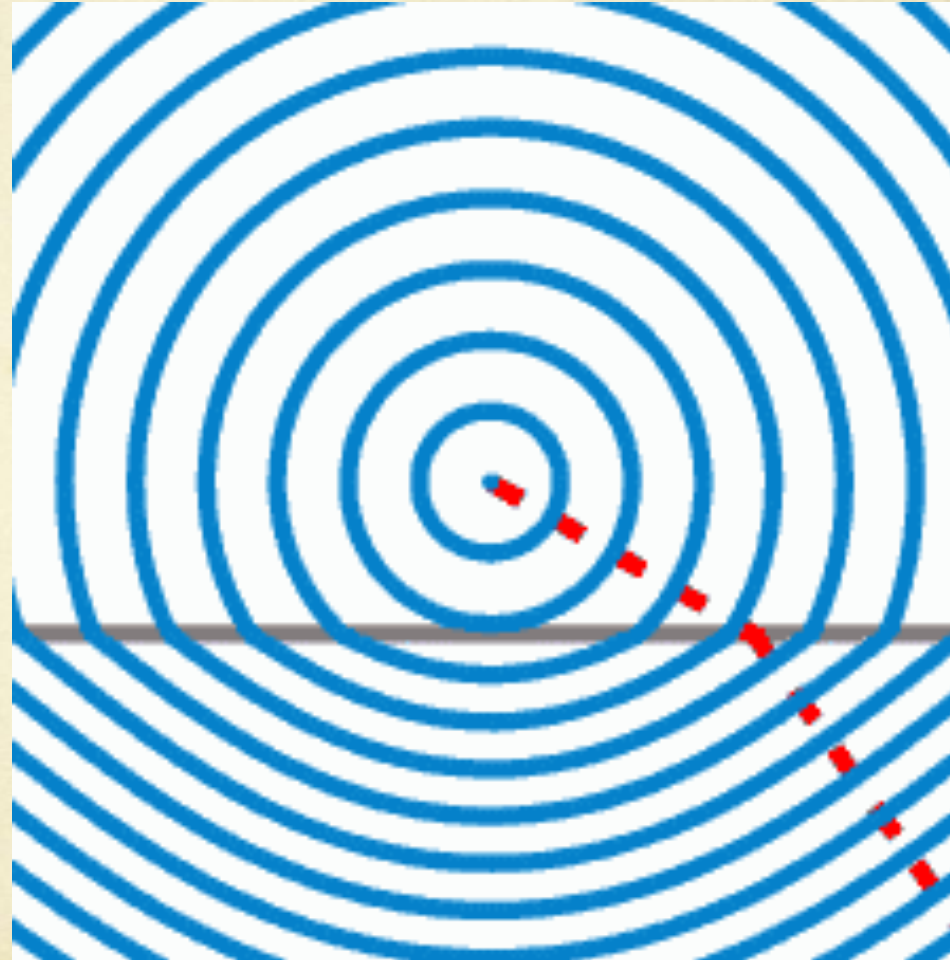
# What is refractive index?

*The refractive index  $n$  (or index of refraction) of a medium is a measure of how much the velocity of a wave is reduced inside that medium.*

$$n = \frac{c}{v_p} = \frac{\lambda_{\text{vacuum}}}{\lambda_{\text{medium}}}$$

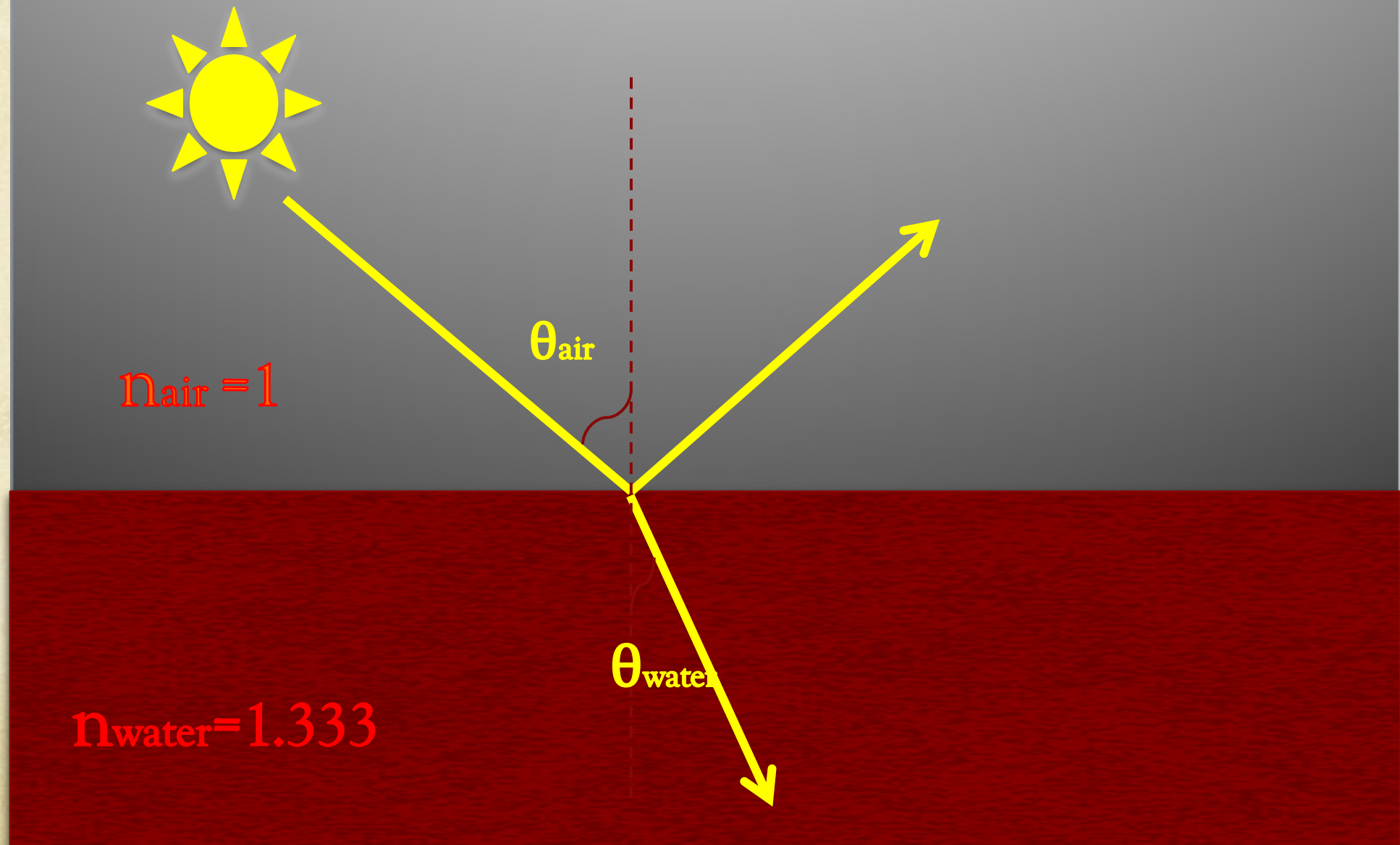
Wavefronts from a point source in the context of Snell's law. The region below the gray line has a higher index of refraction and proportionally lower wave velocity than the region above it.

Birefringent materials like  $\text{CaCO}_3$  have different  $n$  for different polarization elements and light directions....



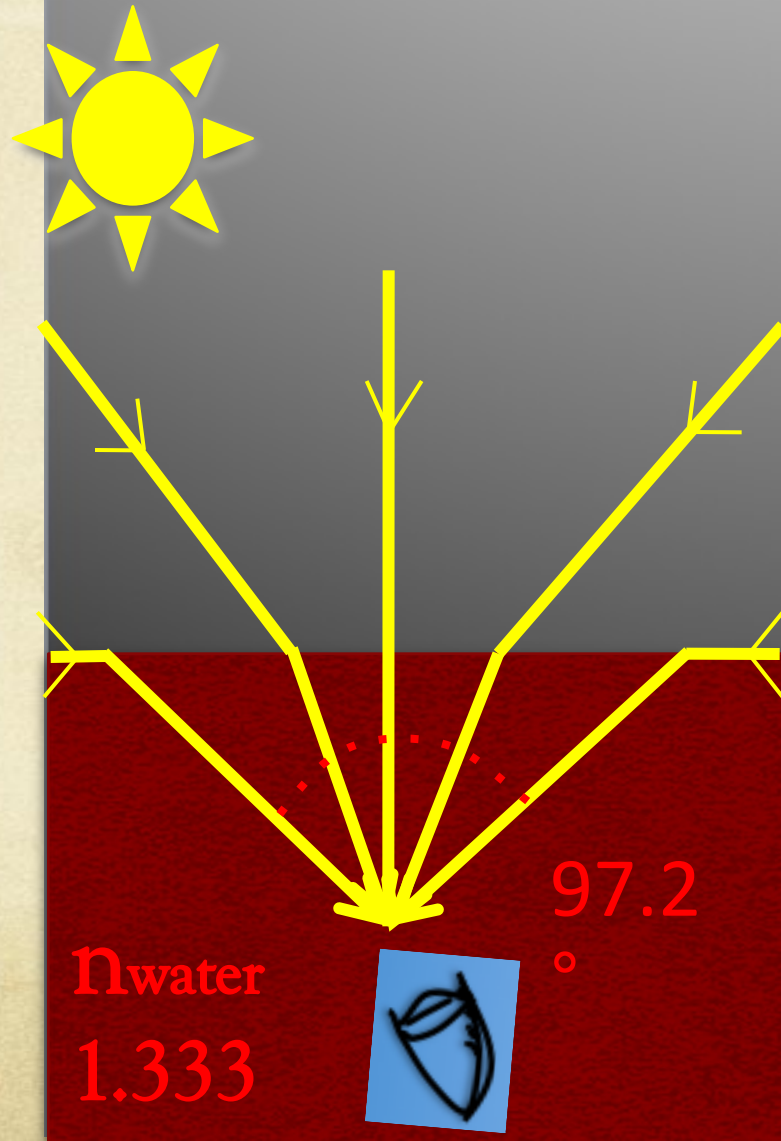
# Snell's Law

$$n_1 \sin \theta_1 = n_2 \sin \theta_2$$





# Snell's Window





# Polarized scattering: effects of bubbles

